Module	Nod	Color
SL1	first	lime-green
SL1	second	magenta
SL2	first	red
SL2	second	sky blue
LL1	first	brown
LL1	second	purple
LL2	first	dark blue
LL2	second	orange

Table 1. Colors used for each nod and module.

1 APPENDIX C

In this appendix we present the final Spitzer-IRS spectra for our sample. In the text we discuss the general data reduction recipe that was applied to all the targets. However, in few exceptional cases slight modification to the general recipe was necessary. Here, we provide a brief per-target recipe that will allow the reader to achieve identical results.

In the following pages, the first plot (top) shows the extracted spectrum of each target. Note that the first and the second nod and module is distinguished by a certain color as shown in Table 1.

In the second plot (bottom) on each page, we show the point spread functions for each nod and module after correction for the background. The observed point spread function is shown in black and our best fit point spread functions are shown in different colors depending on the number of sources detected in each of them. The caption of each figure shows the nod and module and its corresponding scale factor.

In most of our targets after extraction, there still appears a residual from insufficient bad pixel removal in form of unrealistic features (e.g. around 19.5-μm or 20.5-μm). We have manually removed those features by masking (removing from the flux array) those points from our spectra. The two nods within each module have been scaled to their common median in all of our targets.

The photometry data from ISOGAL (7, 15-μm), IRAC (3.6, 4.5, 5.8, 8-μm) and MIPS (24-μm) are also over-plotted. In most cases the flux values we extract are in good agreement with the photometry values.

However, in some cases there appears to be a mismatch between the two. We do not have a clear reason that can explain these discrepencies in all targets. These occasional differences can be introduced by a combination of error sources (e.g. instrumental, data processing, variability etc). The intrinsic variability of the star over time might be a plausible contributing factor to the discrepencies. In the whole sample (except of OH/IR stars), we chose SL1 to be our reference module because it has the most reliable and the least noisy flux compared to other modules. We have also tried using other modules as references as well, but in some cases it alleviates and in some other cases it aggravates the discrepencies. The scale factors applied on the Long-Low modules range between $\sim 0.11-0.97$ **and for SL2 they range between** $\sim 0.85-1.5$**. The typical offset between photometric data and spectroscopic data range between** $\sim 0-2$**Jy in flux.**

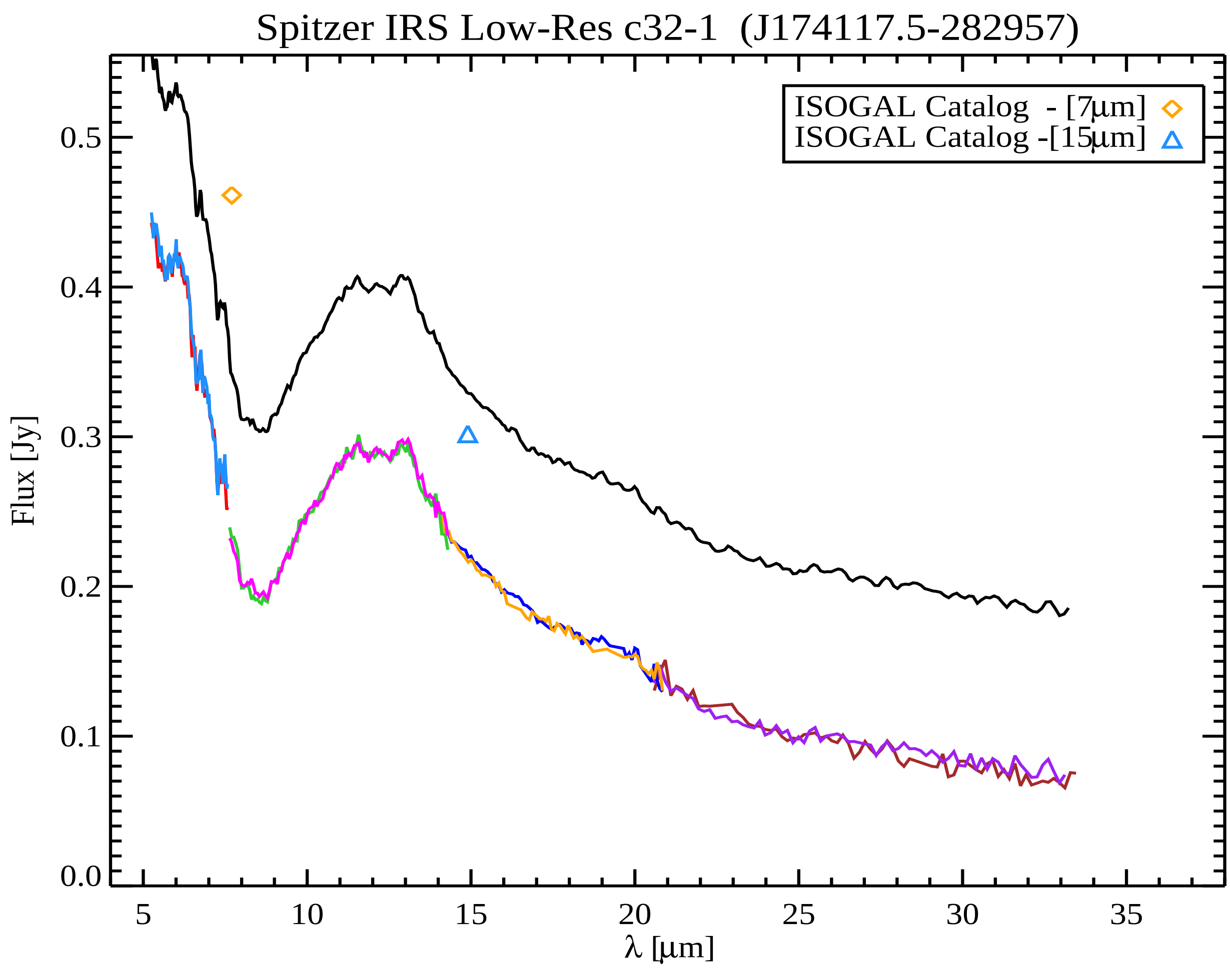

Figure 1. (c32-1) Both nods of the short low modules (SL1 & SL2) of this target contain only one target in the slit whereas in the long low module (LL1 & LL2) a second source appears very close to c32-1 (see Fig. 2). The position of the extracted sources are shown in the Figure 2. The spectrum shows residuals from insufficient bad pixel removal around 20.5-μm which was properly masked. The background of this source is strong and variable with prominent PAH features. However, it can be properly modeled and corrected using the IDL program discussed in the text. In the obtained spectrum, there is a slight mismatch between long low and short low modules. We treated this mismatch by scaling the long low modules with respect to the short low modules. The scaling factors used are listed below.

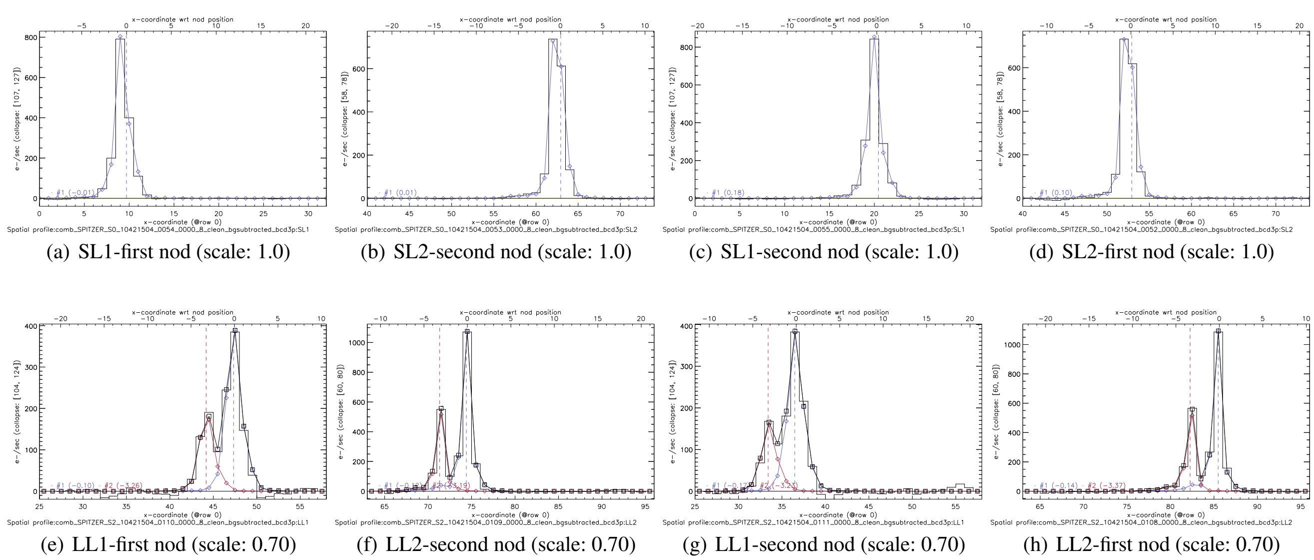

(a) SL1-first nod (scale: 1.0) (b) SL2-second nod (scale: 1.0) (c) SL1-second nod (scale: 1.0) (d) SL2-first nod (scale: 1.0)

(e) LL1-first nod (scale: 0.70) (f) LL2-second nod (scale: 0.70) (g) LL1-second nod (scale: 0.70) (h) LL2-first nod (scale: 0.70)

Figure 2. SL and LL modules spatial profiles after subtraction of the background

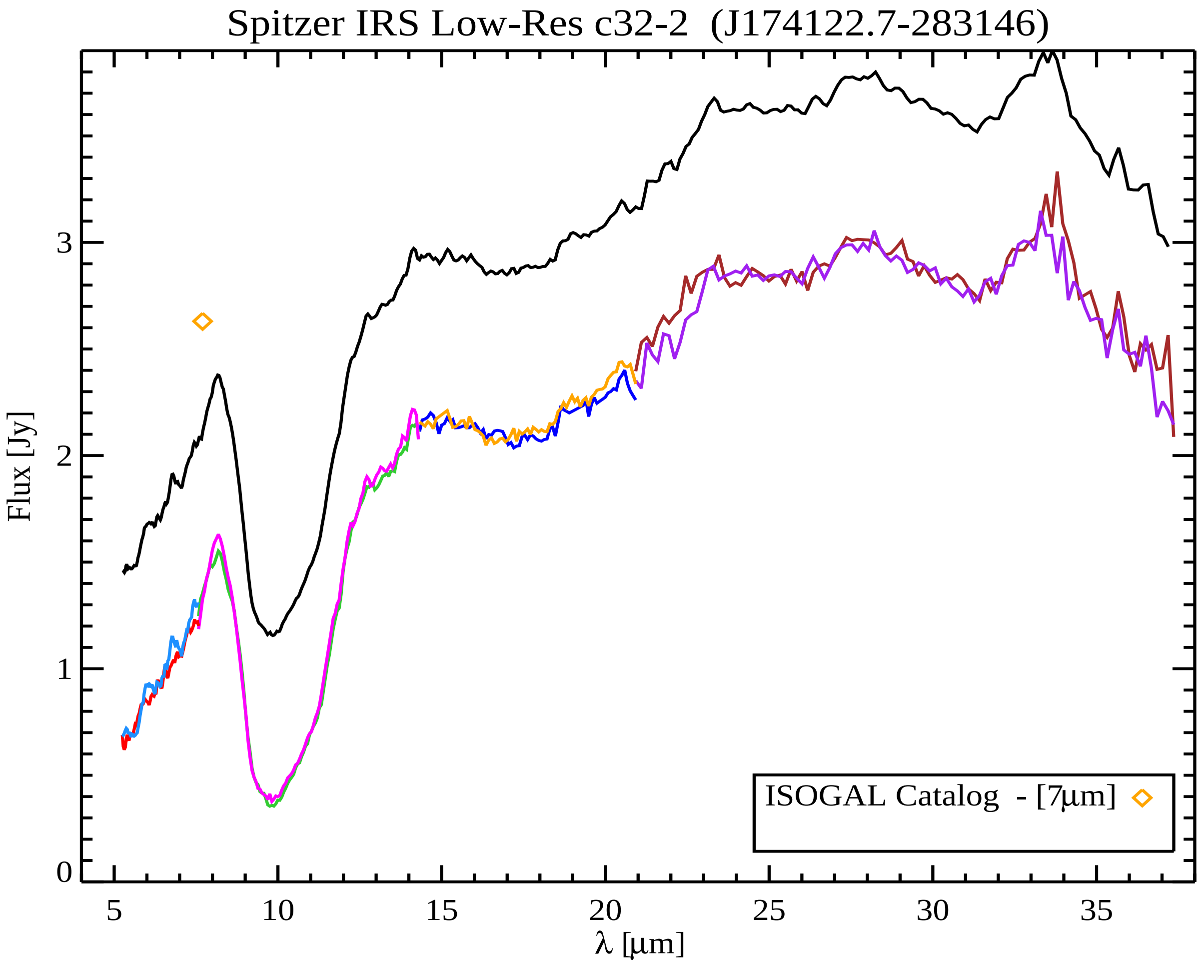

Figure 3. **(c32-2)** The number of extracted sources in each nod and module is shown in Fig. 4 along with their position. In the extracted spectrum, there was a mismatch between the two nods of the SL1 module. Specifically, close to the edges of the module this mismatch was more noticeable. In order to correct for that we have modified the point spread function in SMART by specifying new parameters for the central position and full-width-half-maximum(FWHM)of the PSF. The background of this target was strong and variable and quite similar to c32-1 since they are both in the field c32. The background for the long low modules was properly modeled by the program explained in the text but for the SL2 module we have subtracted the background assuming a first order polynomial within optimal extraction of SMART. Finally, The mismatch between the modules was corrected by scaling the short low modules with respect to long low modules, with the following scale factors.

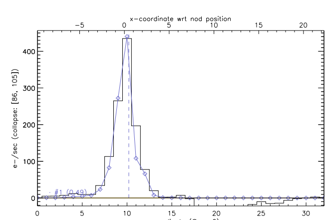

(a) SL1-first nod (scale: 2.3)

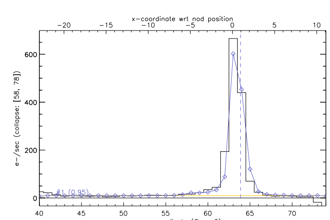

(b) SL2-second nod (scale: 1.4)

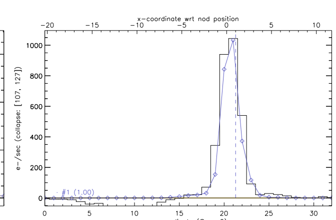

(c) SL1-second nod (scale: 2.3)

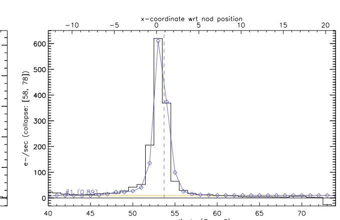

(d) SL2-first nod (scale: 1.4)

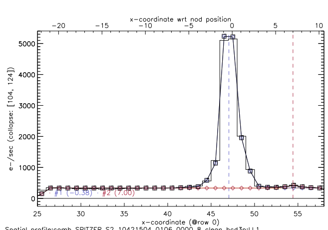

(e) LL1-first nod (scale: 1.0)

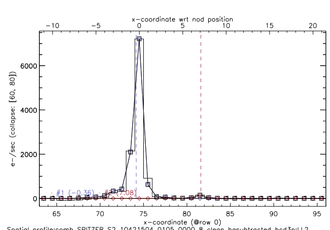

(f) LL2-second nod (scale: 1.0)

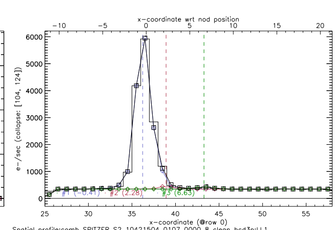

(g) LL1-second nod (scale: 1.0)

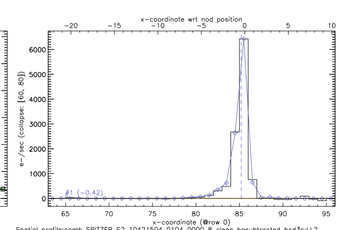

(h) LL2-first nod (scale: 1.0)

Figure 4. SL and LL modules spatial profiles after subtraction of the background

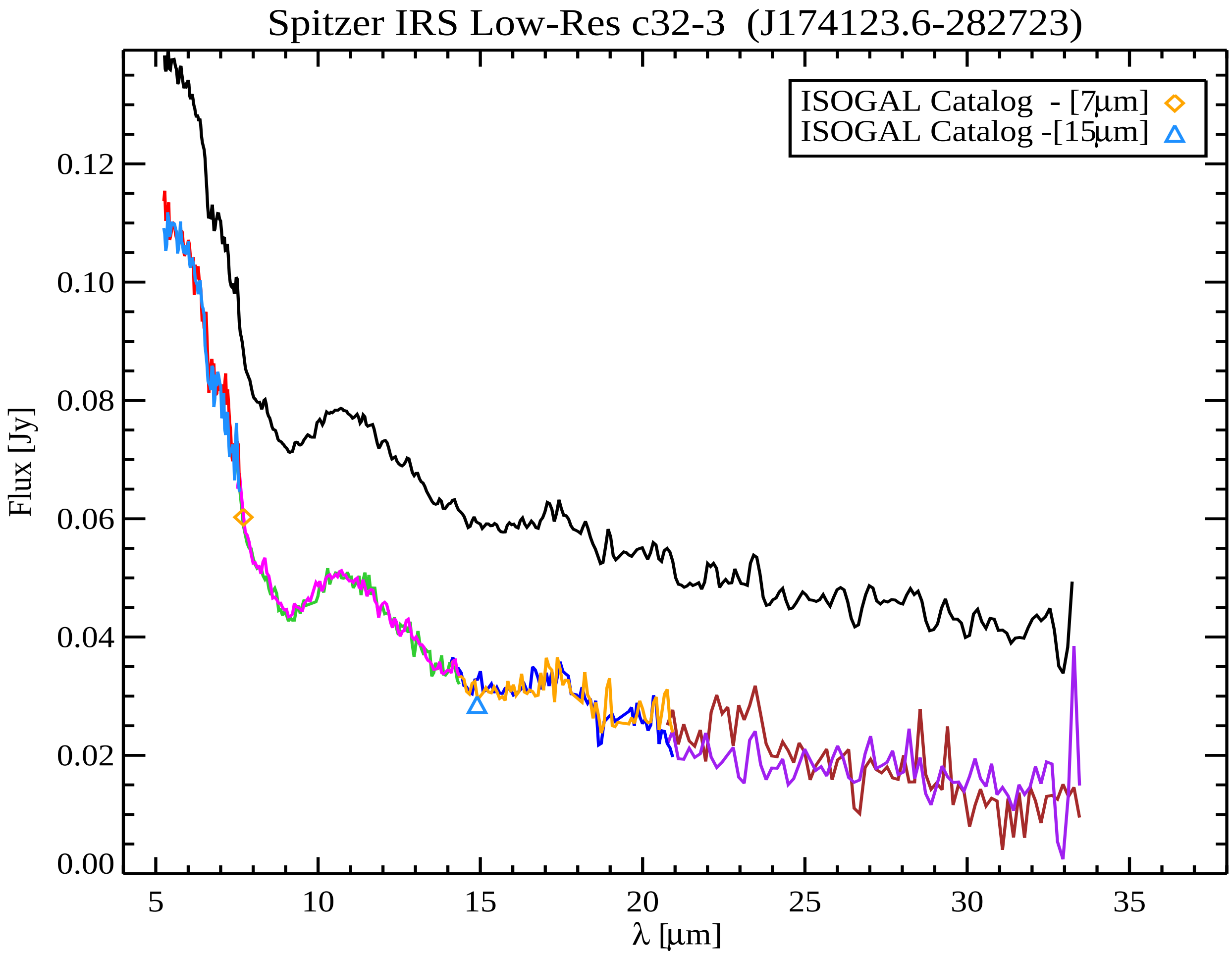

Figure 5. (c32-3) As indicated in Figure 6, the number of sources that have been extracted in each nod and module. There was a significant mismatch between the two nods of SL1 module which was corrected by modifying the point spread function(central position and FWHM). After extraction the residual features were masked properly (e.g. 19.5-μm). This target is located in field c32 but the background is properly corrected through modeling except SL1 module. For this module, we have assumed **a constant offset for the background (polynomial order zero)** and performed the subtraction using optimal extraction within SMART. Finally, we scaled long low modules with respect to the short low modules using the following scale factors, in order to eliminate the mismatch between modules and obtain the continuum shown here.

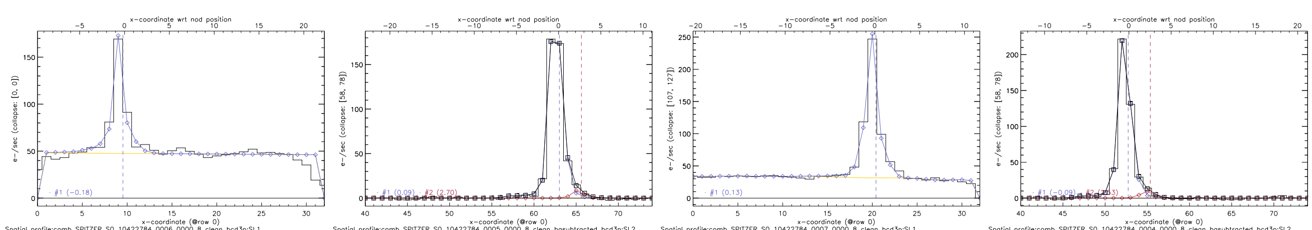

(a) SL1-first nod (scale: 1.0) (b) SL2-second nod (scale: 1.0) (c) SL1-second nod (scale: 1.0) (d) SL2-first nod (scale: 1.0)

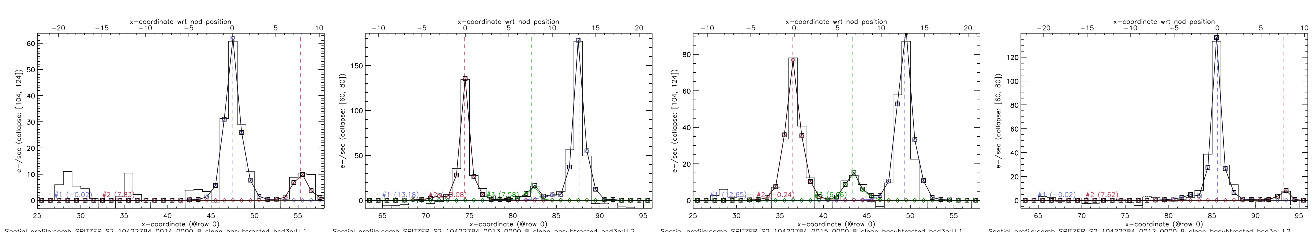

(e) LL1-first nod (scale: 0.77) (f) LL2-second nod (scale: 0.77) (g) LL1-second nod (scale: 0.77) (h) LL2-first nod (scale: 0.77)

Figure 6. SL and LL modules spatial profiles after subtraction of the background

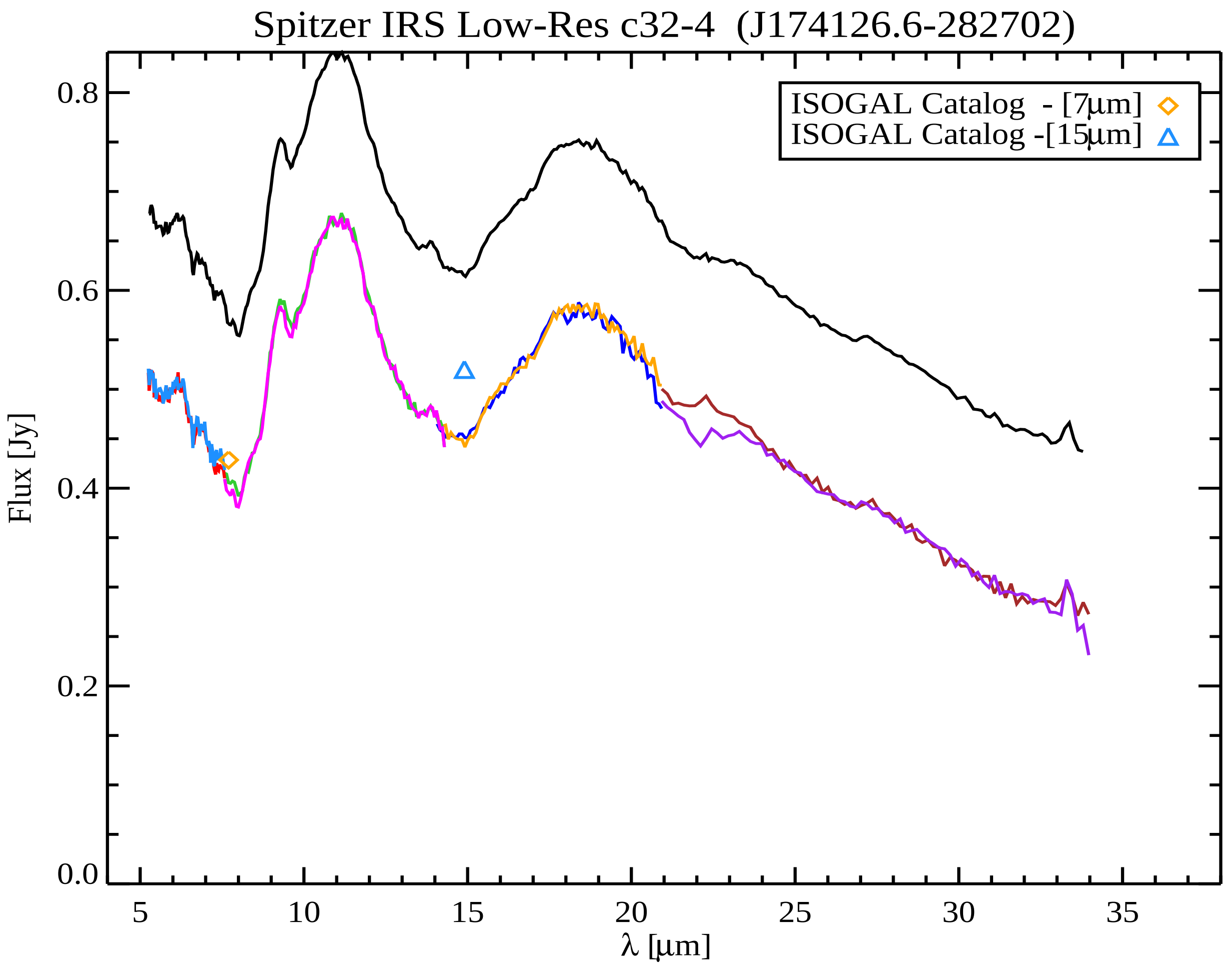

Figure 7. (c32-4) All nods of both modules (SL and LL) of this target contain only one source in the slit except first nod of SL2 module which contains a very faint second source (see Fig. 8). The position of the extracted targets are shown in the figure 8. The residuals we represent after extraction which were properly masked (e.g. 18.5-μm) The background for this source is strong and variable but properly modeled and corrected. Finally, we applied the following scale factors on the corresponding module to eliminate the mismatch between modules and obtain the final continuum shown here.

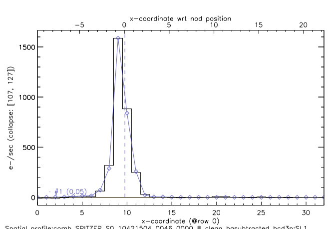
(a) SL1-first nod (scale: 1.0)

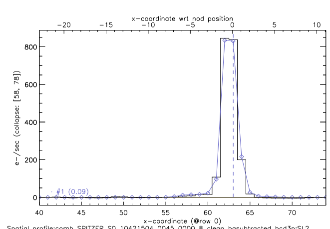
(b) SL2-second nod (scale: 0.95)

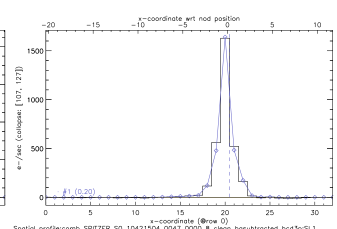
(c) SL1-second nod (scale: 1.0)

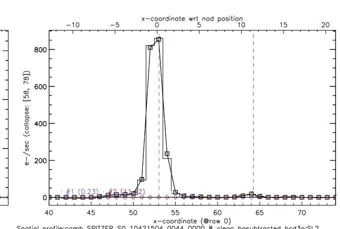
(d) SL2-first nod (scale: 0.95)

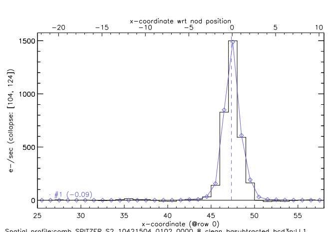
(e) LL1-first nod (scale: 0.72)

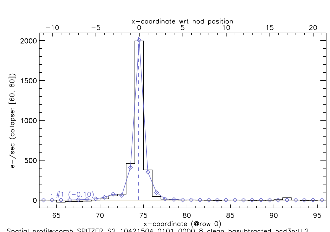
(f) LL2-second nod (scale: 0.76)

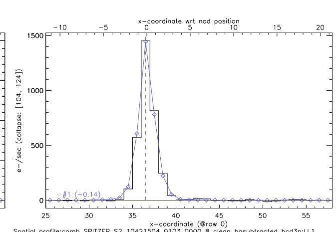
(g) LL1-second nod (scale: 0.72)

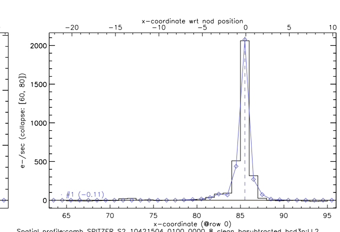
(h) LL2-first nod (scale: 0.76)

Figure 8. SL and LL modules spatial profiles after subtraction of the background

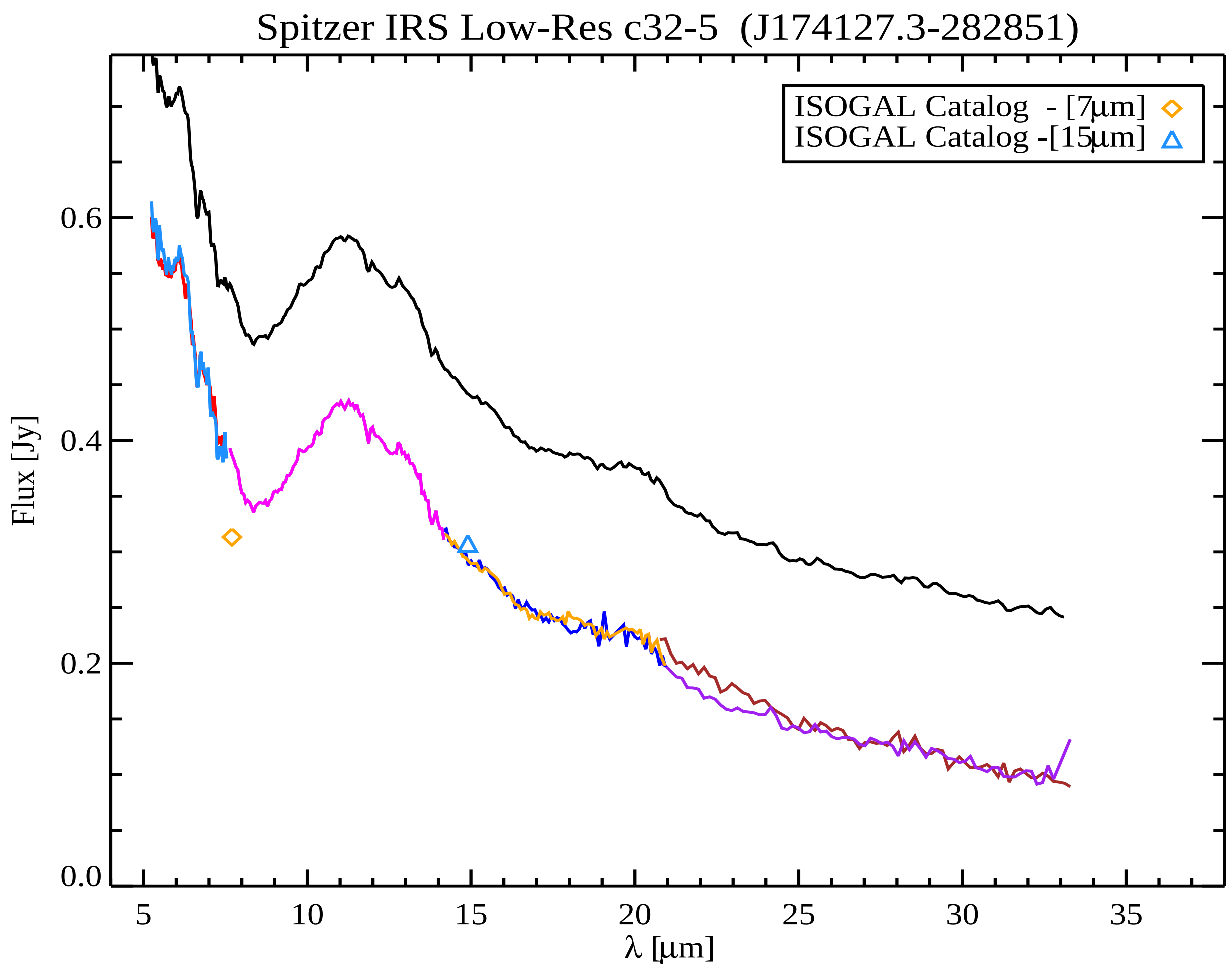

Figure 9. (c32-5) This is the final spectrum of c32-5. Figure 10 indicates the number of sources that have been extracted in each nod of each module. After extraction there was no obvious residuals left for us to remove manually. As shown in Figure 10 the observation for the second nod of SL1 module did not contain any useful information to extract, therefore for this module, we only took into account the data in the first nod. **The background for this source is strong and variable but properly modeled and corrected.** Finally, we scaled the long low modules with respect to the short low in order to eliminate the mismatch between modules and obtain the continuum shown here.

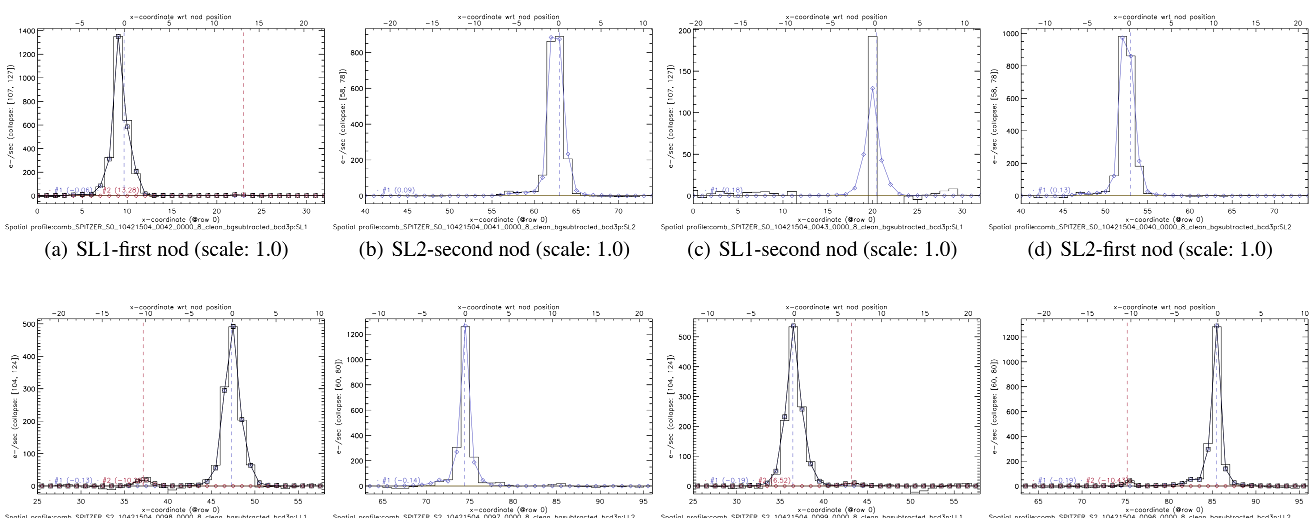

(a) SL1-first nod (scale: 1.0) (b) SL2-second nod (scale: 1.0) (c) SL1-second nod (scale: 1.0) (d) SL2-first nod (scale: 1.0)

(e) LL1-first nod (scale: 0.80) (f) LL2-second nod (scale: 0.80) (g) LL1-second nod (scale: 0.80) (h) LL2-first nod (scale: 0.80)

Figure 10. SL and LL modules spatial profiles after subtraction of the background

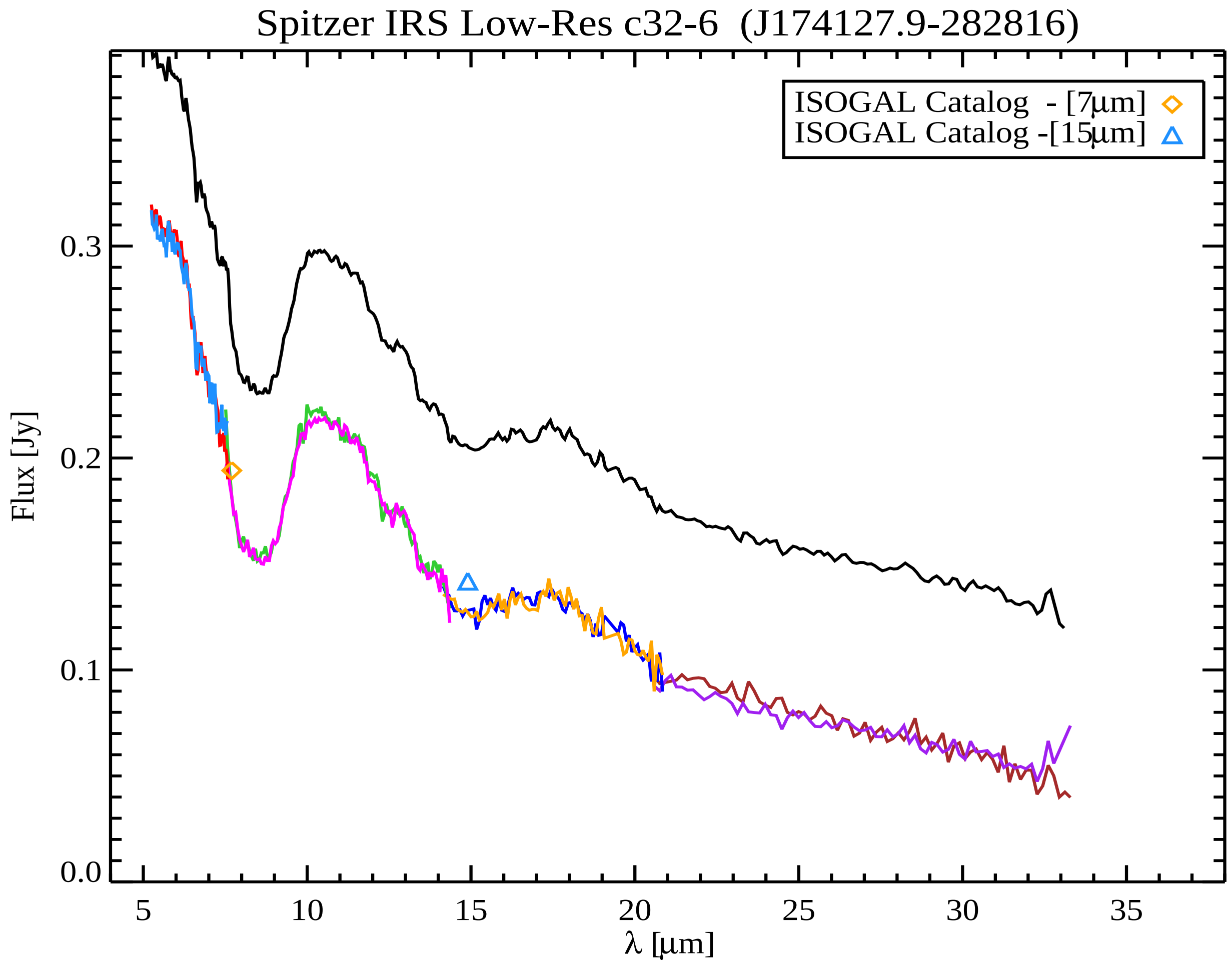

Figure 11. (c32-6) This is the final spectrum of c32-6. Figure 12 indicates the number of sources that have been extracted in each nod of each module. The mismatch between the nods of SL1 module was removed by modifying the point spread function (central position and FWHM). After extraction the residual features were masked (e.g. 19.5-μm). In all modules, the background could be corrected by means of modeling except the LL1 module, in which case we have subtracted the background assuming **an order one polynomial (linear gradient)** in manual optimal extraction within Smart. Finally, we scaled the long low modules with respect to the short low modules in order to eliminate the mismatch between modules and obtain the continuum shown here.

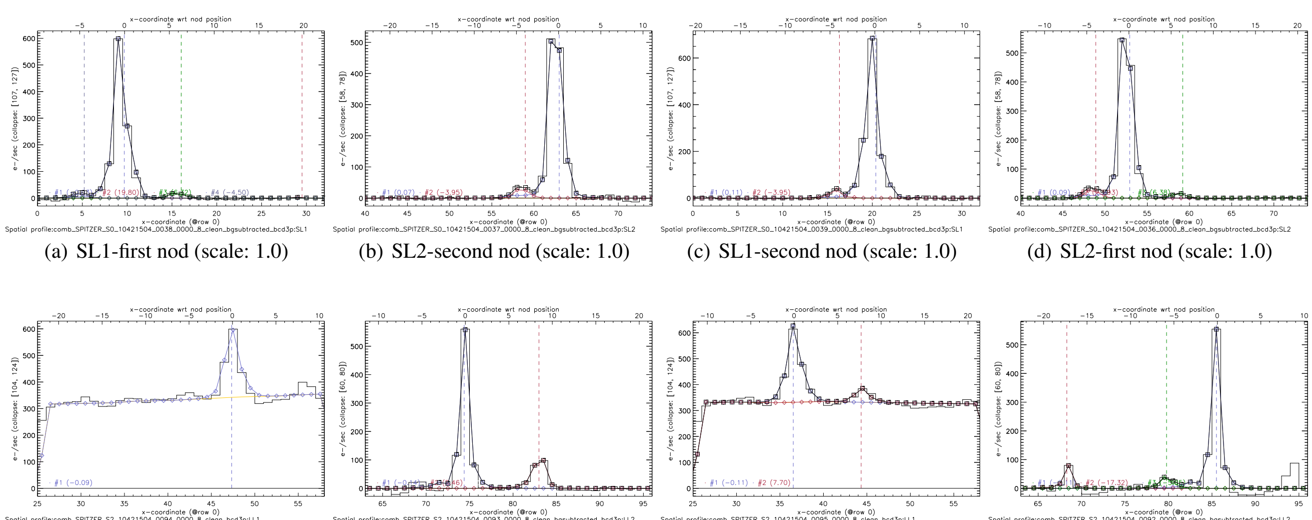

(a) SL1-first nod (scale: 1.0) (b) SL2-second nod (scale: 1.0) (c) SL1-second nod (scale: 1.0) (d) SL2-first nod (scale: 1.0)

(e) LL1-first nod (scale: 0.78) (f) LL2-second nod (scale: 0.80) (g) LL1-second nod (scale: 0.78) (h) LL2-first nod (scale: 0.80)

Figure 12. SL and LL modules spatial profiles after subtraction of the background

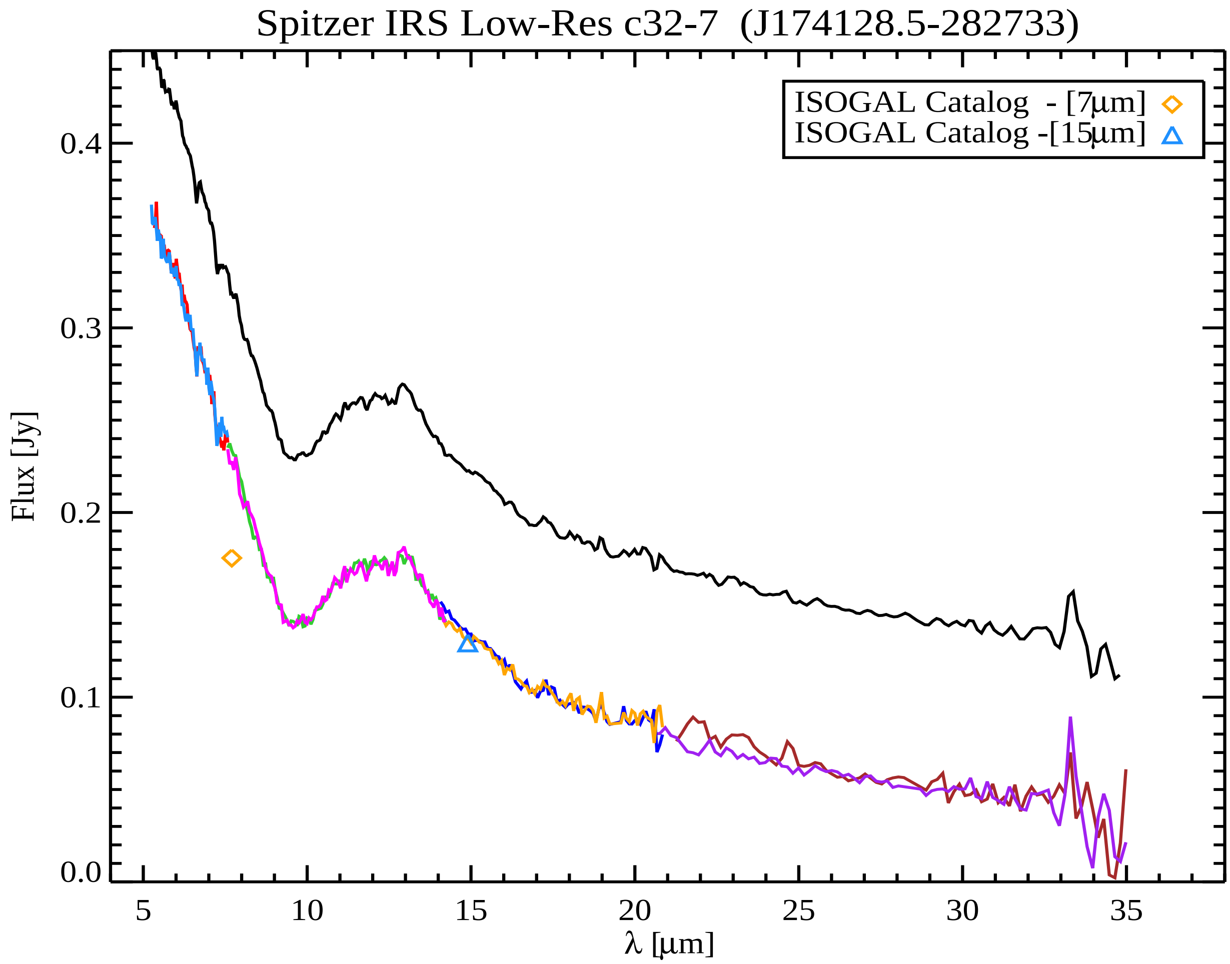

Figure 13. (c32-7) This is the final spectrum of c32-7. Figure 14 indicates the number of sources that have been extracted in each nod and module. There was a slight mismatch between the two nods of SL1 module which was removed by modifying the point spread function (central position and FWHM). After extraction the sharp and unrealistic residual features were masked (e.g. 19.5-μm). The background for this source is properly corrected through modeling. Finally, we applied the following scale factors on the corresponding module to eliminate the mismatch between modules and obtain the final continuum shown here.

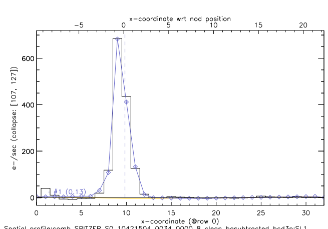
(a) SL1-first nod (scale: 1.0)

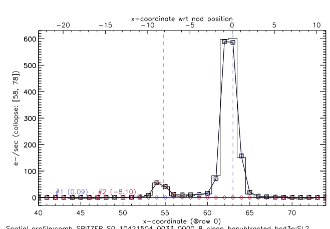
(b) SL2-second nod (scale: 0.92)

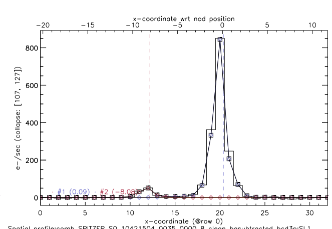
(c) SL1-second nod (scale: 1.0)

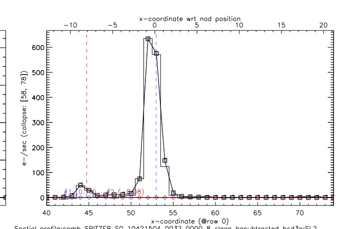
(d) SL2-first nod (scale: 0.92)

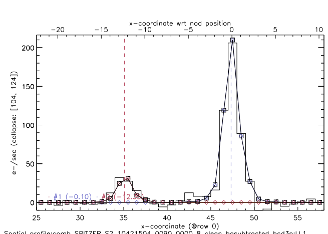
(e) LL1-first nod (scale: 0.80)

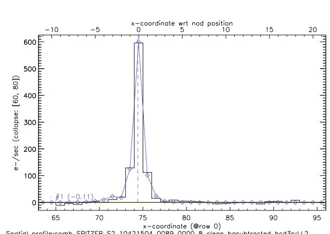
(f) LL2-second nod (scale: 0.75)

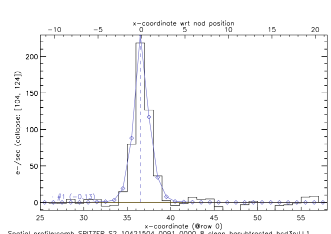
(g) LL1-second nod (scale: 0.80)

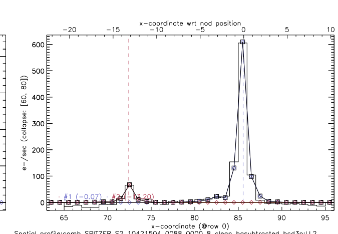
(h) LL2-first nod (scale: 0.75)

Figure 14. SL and LL modules spatial profiles after subtraction of the background

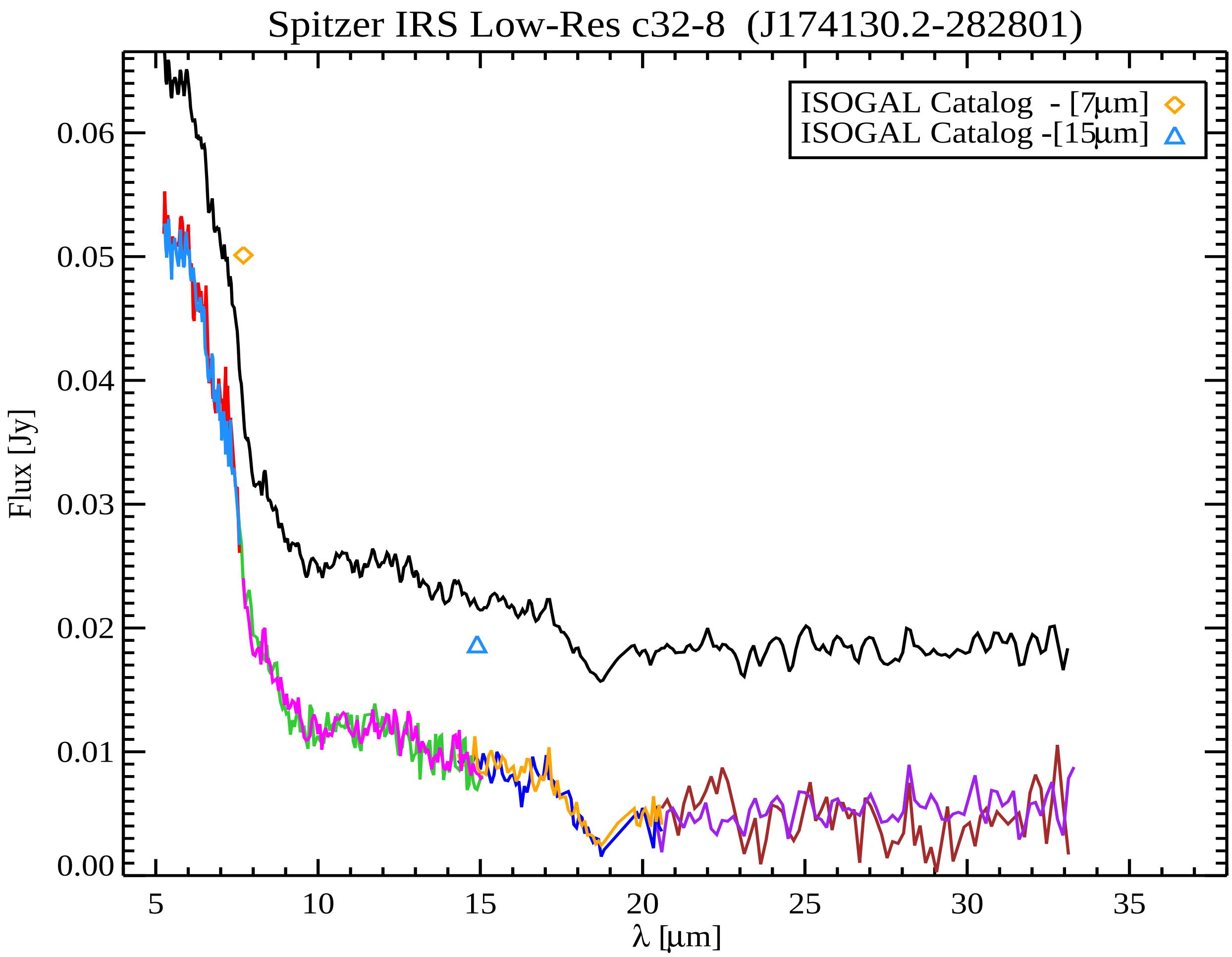

Figure 15. (c32-8) This is the final spectrum of c32-8. Figure 16 indicates the number of sources that have been extracted in each nod and module. There was a slight mismatch between the two nods of SL1 module which was removed by modifying the point spread function (central position and FWHM). After extraction there were no significant residuals to mask. The background is properly corrected through modeling. Finally, we scaled the long low modules with respect to the short low modules using the following scale factors, in order to eliminate the mismatch between them and obtain the continuum shown here.

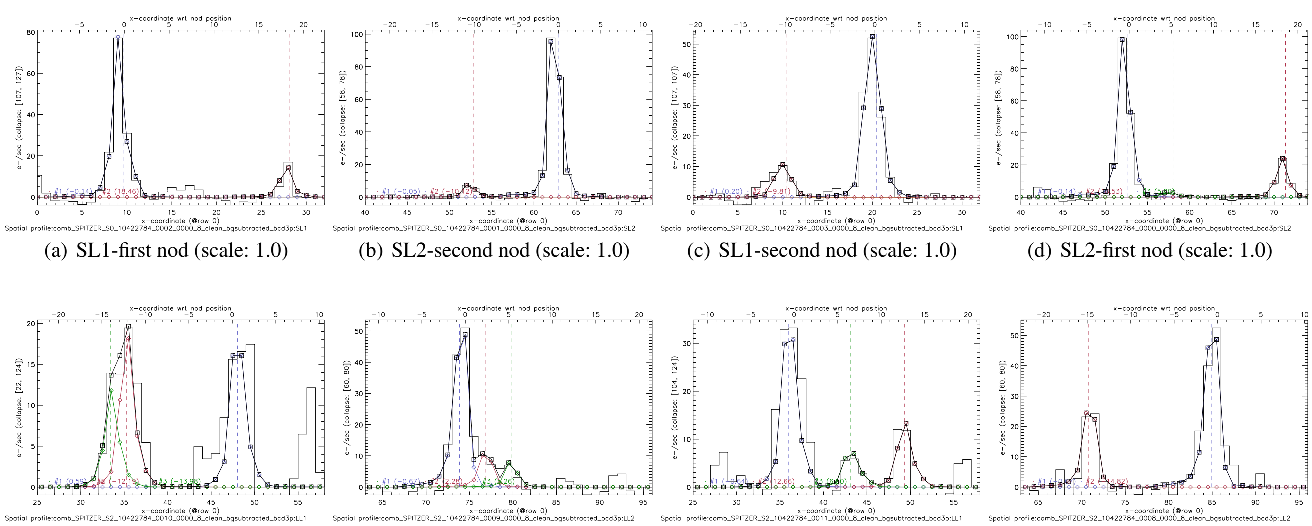

(a) SL1-first nod (scale: 1.0) (b) SL2-second nod (scale: 1.0) (c) SL1-second nod (scale: 1.0) (d) SL2-first nod (scale: 1.0)

(e) LL1-first nod (scale: 0.40) (f) LL2-second nod (scale: 0.40) (g) LL1-second nod (scale: 0.40) (h) LL2-first nod (scale: 0.40)

Figure 16. SL and LL modules spatial profiles after subtraction of the background

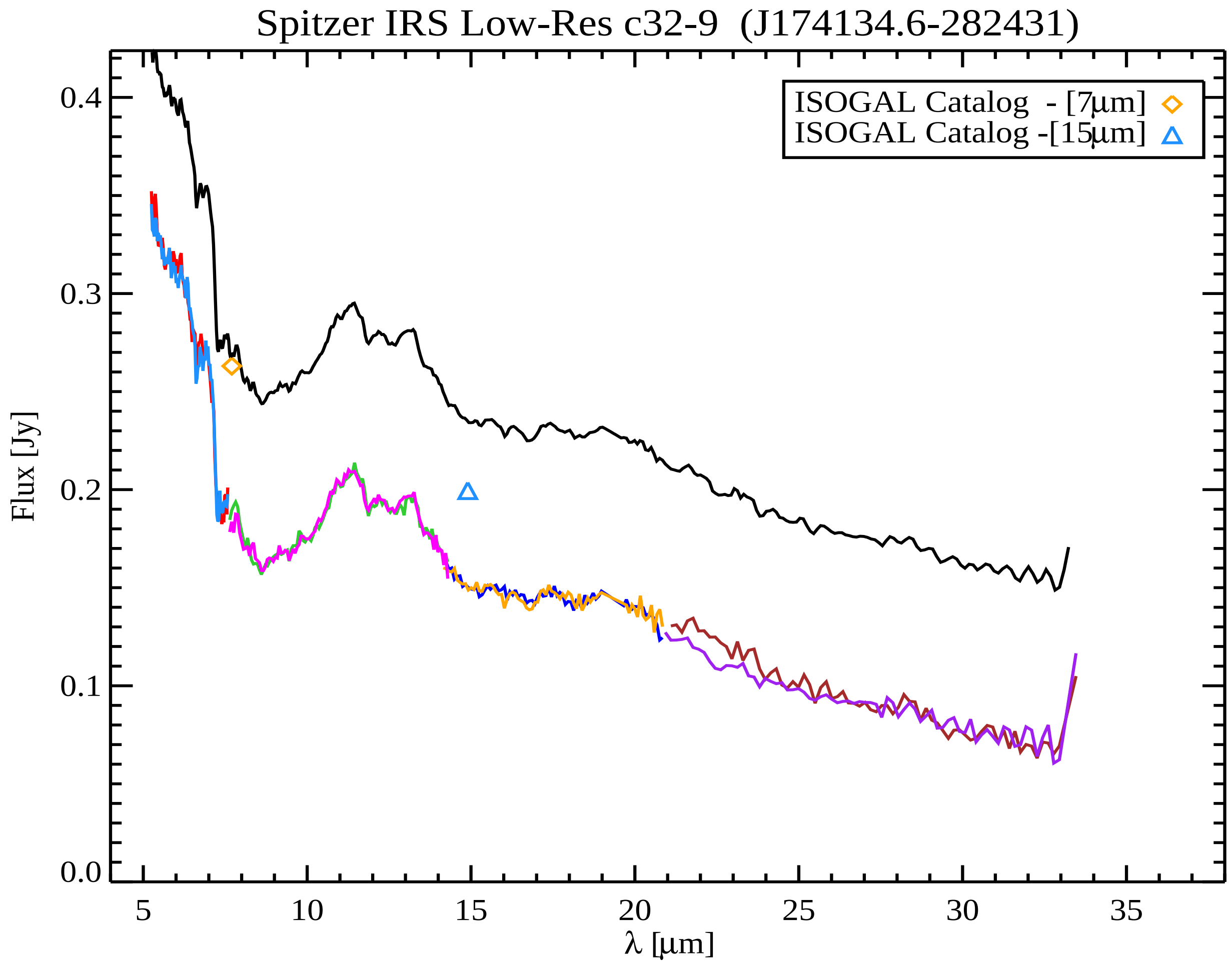

Figure 17. (c32-9) This is the final spectrum of c32-9. Figure 18 indicates the number of sources that have been extracted in each nod and module. There was a slight mismatch between the two nods of SL1 module which was removed by modifying the point spread function (central position and FWHM). After extraction the sharp and unrealistic residual features were masked (e.g. 19.5-μm). The background is properly modelled and corrected. Finally, we scaled the long low modules with respect to the short low modules using the following scale factors, in order to eliminate the mismatch between modules and obtain the continuum shown here.

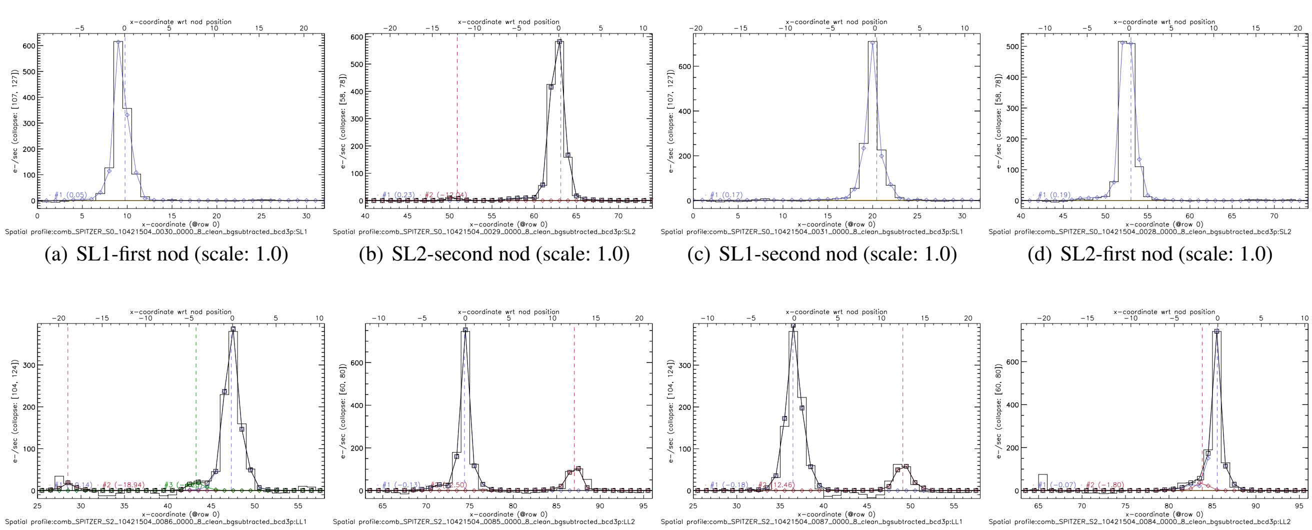

(a) SL1-first nod (scale: 1.0) (b) SL2-second nod (scale: 1.0) (c) SL1-second nod (scale: 1.0) (d) SL2-first nod (scale: 1.0)

(e) LL1-first nod (scale: 0.70) (f) LL2-second nod (scale: 0.70) (g) LL1-second nod (scale: 0.70) (h) LL2-first nod (scale: 0.70)

Figure 18. SL and LL modules spatial profiles after subtraction of the background

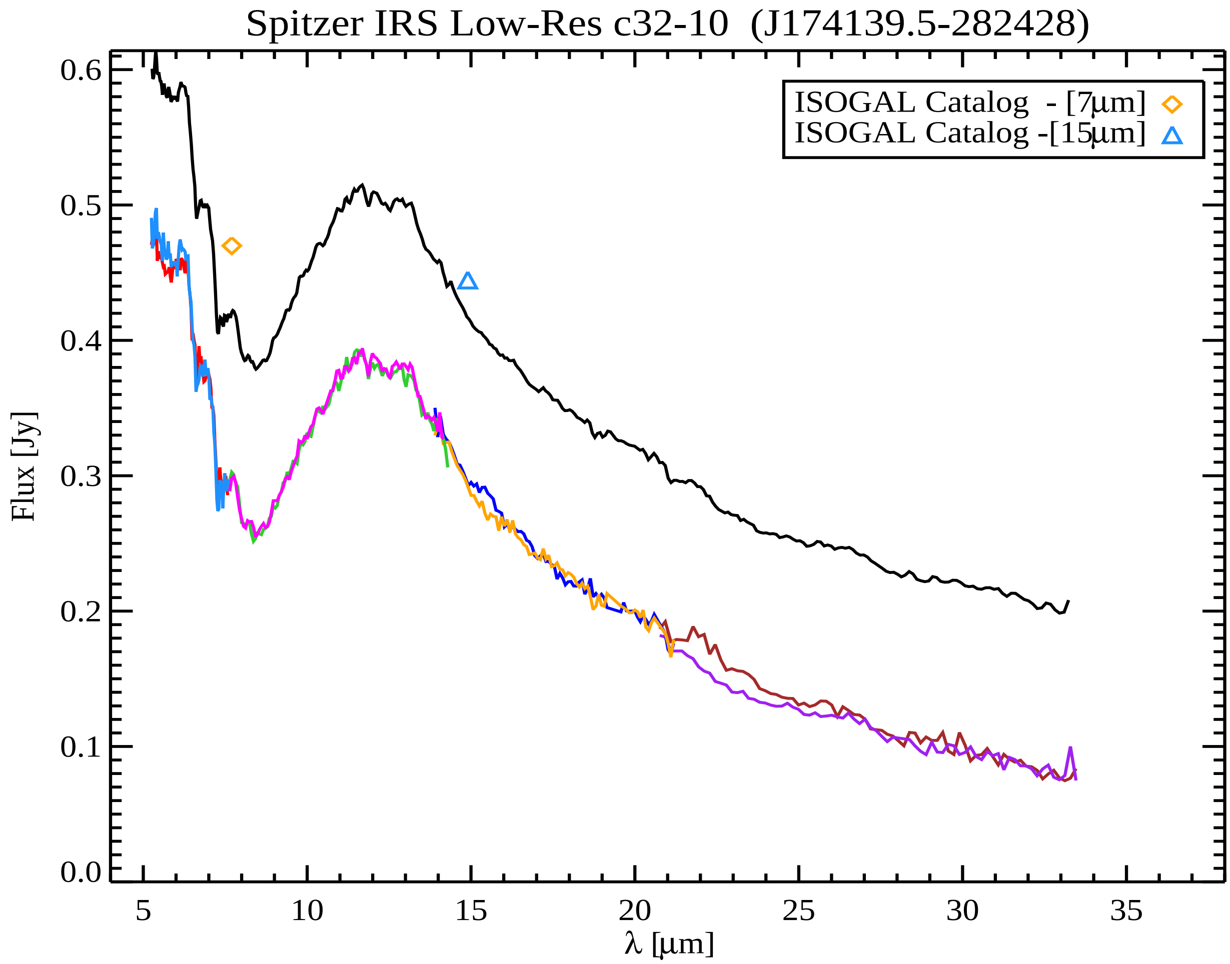

Figure 19. (c32-10) This is the final spectrum of c32-10. Figure 20 indicates the number of sources that have been extracted in each nod and module. There was a slight mismatch between the two nods of SL1 module which was removed by modifying the point spread function (central position and FWHM). After extraction the sharp and unrealistic residual features were masked (e.g. 19.5-μm). The background for this source is properly corrected through modeling. Finally, we scaled all modules with respect to the SL1 module using the following scale factors, in order to eliminate the mismatch between modules and obtain the continuum shown here.

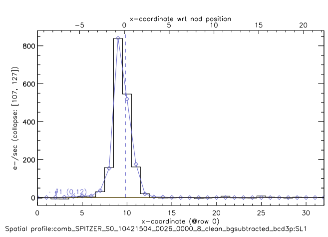
(a) SL1-first nod (scale: 1.0)

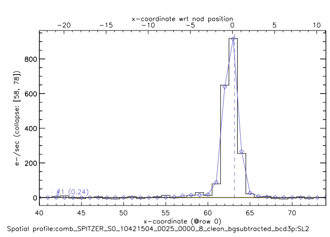
(b) SL2-second nod (scale: 0.90)

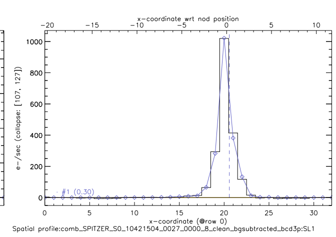
(c) SL1-second nod (scale: 1.0)

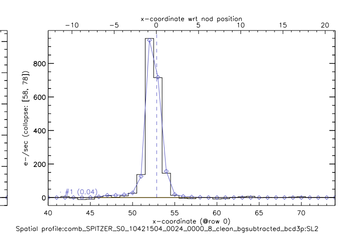
(d) SL2-first nod (scale: 0.90)

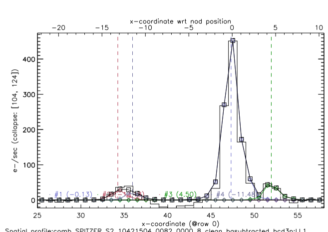
(e) LL1-first nod (scale: 0.78)

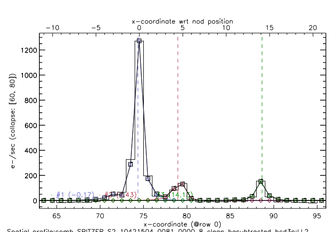
(f) LL2-second nod (scale: 0.80)

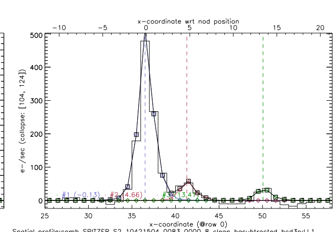
(g) LL1-second nod (scale: 0.78)

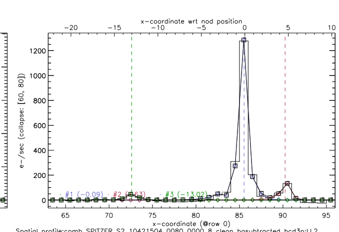
(h) LL2-first nod (scale: 0.80)

Figure 20. SL and LL modules spatial profiles after subtraction of the background

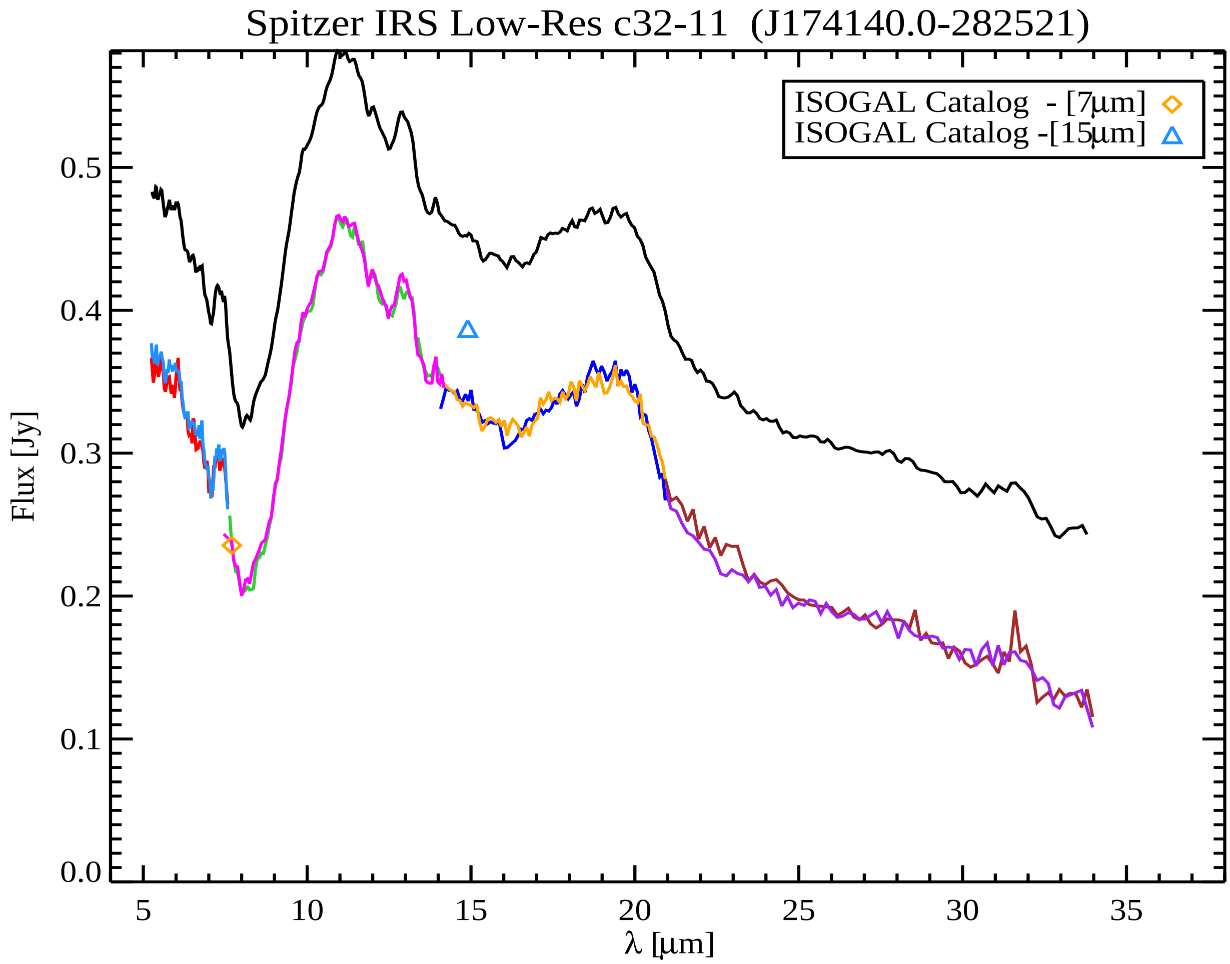

Figure 21. (c32-11) This is the final spectrum of c32-11. Figure 22 indicates the number of sources that have been extracted in each nod and module. There was a significant mismatch between the two nods of SL1 module which was corrected by modifying the point spread function (central position and FWHM). After extraction there were no significant residuals to mask. The background for all modules is properly corrected through modeling except SL1 module. For this module, we have assumed **a constant offset for the background (polynomial order zero)** and performed the subtraction using optimal extraction within SMART. Finally, we scaled all modules with respect to the SL1 module using the following scale factors, in order to eliminate the mismatch between modules and obtain the continuum shown here.

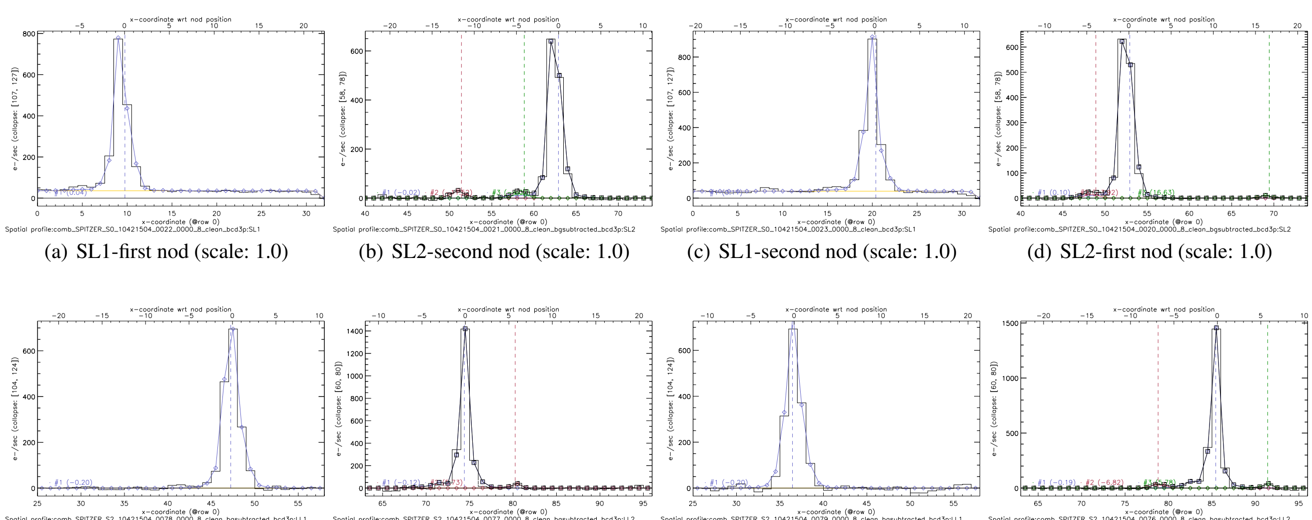

(a) SL1-first nod (scale: 1.0) (b) SL2-second nod (scale: 1.0) (c) SL1-second nod (scale: 1.0) (d) SL2-first nod (scale: 1.0)

(e) LL1-first nod (scale: 0.75) (f) LL2-second nod (scale: 0.80) (g) LL1-second nod (scale: 0.75) (h) LL2-first nod (scale: 0.80)

Figure 22. SL and LL modules spatial profiles after subtraction of the background

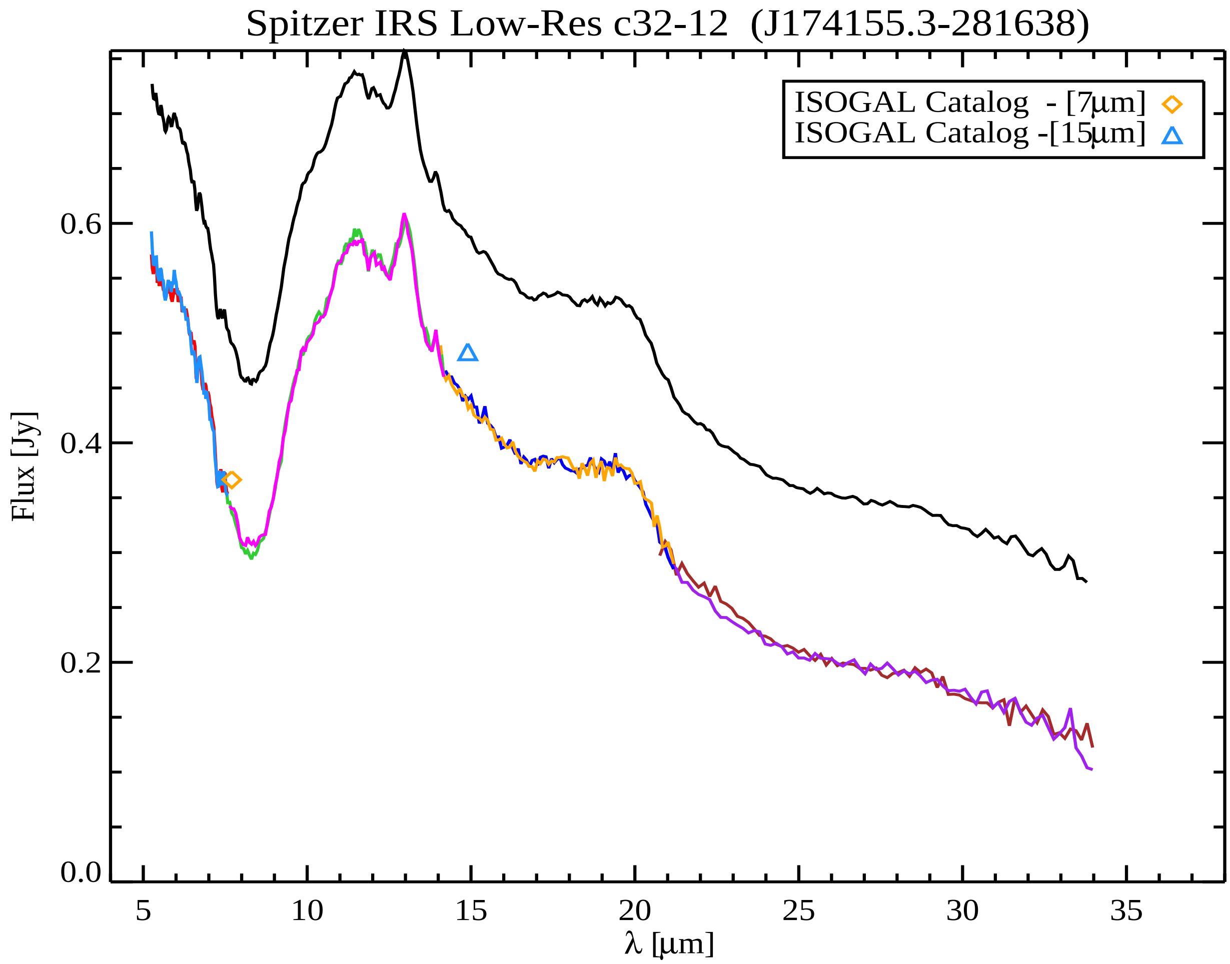

Figure 23. (c32-12) This is the final spectrum of c32-12. Figure 24 indicates the number of sources that have been extracted in each nod and module. There was a significant mismatch between the two nods of SL1 module which was removed by modifying the point spread function (central position and FWHM). After extraction there were no significant residuals to mask. The background is properly corrected through modeling. Finally, we scaled all modules with respect to the SL1 module using the following scale factors, in order to eliminate the mismatch between modules and obtain the continuum shown here.

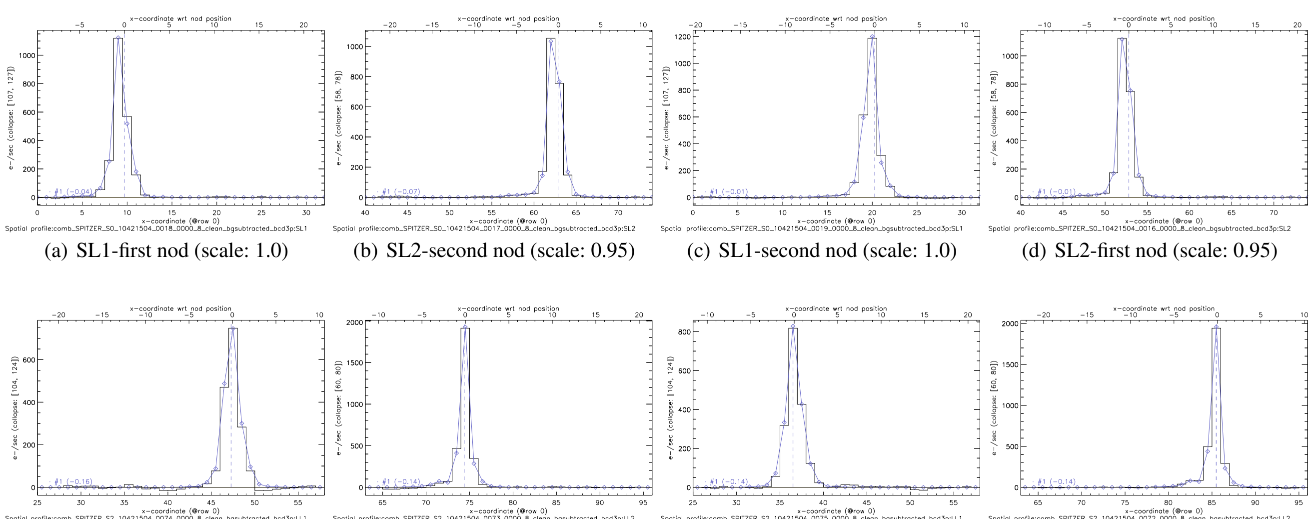

(a) SL1-first nod (scale: 1.0)
(b) SL2-second nod (scale: 0.95)
(c) SL1-second nod (scale: 1.0)
(d) SL2-first nod (scale: 0.95)
(e) LL1-first nod (scale: 0.75)
(f) LL2-second nod (scale: 0.78)
(g) LL1-second nod (scale: 0.75)
(h) LL2-first nod (scale: 0.78)

Figure 24. SL and LL modules spatial profiles after subtraction of the background

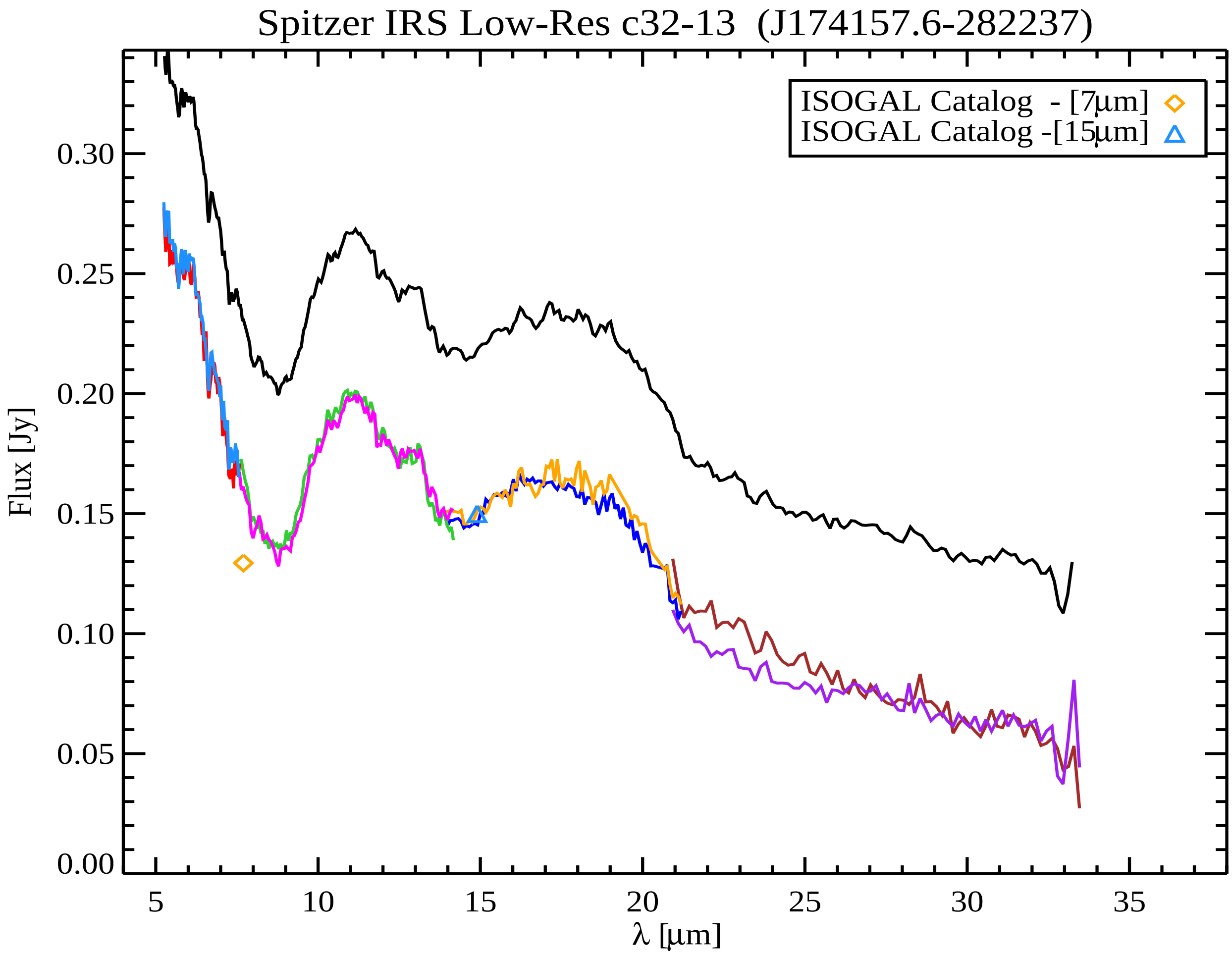

Figure 25. (c32-13) This is final spectrum of c32-13. Figure 26 indicates the number of sources that have been extracted in each nod and module. There was an extreme mismatch between the two nods of SL1 module which was corrected by modifying the point spread function (central position and FWHM). After extraction the residual features were masked properly (e.g. 19-μm). The background for all modules was properly corrected through modeling except LL2 module. For this module, we have assumed **a constant offset for the background (polynomial order zero)** and performed the subtraction using optimal extraction within SMART. Finally, we scaled all modules with respect to the SL1 module using the following scale factors, in order to eliminate the mismatch between modules and obtain the continuum shown here.

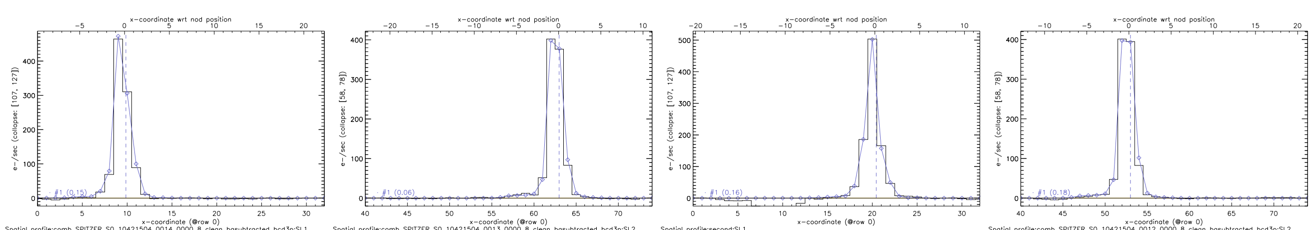

(a) SL1-first nod (scale: 1.0) (b) SL2-second nod (scale: 1.0) (c) SL1-second nod (scale: 1.0) (d) SL2-first nod (scale: 1.0)

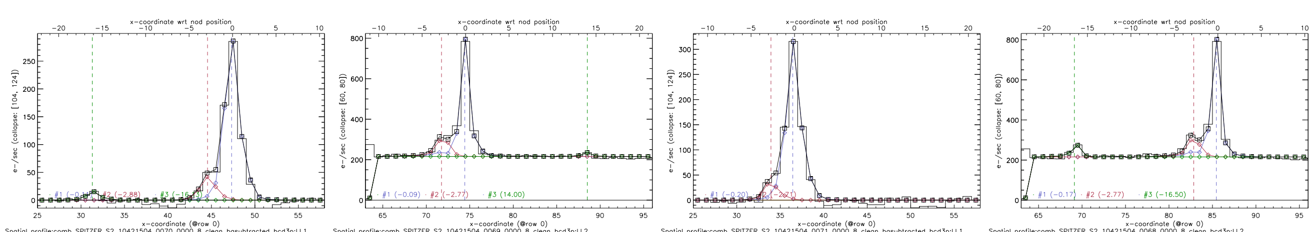

(e) LL1-first nod (scale: 0.78) (f) LL2-second nod (scale: 0.88) (g) LL1-second nod (scale: 0.78) (h) LL2-first nod (scale: 0.88)

Figure 26. SL and LL modules spatial profiles after subtraction of the background

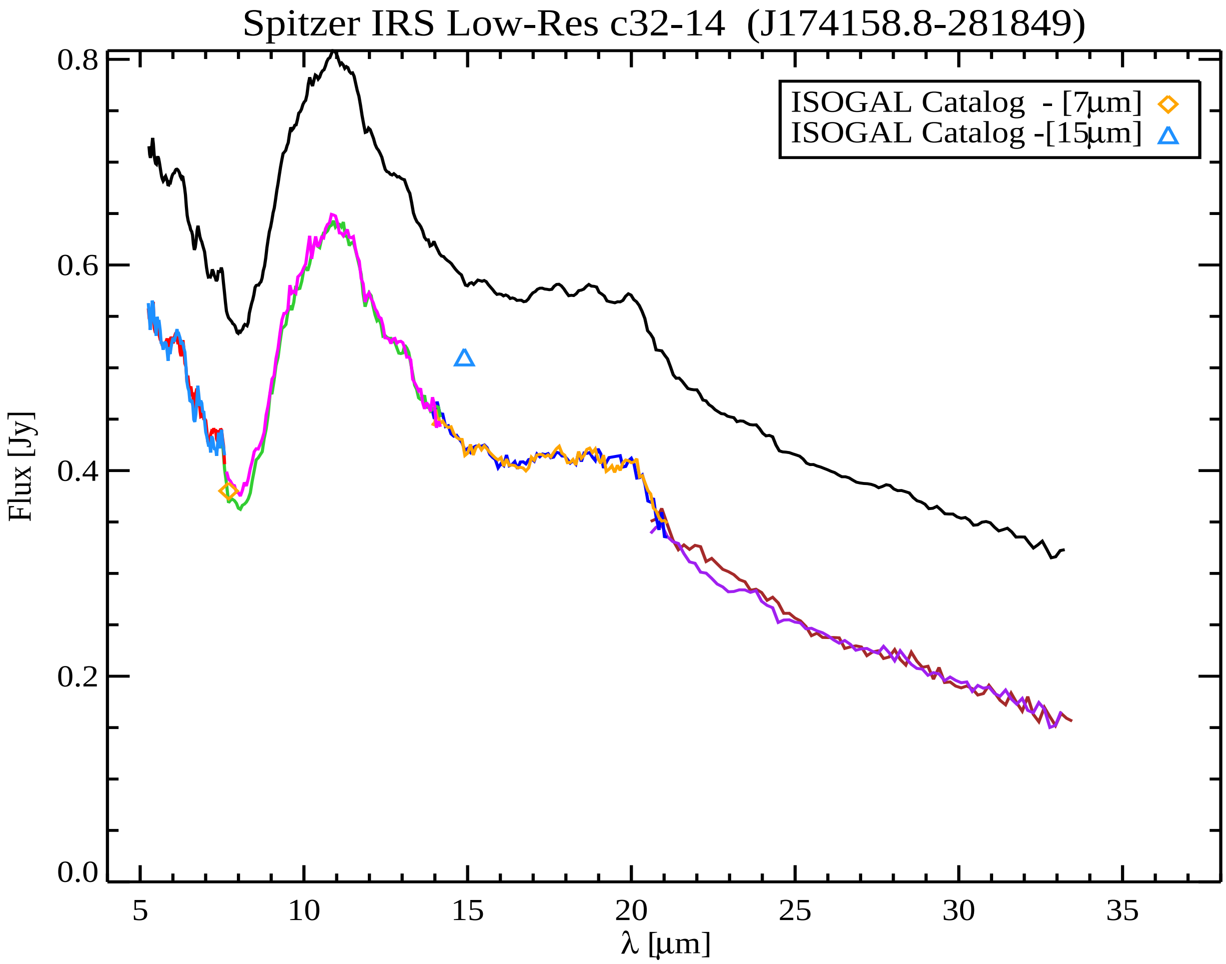

Figure 27. (c32-14) This is the final spectrum of c32-14. Figure 28 indicates the number of sources that have been extracted in each nod and module. There was an extreme mismatch between the two nods of SL1 module which was removed by modifying the point spread function (central position and FWHM). After extraction a few residual features were masked (e.g. 19.5-μm).The background for this source was properly corrected through modeling. Finally, we scaled long low modules with respect to the short low modules using the following scale factors, in order to eliminate the mismatch between modules and obtain the continuum shown here.

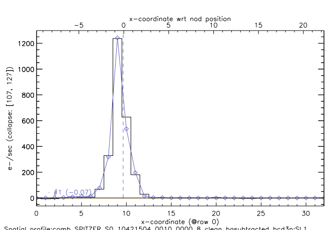
(a) SL1-first nod (scale: 1.0)

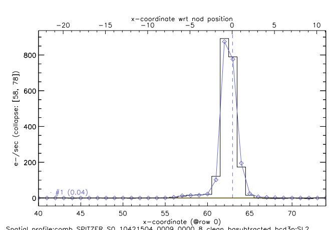
(b) SL2-second nod (scale: 1.0)

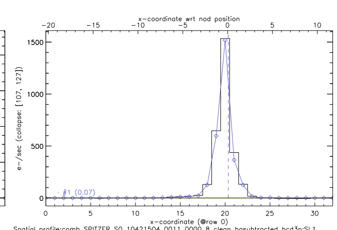
(c) SL1-second nod (scale: 1.0)

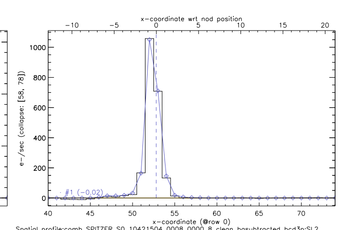
(d) SL2-first nod (scale: 1.0)

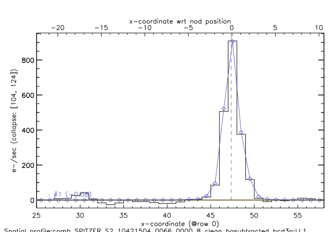
(e) LL1-first nod (scale: 0.75)

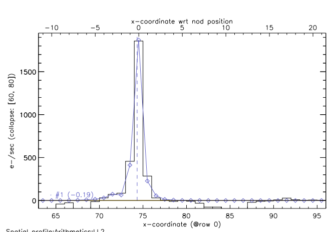
(f) LL2-second nod (scale: 0.80)

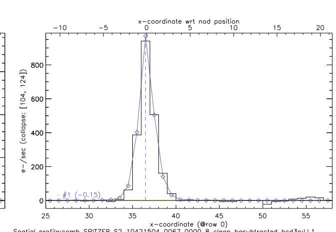
(g) LL1-second nod (scale: 0.75)

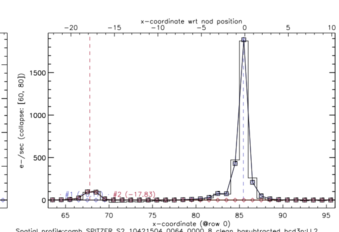
(h) LL2-first nod (scale: 0.80)

Figure 28. SL and LL modules spatial profiles after subtraction of the background

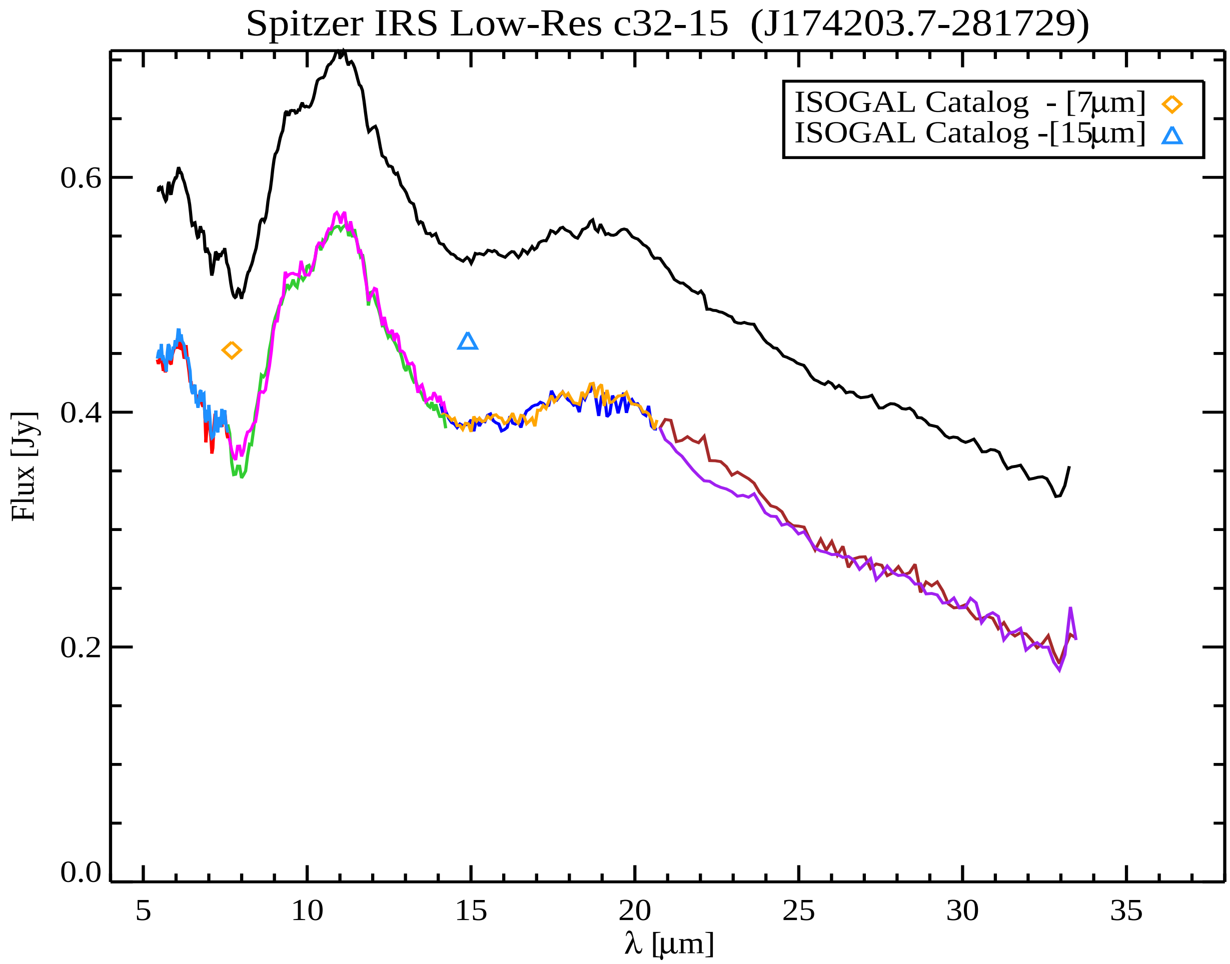

Figure 29. (c32-15) This is the final spectrum of c32-15. Figure 30 indicates the number of sources that have been extracted in each nod and module. There was a significant mismatch between the two nods of SL1 module which was removed by modifying the point spread function (central position and FWHM). After extraction the sharp and unrealistic residual features were masked (e.g. 19.5-μm). The background for this source was properly corrected through modeling. Finally, we scaled long low modules with respect to the short low modules using the following scale factors, in order to eliminate the mismatch between modules and obtain the continuum shown here.

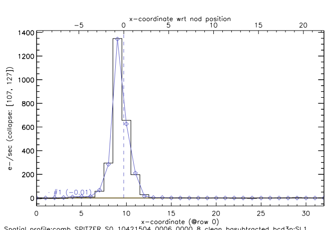
(a) SL1-first nod (scale: 1.0)

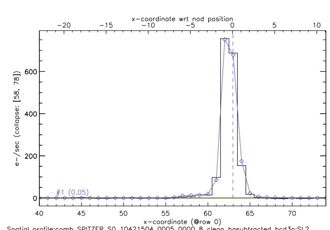
(b) SL2-second nod (scale: 1.0)

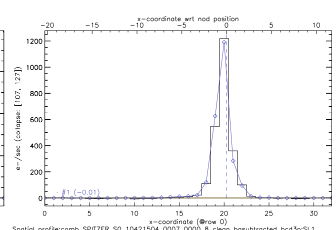
(c) SL1-second nod (scale: 1.0)

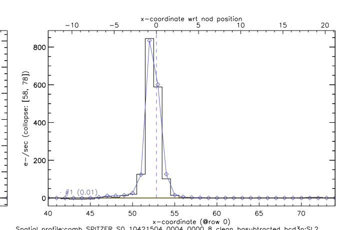
(d) SL2-first nod (scale: 1.0)

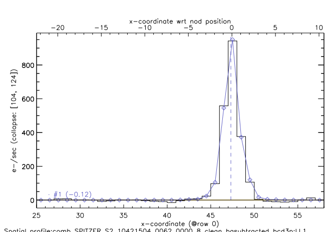
(e) LL1-first nod (scale: 0.84)

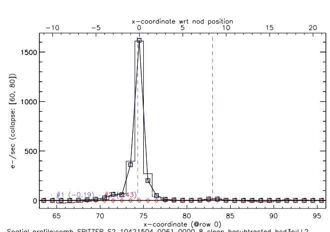
(f) LL2-second nod (scale: 0.84)

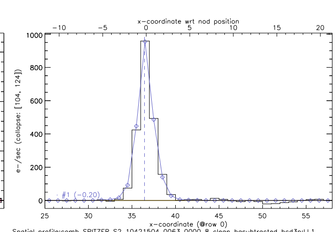
(g) LL1-second nod (scale: 0.84)

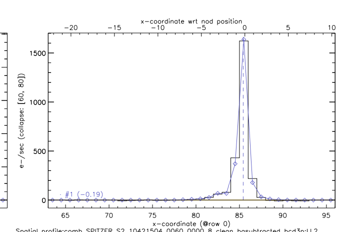
(h) LL2-first nod (scale: 0.84)

Figure 30. SL and LL modules spatial profiles after subtraction of the background

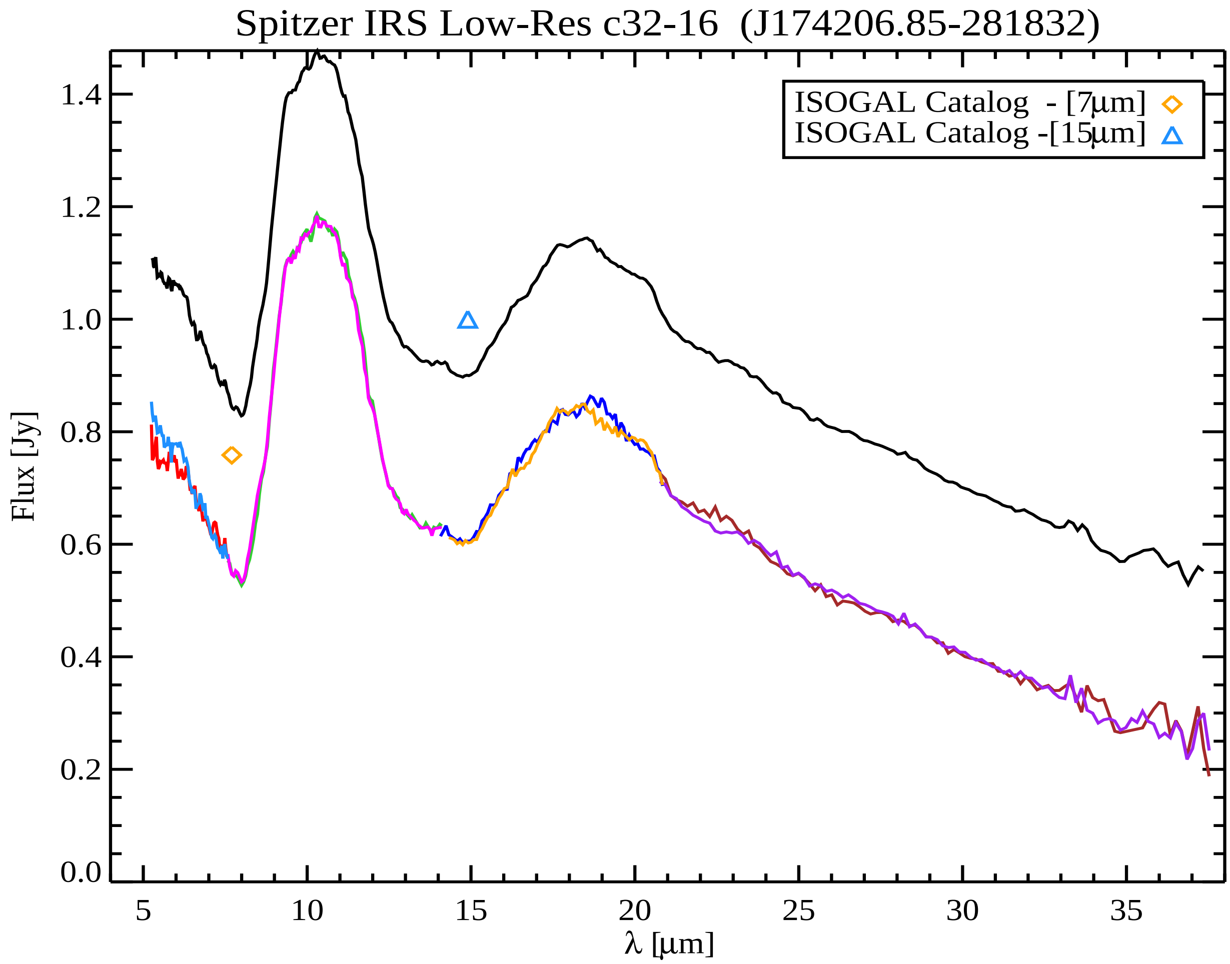

Figure 31. (c32-16) This is the final spectrum of c32-16. Figure 32 indicates the number of sources that have been extracted in each nod and module. There was a slight mismatch between the two nods of SL1 and SL2 modules which were removed by modifying the point spread function (central position and FWHM). After extraction there was no significant residual left to mask. The background for this source is properly corrected through modeling. Finally,we scaled all modules with respect to the SL1 module using the following scale factors, in order to eliminate the mismatch between modules and obtain the continuum shown here.

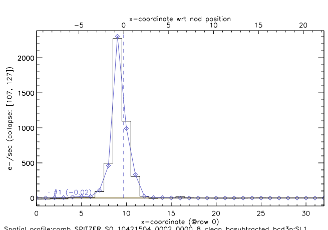

(a) SL1-first nod (scale: 1.0)

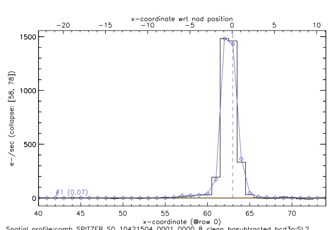

(b) SL2-second nod (scale: 0.85)

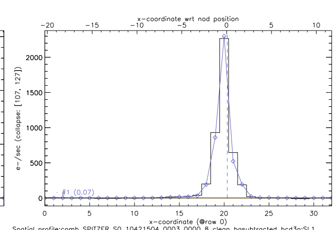

(c) SL1-second nod (scale: 1.0)

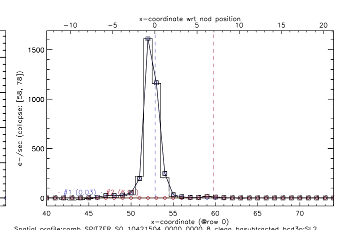

(d) SL2-first nod (scale: 0.85)

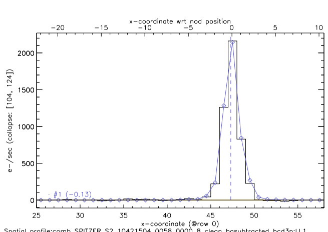

(e) LL1-first nod (scale: 0.68)

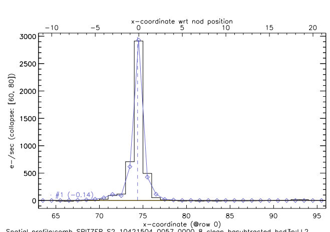

(f) LL2-second nod (scale: 0.72)

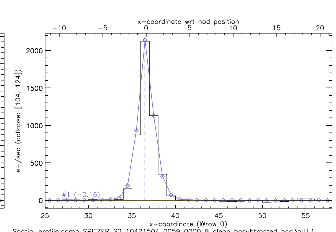

(g) LL1-second nod (scale: 0.68)

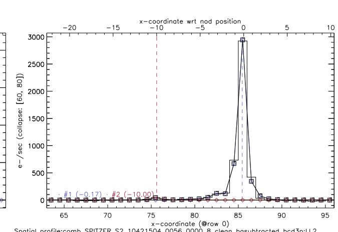

(h) LL2-first nod (scale: 0.72)

Figure 32. SL and LL modules spatial profiles after subtraction of the background

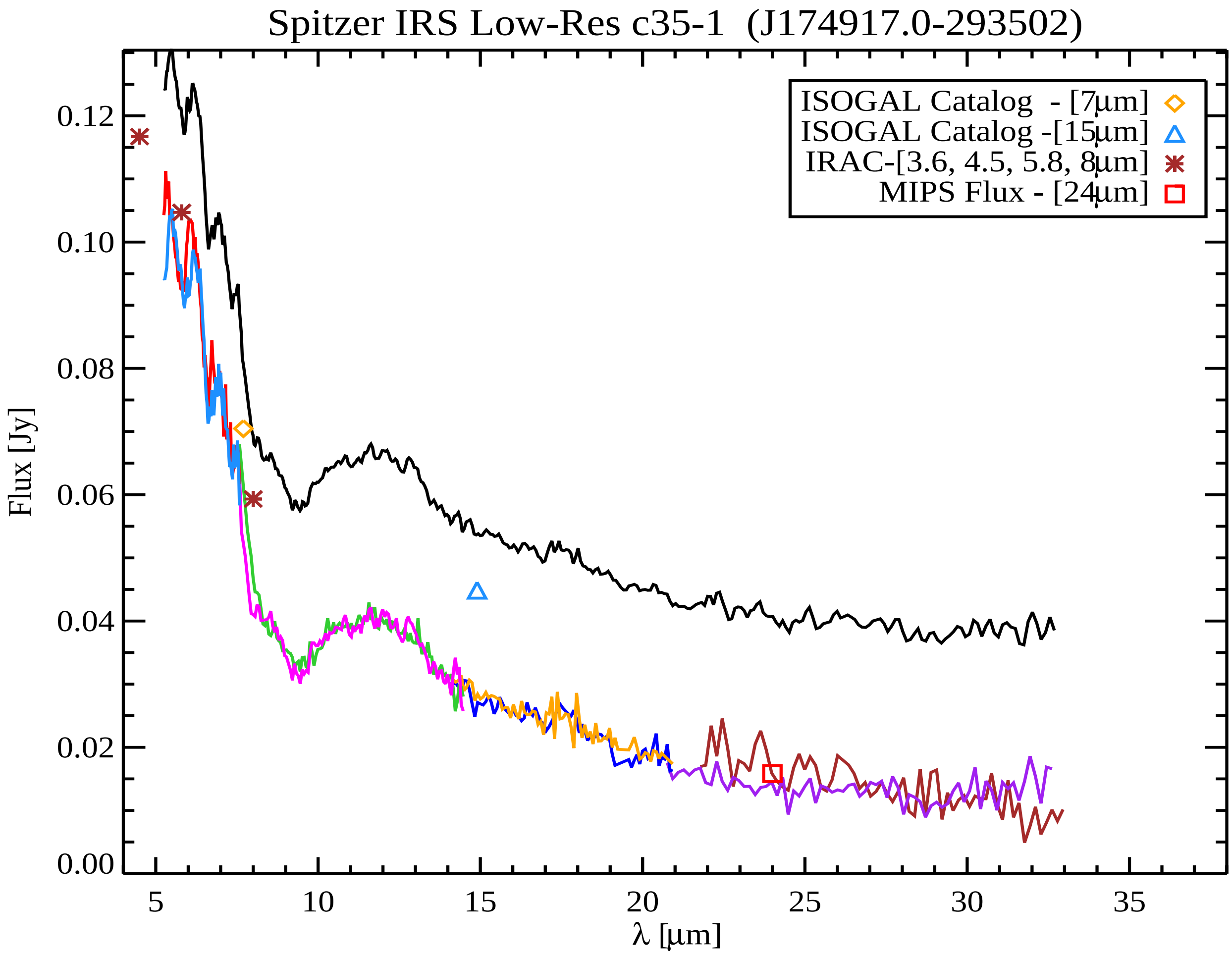

Figure 33. (c35-1) This is the final spectrum of c35-1. Figure 34 indicates the number of sources that have been extracted in each nod and module. After extraction the sharp and unrealistic residual features were masked (e.g. 19.5-μm). The strong and variable background with prominent PAH feature was properly modeled and corrected. Finally, we scaled long low modules with respect to the short low modules using the following scale factors, in order to eliminate the mismatch between them and obtain the continuum shown here.

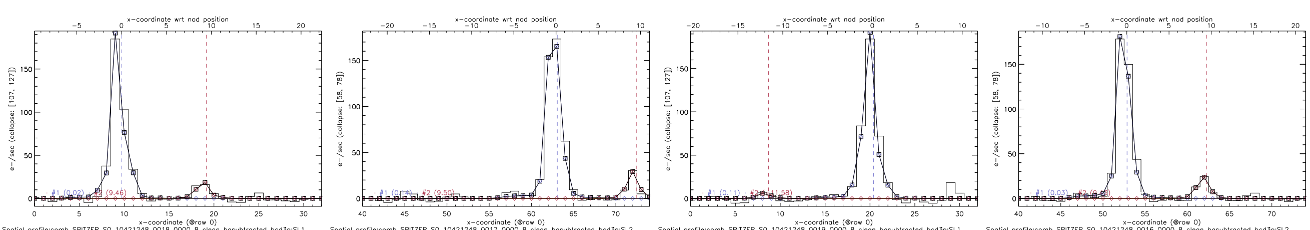

(a) SL1-first nod (scale: 1.0) (b) SL2-second nod (scale: 1.0) (c) SL1-second nod (scale: 1.0) (d) SL2-first nod (scale: 1.0)

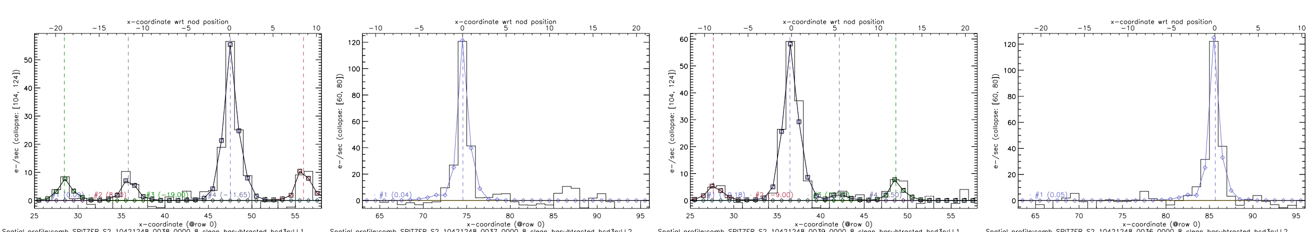

(e) LL1-first nod (scale: 0.70) (f) LL2-second nod (scale: 0.70) (g) LL1-second nod (scale: 0.70) (h) LL2-first nod (scale: 0.70)

Figure 34. SL and LL modules spatial profiles after subtraction of the background

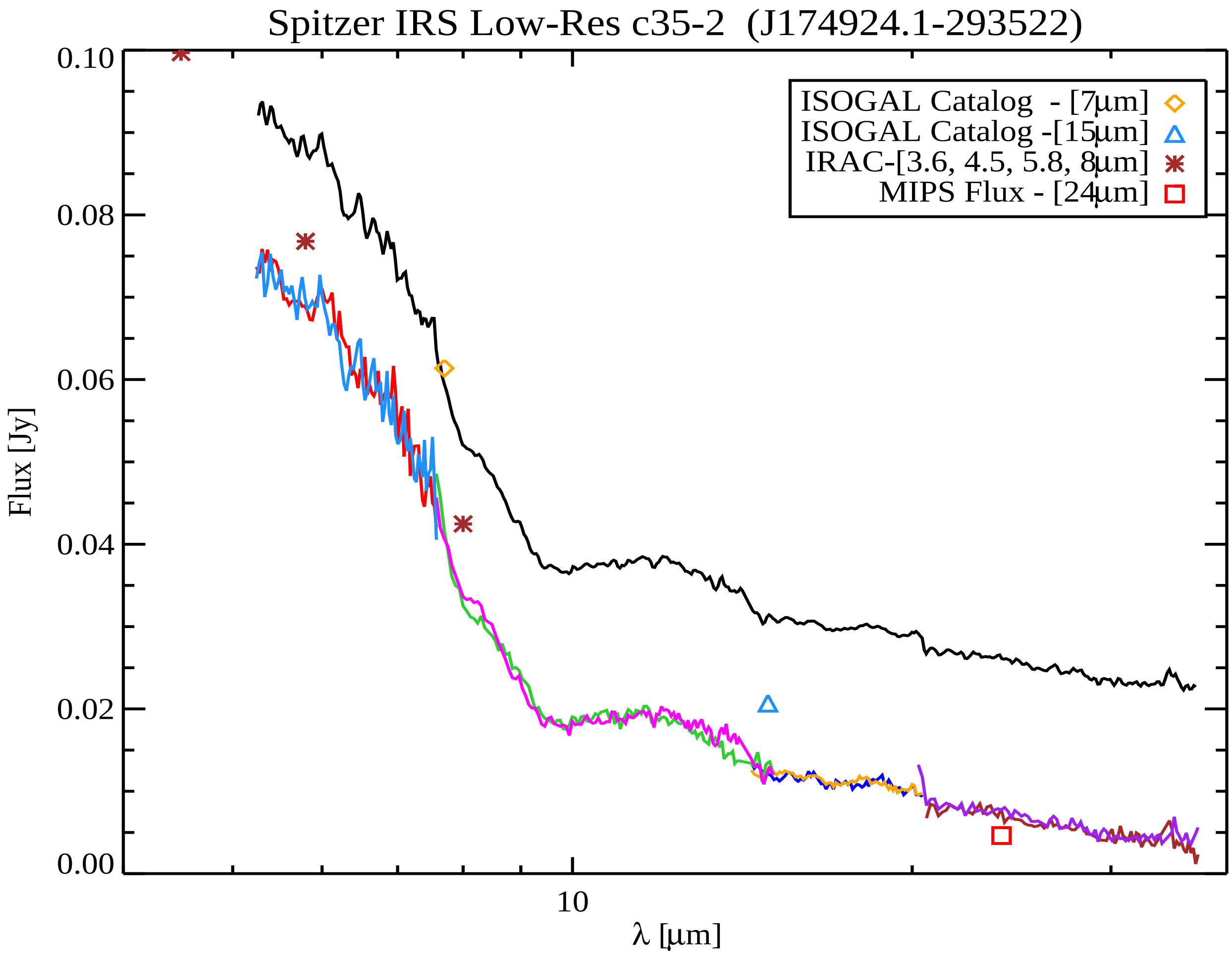

Figure 35. (c35-2) This is the final spectrum of c35-2. Figure 36 indicates the number of sources that have been extracted in each nod and module. After extraction the sharp and unrealistic residual features were masked (e.g. 19.5-μm). The strong and variable background with prominent PAH feature was properly modeled and corrected. Finally, we scaled long low modules with respect to the short low modules using the following scale factors, in order to eliminate the mismatch between them and obtain the continuum shown here.

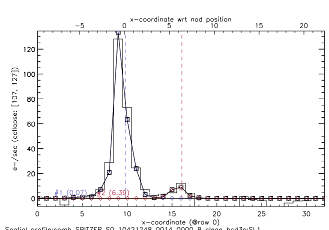

(a) SL1-first nod (scale: 1.1)

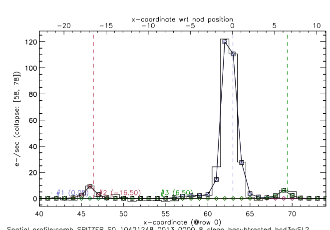

(b) SL2-second nod (scale: 1.0)

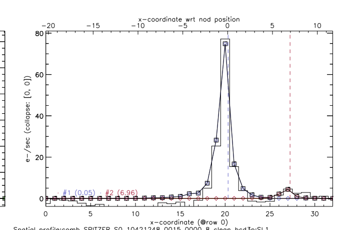

(c) SL1-second nod (scale: 1.1)

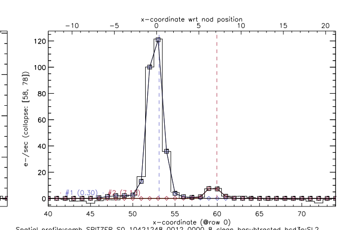

(d) SL2-first nod (scale: 1.0)

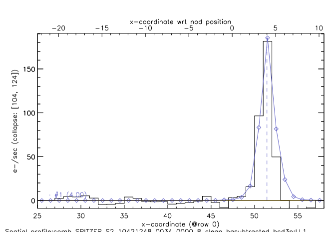

(e) LL1-first nod (scale: 0.13)

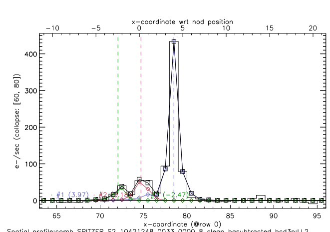

(f) LL2-second nod (scale: 0.11)

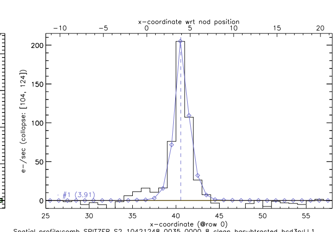

(g) LL1-second nod (scale: 0.13)

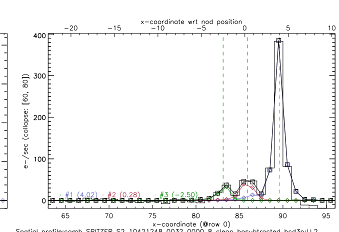

(h) LL2-first nod (scale: 0.11)

Figure 36. SL and LL modules spatial profiles after subtraction of the background

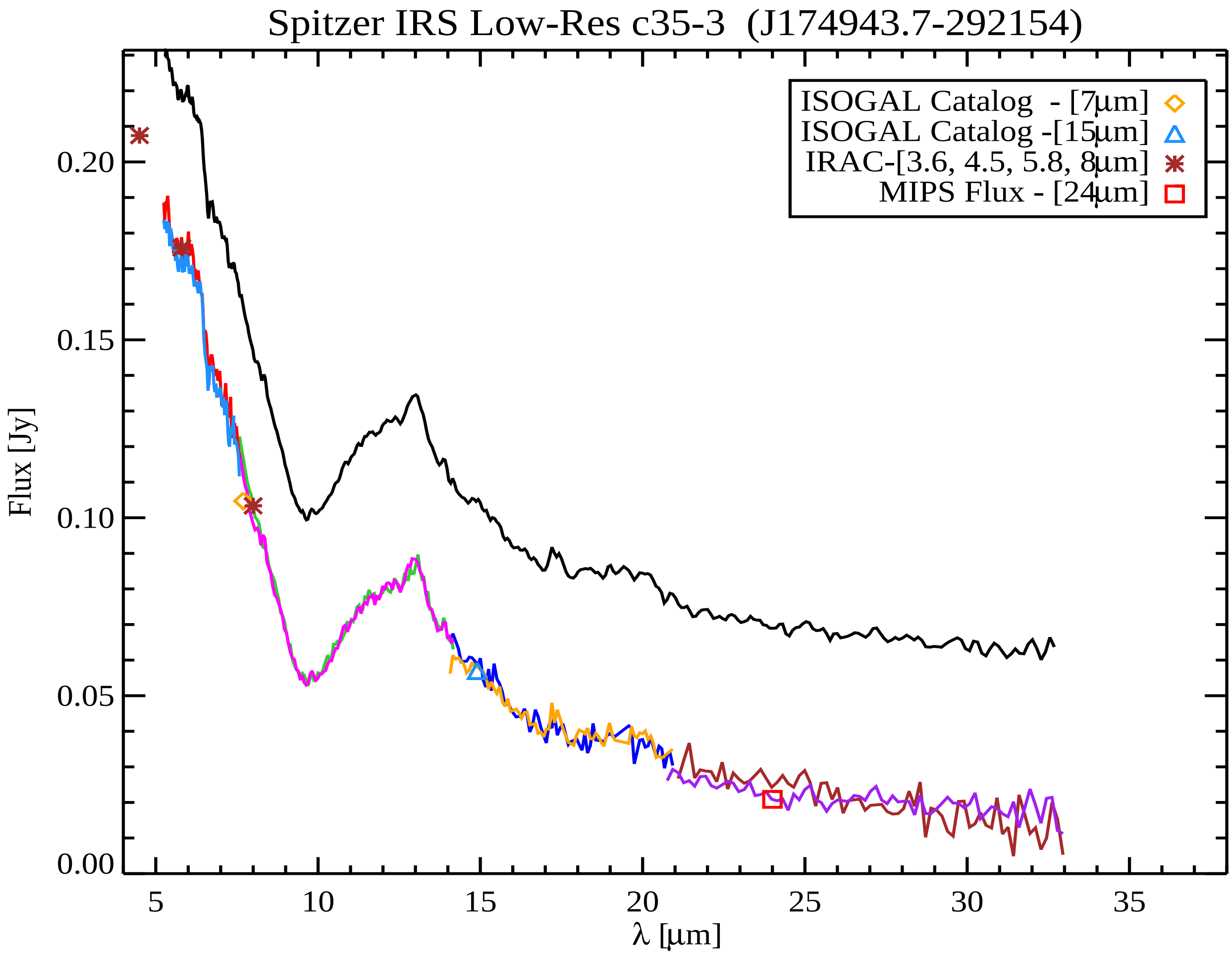

Figure 37. (c35-3) This is the final spectrum of c35-3. Figure 38 indicates the number of sources that have been extracted in each nod and module. After extraction the residual features were masked (e.g. 19.5-μm). The strong and variable background with prominent PAH feature was properly modeled and corrected. Finally, we scaled long low modules with respect to the short low modules using the following scale factors, in order to eliminate the mismatch between modules and obtain the continuum shown here.

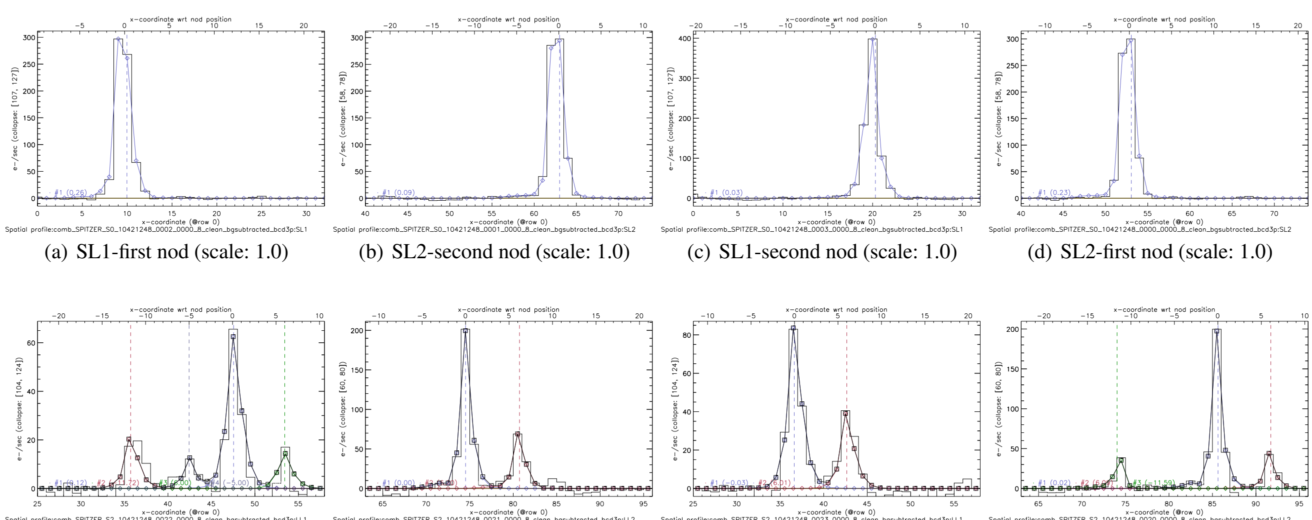

(a) SL1-first nod (scale: 1.0) (b) SL2-second nod (scale: 1.0) (c) SL1-second nod (scale: 1.0) (d) SL2-first nod (scale: 1.0)

(e) LL1-first nod (scale: 0.90) (f) LL2-second nod (scale: 0.90) (g) LL1-second nod (scale: 0.90) (h) LL2-first nod (scale: 0.90)

Figure 38. SL and LL modules spatial profiles after subtraction of the background

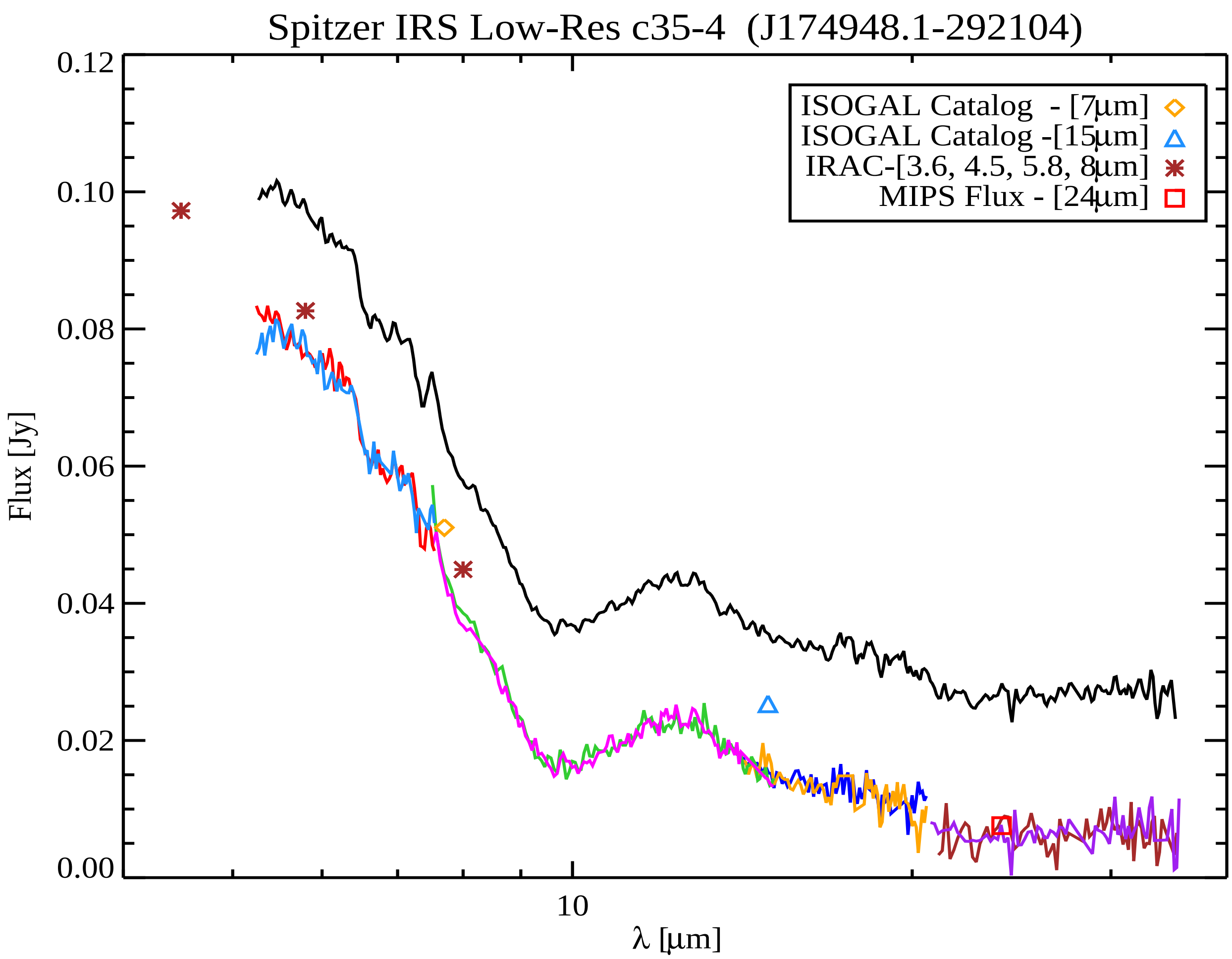

Figure 39. (c35-4) This is the final spectrum of c35-4. Figure 40 indicates the number of sources that have been extracted in each nod and module. There was a slight mismatch between the two nods of LL2 module which was removed by modifying the point spread function (central position and FWHM). After extraction the residual features were masked (e.g. 19.5-μm). The strong and variable background with prominent PAH feature was properly modeled and corrected. Finally, we scaled long low modules with respect to the short low modules using the following scale factors, in order to eliminate the mismatch between modules and obtain the continuum shown here.

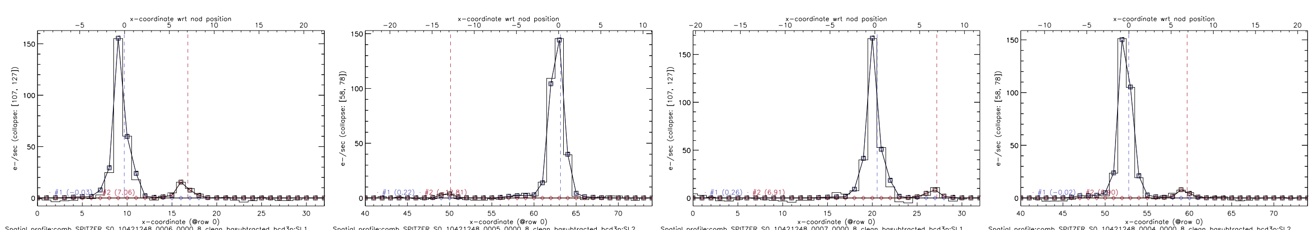

(a) SL1-first nod (scale: 1.0) (b) SL2-second nod (scale: 1.0) (c) SL1-second nod (scale: 1.0) (d) SL2-first nod (scale: 1.0)

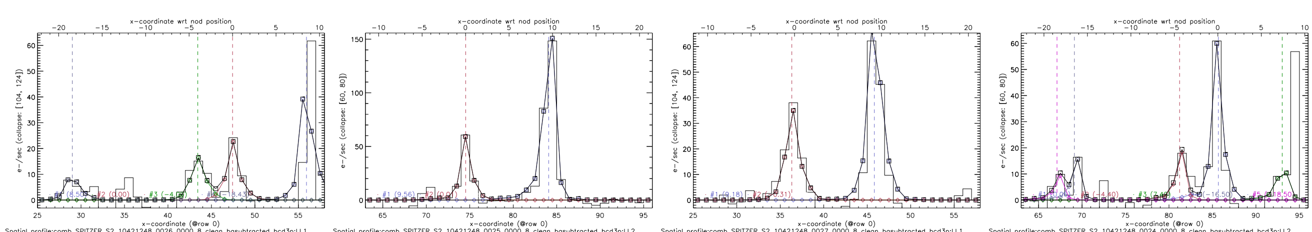

(e) LL1-first nod (scale: 0.80) (f) LL2-second nod (scale: 0.80) (g) LL1-second nod (scale: 0.80) (h) LL2-first nod (scale: 0.80)

Figure 40. SL and LL modules spatial profiles after subtraction of the background

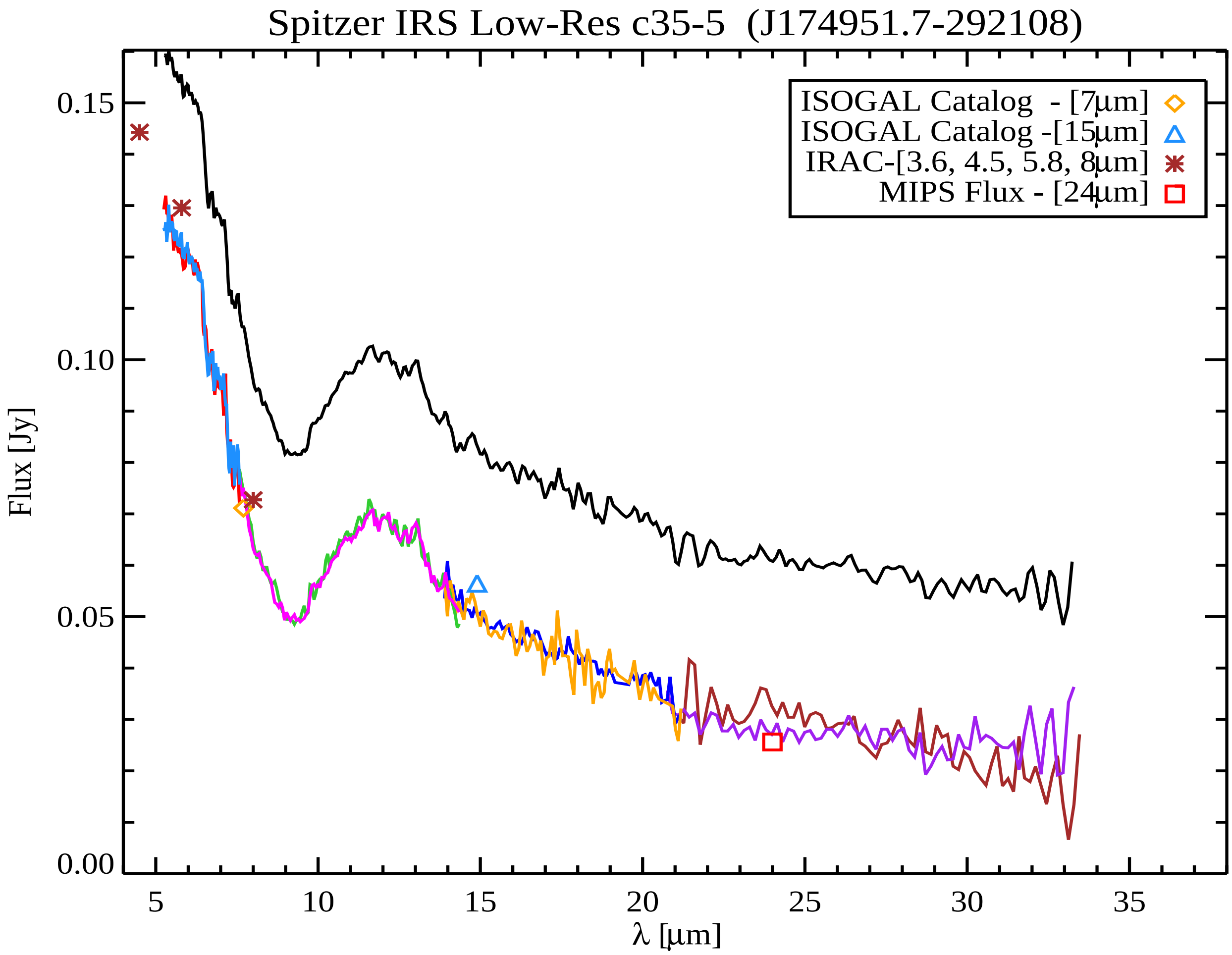

Figure 41. (c35-5) This is the final spectrum of c35-5. Figure 42 indicates the number of sources that have been extracted in each nod and module. After extraction, sharp residual features were masked (e.g. 19.5-μm). The strong and variable background with prominent PAH feature was properly modeled and corrected. Finally, we scaled long low modules with respect to the short low modules using the following scale factors, in order to eliminate the mismatch between modules and obtain the continuum shown here.

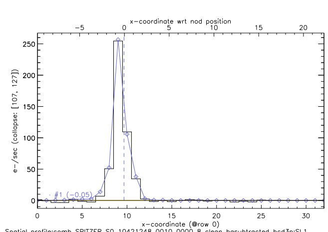
(a) SL1-first nod (scale: 1.0)

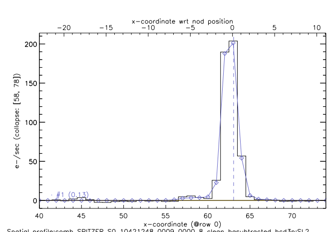
(b) SL2-second nod (scale: 1.0)

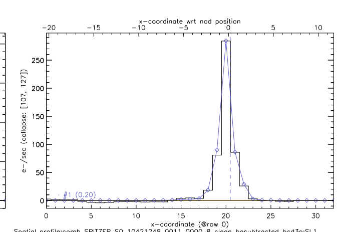
(c) SL1-second nod (scale: 1.0)

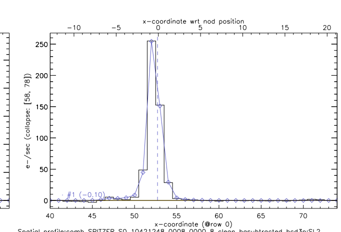
(d) SL2-first nod (scale: 1.0)

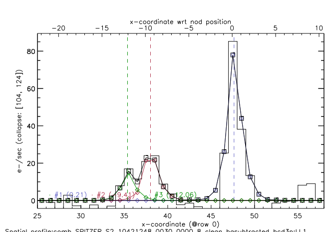
(e) LL1-first nod (scale: 0.88)

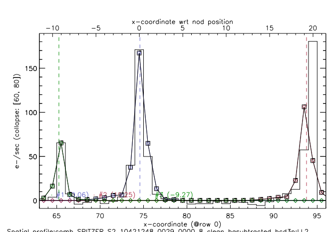
(f) LL2-second nod (scale: 0.88)

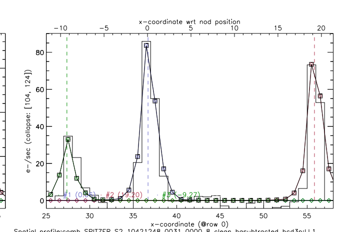
(g) LL1-second nod (scale: 0.88)

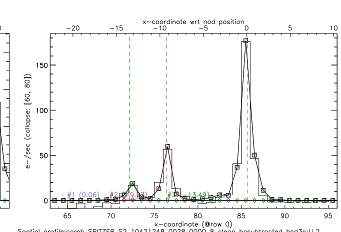
(h) LL2-first nod (scale: 0.88)

Figure 42. SL and LL modules spatial profiles after subtraction of the background

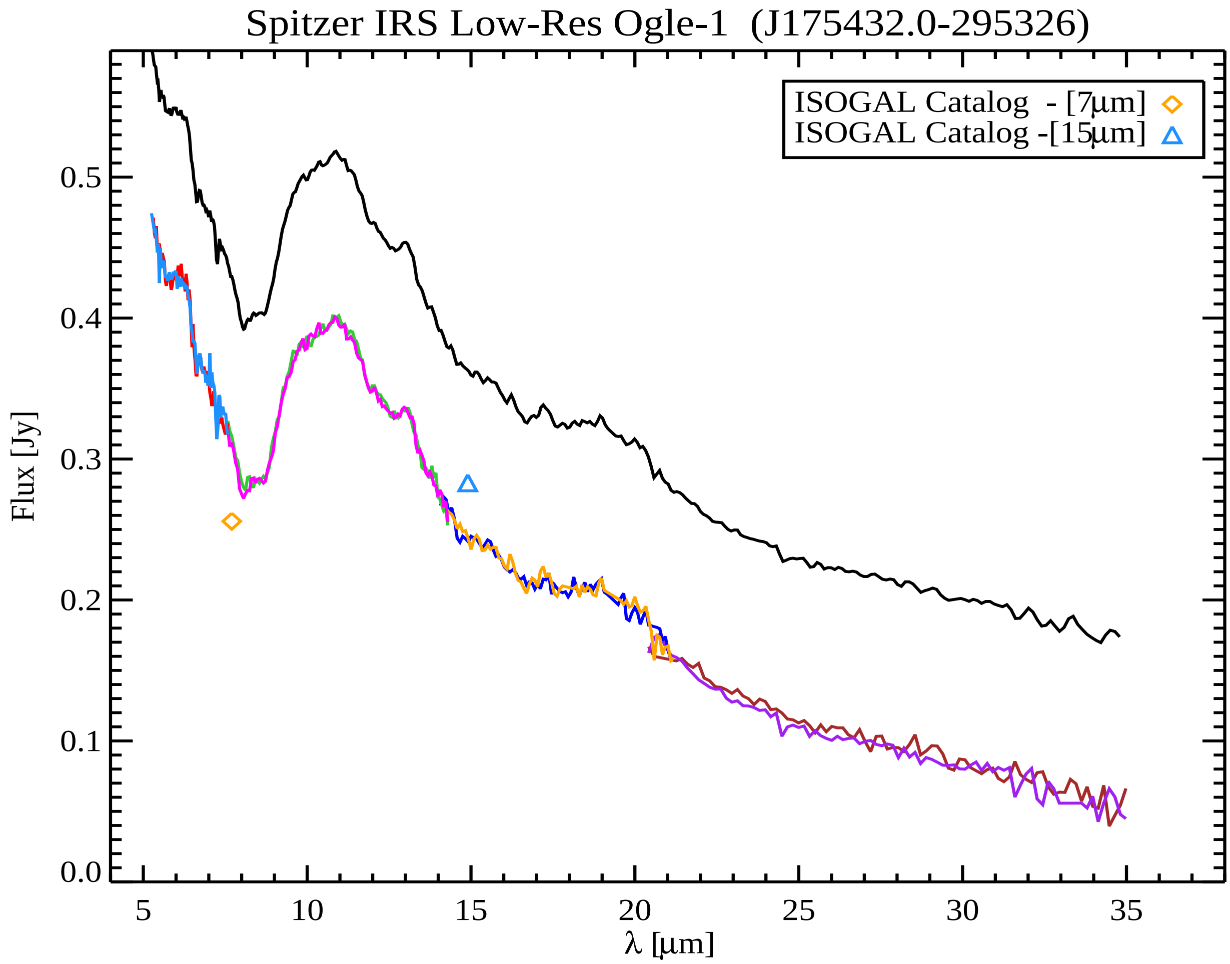

Figure 43. (Ogle-1) This is the final spectrum of Ogle-1. Figure 44 indicates the number of sources that have been extracted in each nod and module. After extraction the sharp and unrealistic residual features were masked (e.g. 19.5-μm). The strong and variable background for this source was properly corrected through modeling. Finally, we scaled long low modules with respect to the short low modules using the following scale factors, in order to eliminate the mismatch between modules and obtain the continuum shown here.

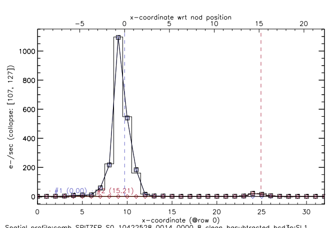
(a) SL1-first nod (scale: 1.0)

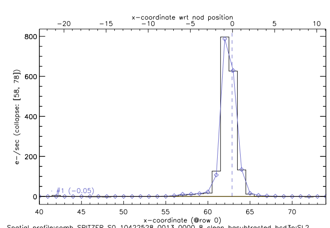
(b) SL2-second nod (scale: 1.0)

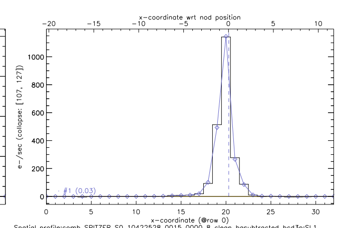
(c) SL1-second nod (scale: 1.0)

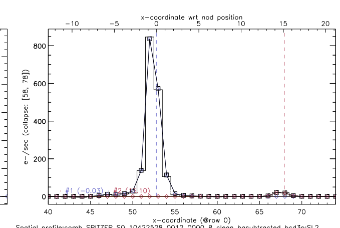
(d) SL2-first nod (scale: 1.0)

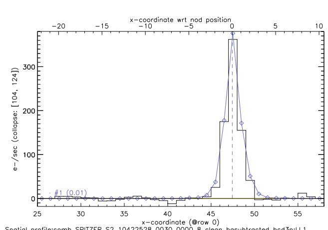
(e) LL1-first nod (scale: 0.89)

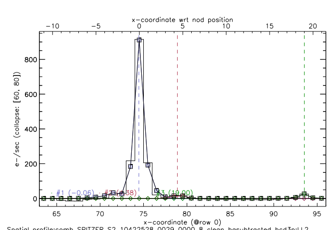
(f) LL2-second nod (scale: 0.89)

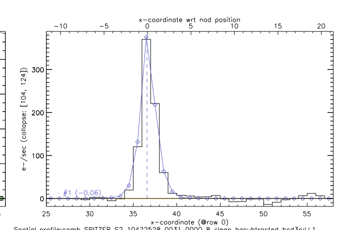
(g) LL1-second nod (scale: 0.89)

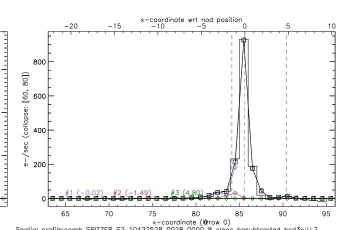
(h) LL2-first nod (scale: 0.89)

Figure 44. SL and LL modules spatial profiles after subtraction of the background

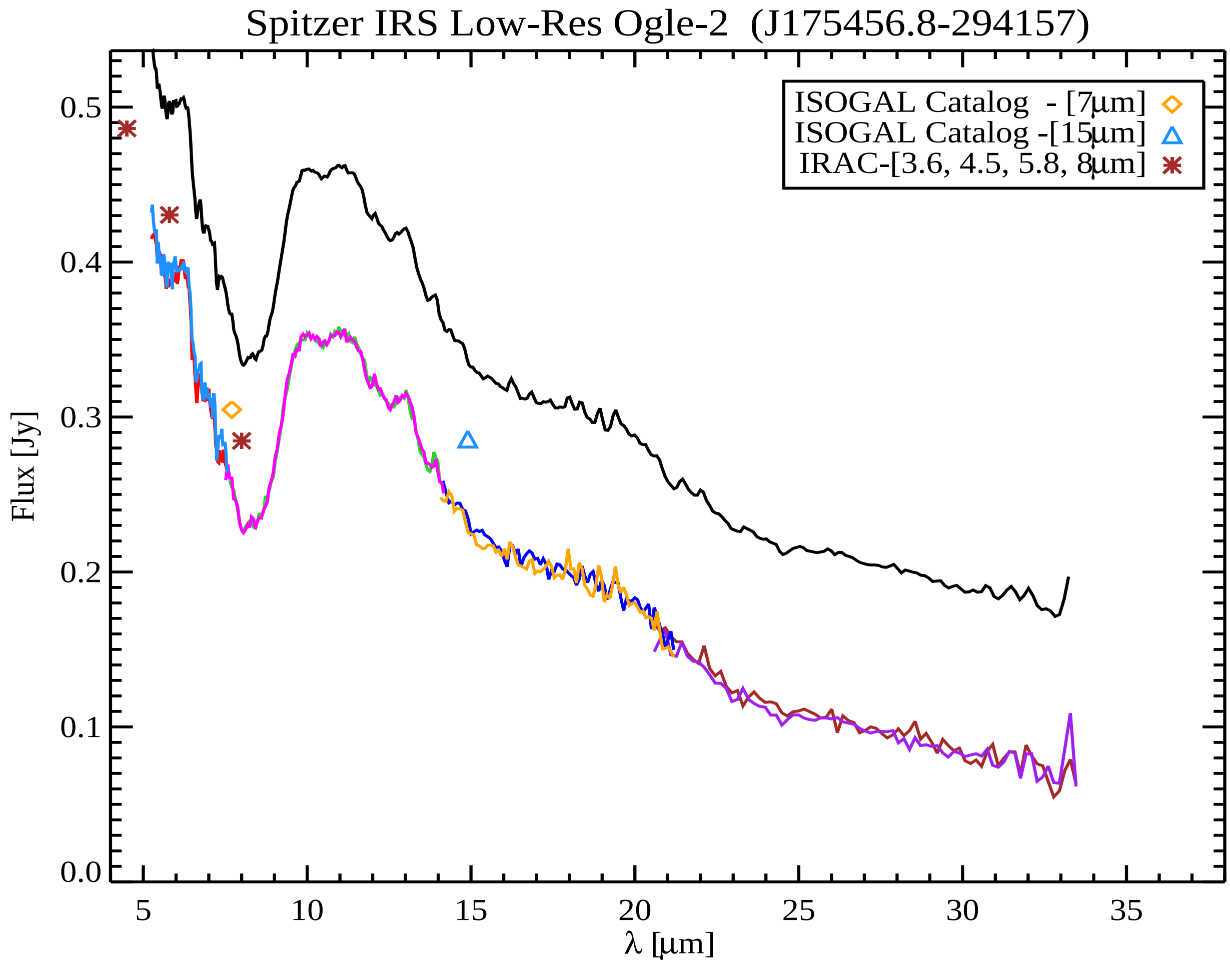

Figure 45. (Ogle-2) This is the final spectrum of Ogle-2. Figure 46 indicates the number of sources that have been extracted in each nod and module. After extraction the residual features were masked (e.g. 19.5-μm). The strong and variable background for this source was properly corrected through modeling. Finally, we scaled long low modules with respect to the short low modules using the following scale factors, in order to eliminate the mismatch between modules and obtain the continuum shown here.

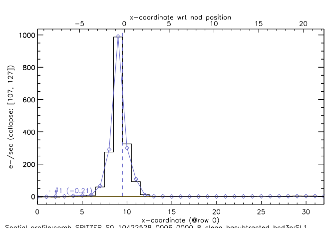
(a) SL1-first nod (scale: 1.0)

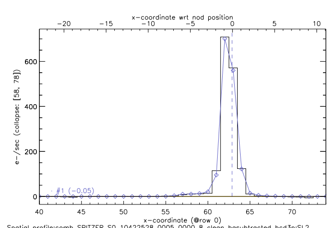
(b) SL2-second nod (scale: 1.0)

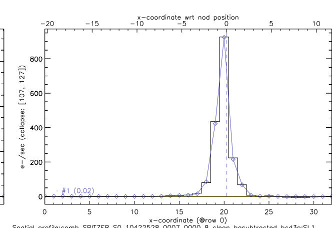
(c) SL1-second nod (scale: 1.0)

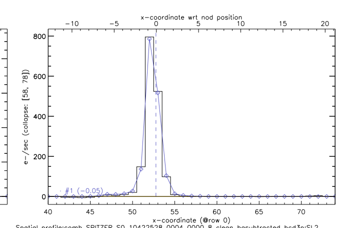
(d) SL2-first nod (scale: 1.0)

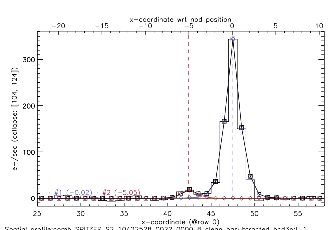
(e) LL1-first nod (scale: 0.90)

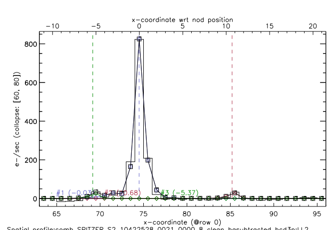
(f) LL2-second nod (scale: 0.90)

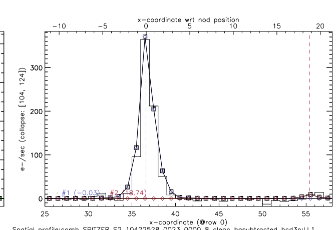
(g) LL1-second nod (scale: 0.90)

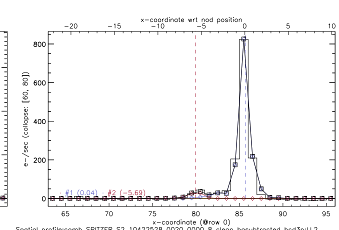
(h) LL2-first nod (scale: 0.90)

Figure 46. SL and LL modules spatial profiles after subtraction of the background

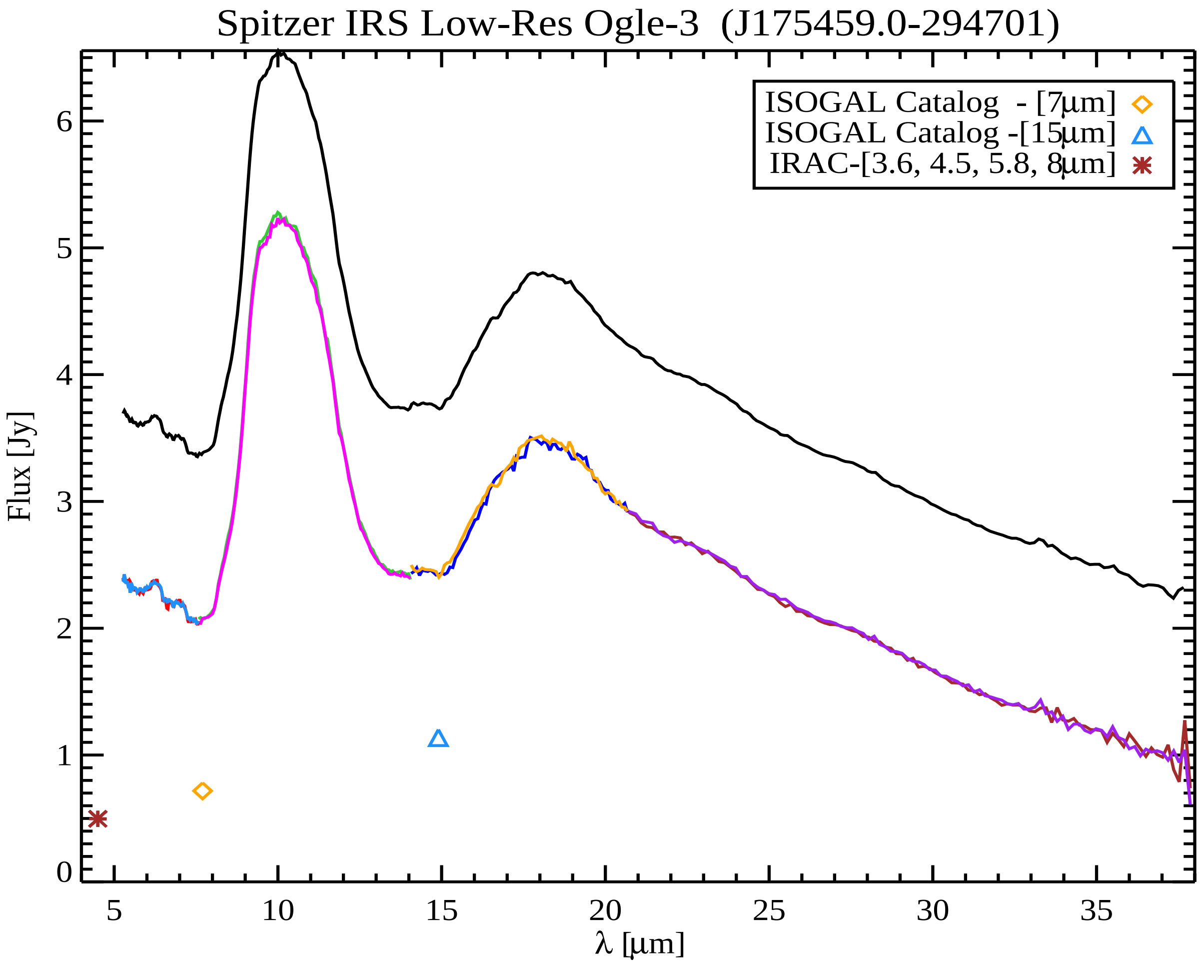

Figure 47. (Ogle-3) This is the final spectrum of Ogle-3. Figure 48 indicates the number of sources that have been extracted in each nod and module. After extraction the residual features were masked (e.g. 16.5-μm). The strong and variable background for this source was properly corrected through modeling. The only exception was the first nod of LL1 module which indicated strong background residuals, therefore we have also subtracted a **constant offset (polynomial order zero) from the background after it has already been corrected through modeling.** In this particular case, there was no mismatch between the modules therefore the continuum shown here was obtained without any further scaling.

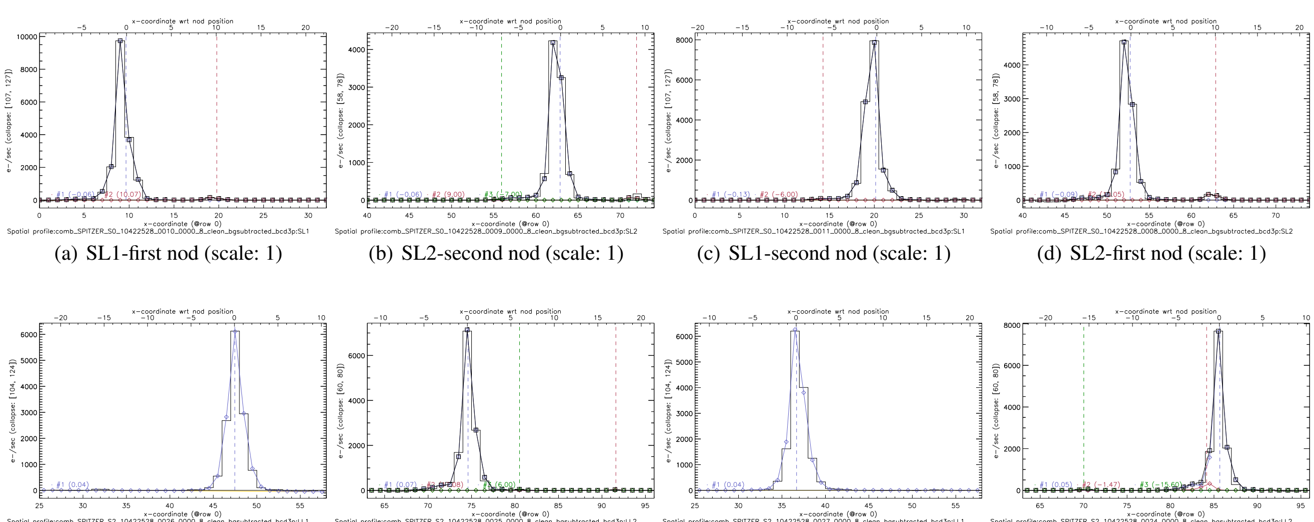

(a) SL1-first nod (scale: 1) (b) SL2-second nod (scale: 1) (c) SL1-second nod (scale: 1) (d) SL2-first nod (scale: 1)

(e) LL1-first nod (scale: 1) (f) LL2-second nod (scale: 1) (g) LL1-second nod (scale: 1) (h) LL2-first nod (scale: 1)

Figure 48. SL and LL modules spatial profiles after subtraction of the background

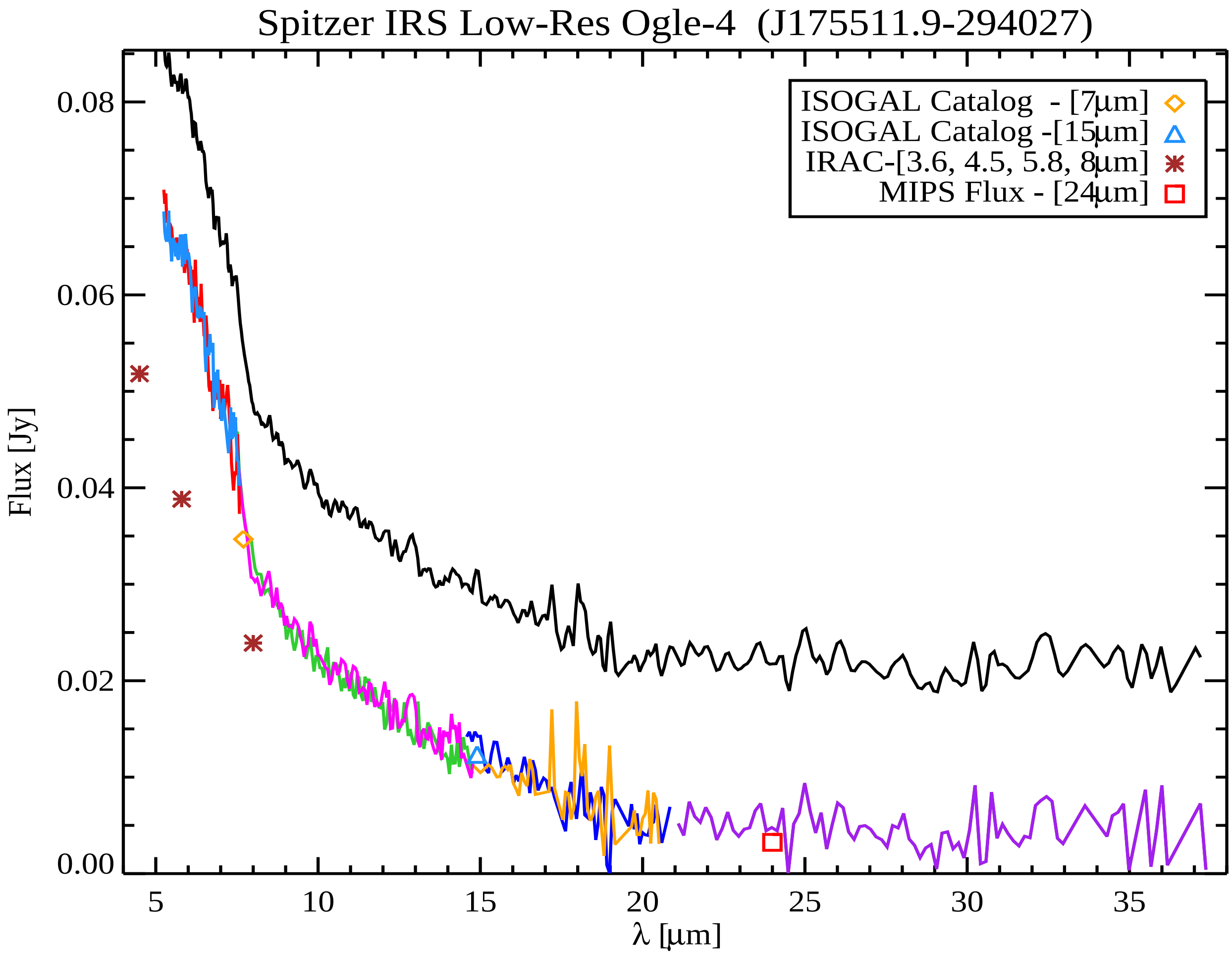

Figure 49. (Ogle-4) This is the final spectrum of Ogle-4. Figure 50 indicates the number of sources that have been extracted in each nod and module. After extraction, residual features were masked (e.g. 19.5-μm). The strong and variable background for this source was properly corrected through modeling. Finally, we scaled long low modules with respect to the short low modules using the following scale factors, in order to eliminate the mismatch between modules and obtain the continuum shown here.

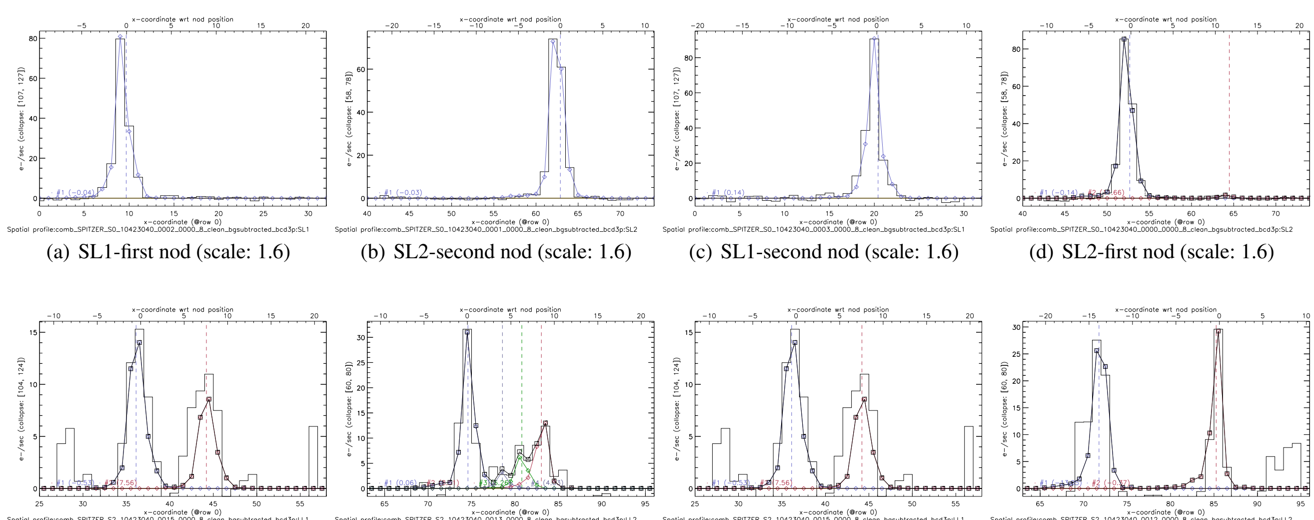

(a) SL1-first nod (scale: 1.6)
(b) SL2-second nod (scale: 1.6)
(c) SL1-second nod (scale: 1.6)
(d) SL2-first nod (scale: 1.6)
(e) LL1-first nod (scale: 0.80)
(f) LL2-second nod (scale: 1.2)
(g) LL1-second nod (scale: 0.80)
(h) LL2-first nod (scale: 1.2)

Figure 50. SL and LL modules spatial profiles after subtraction of the background

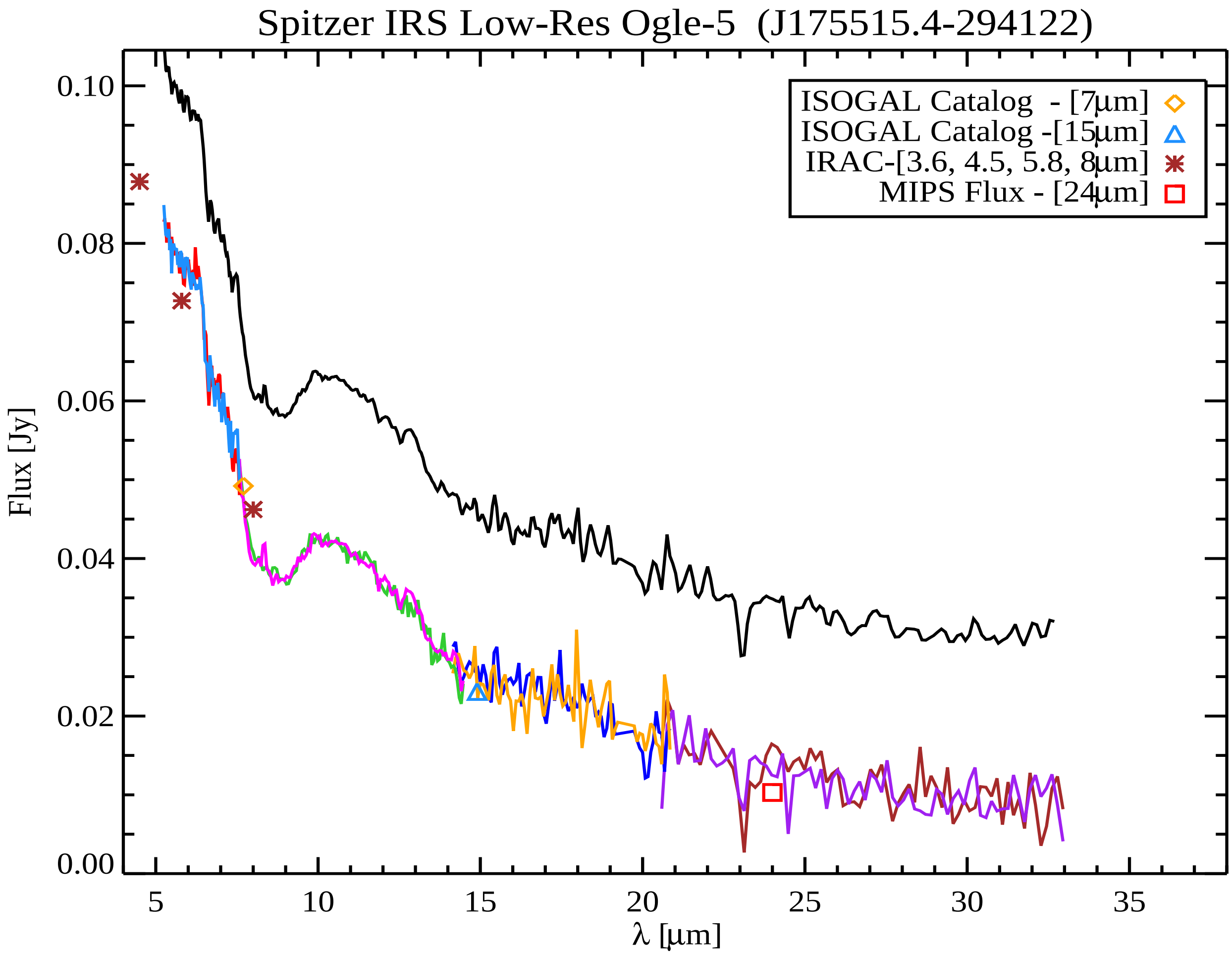

Figure 51. (Ogle-5) This is final spectrum of Ogle-5. Figure 52 indicates the number of sources that have been extracted in each nod and module. After extraction the sharp and unrealistic residual features were masked (e.g. 18-μm). The strong and variable background for this source was properly corrected through modeling. In this particular case, there was no mismatch between the modules therefore the continuum shown here was obtained without any further scaling.

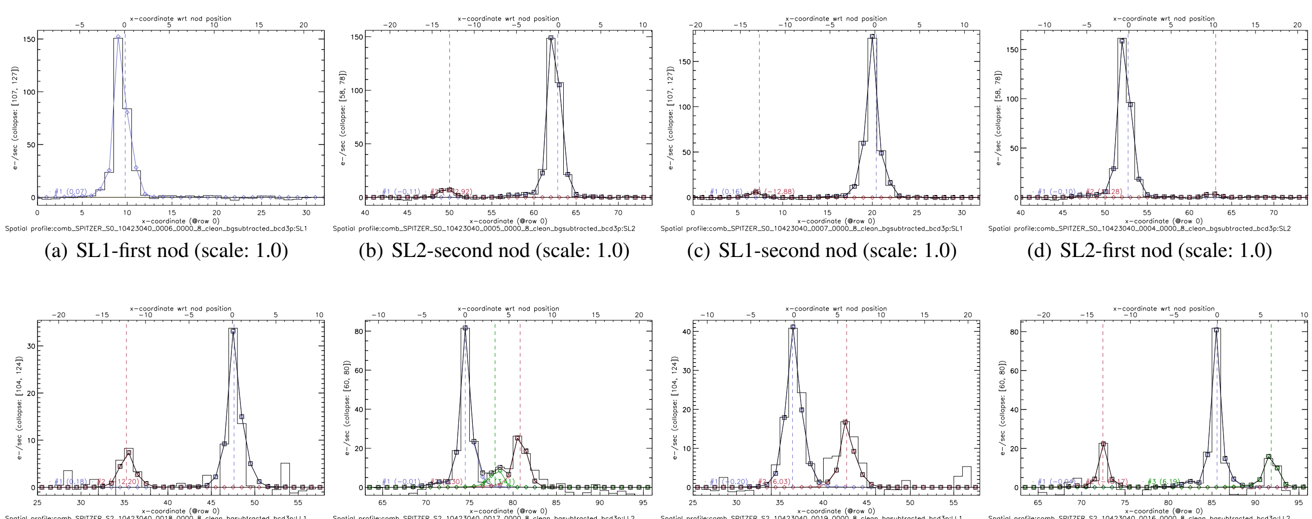

(a) SL1-first nod (scale: 1.0) (b) SL2-second nod (scale: 1.0) (c) SL1-second nod (scale: 1.0) (d) SL2-first nod (scale: 1.0)

(e) LL1-first nod (scale: 1.0) (f) LL2-second nod (scale: 1.0) (g) LL1-second nod (scale: 1.0) (h) LL2-first nod (scale: 1.0)

Figure 52. SL and LL modules spatial profiles after subtraction of the background

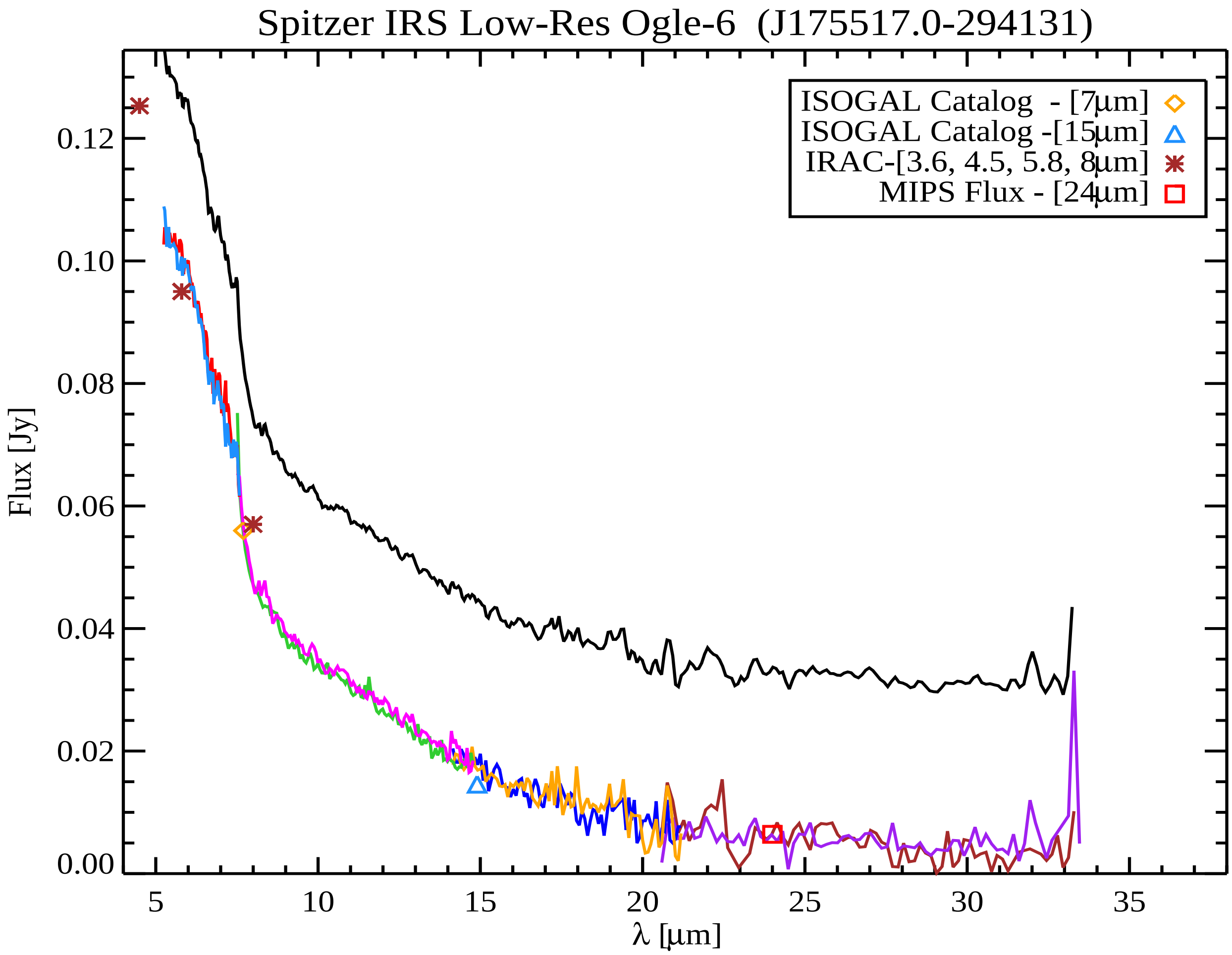

Figure 53. (Ogle-6) This is the final spectrum of Ogle-6. Figure 54 indicates the number of sources that have been extracted in each nod and module. After extraction the sharp and unrealistic residual features were masked (e.g. 19.5-μm). The background for this source is similar to other sources in field Ogle which was properly corrected through modeling. Finally, we scaled long low modules with respect to the short low module using the following scale factors, in order to eliminate the mismatch between modules and obtain the continuum shown here.

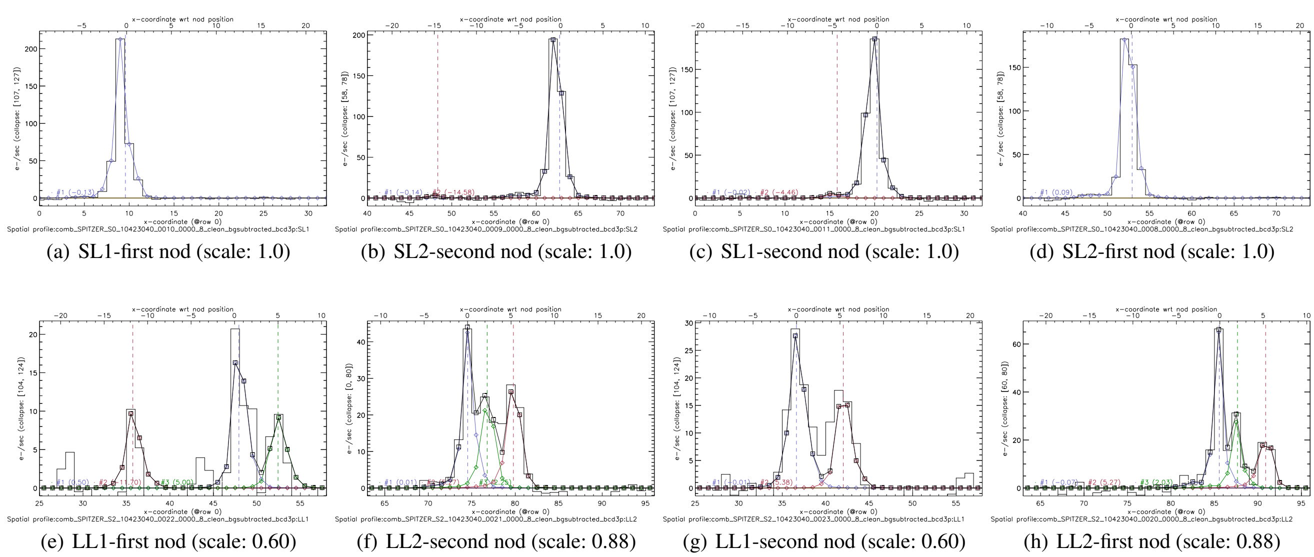

(a) SL1-first nod (scale: 1.0)
(b) SL2-second nod (scale: 1.0)
(c) SL1-second nod (scale: 1.0)
(d) SL2-first nod (scale: 1.0)
(e) LL1-first nod (scale: 0.60)
(f) LL2-second nod (scale: 0.88)
(g) LL1-second nod (scale: 0.60)
(h) LL2-first nod (scale: 0.88)

Figure 54. SL and LL modules spatial profiles after subtraction of the background

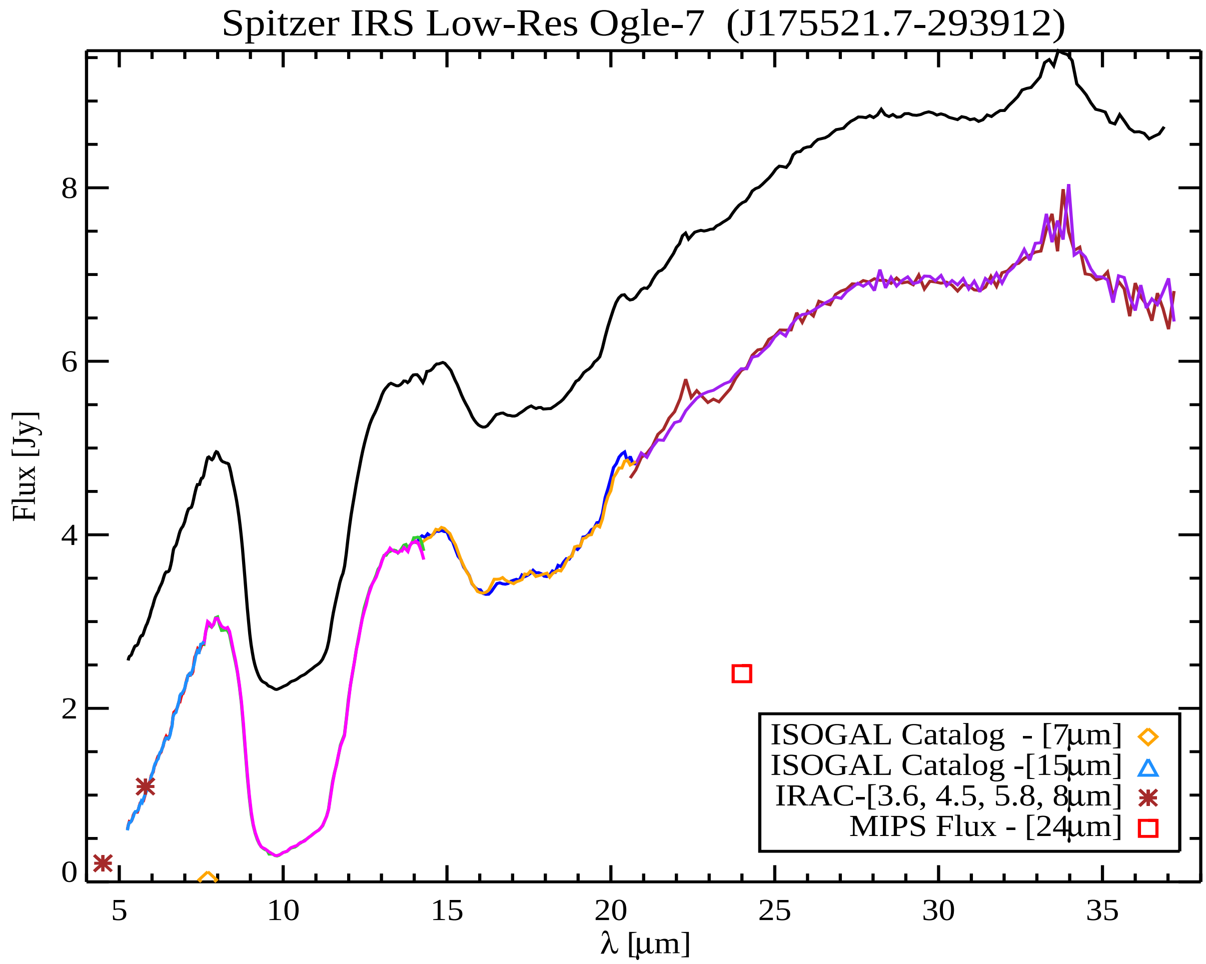

Figure 55. (Ogle-7) This is the final spectrum of Ogle-7. Figure 56 indicates the number of sources that have been extracted in each nod and module. After extraction, residual features were masked (e.g. 16.5-μm). The strong and variable background for this source was properly corrected through modeling. Finally, we scaled all modules with respect to the SL1 module using the following scale factors, in order to eliminate the mismatch between modules and obtain the continuum shown here.

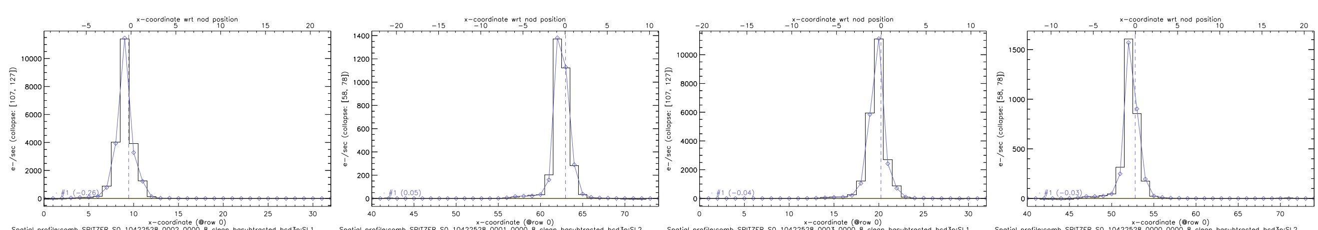

(a) SL1-first nod (scale: 1.0) (b) SL2-second nod (scale: 1.0) (c) SL1-second nod (scale: 1.0) (d) SL2-first nod (scale: 1.0)

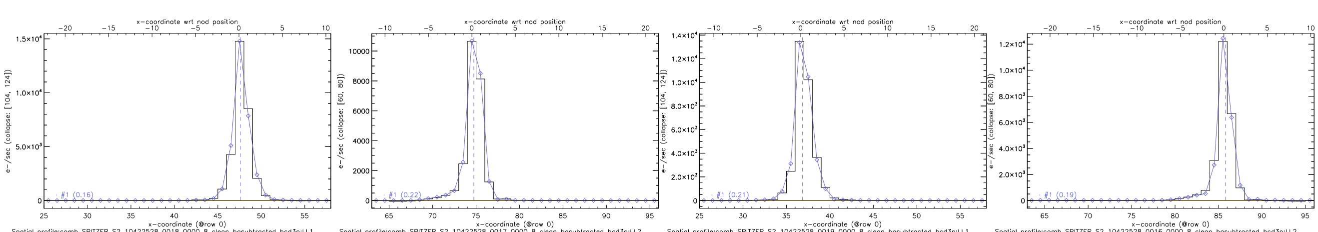

(e) LL1-first nod (scale: 0.85) (f) LL2-second nod (scale: 0.85) (g) LL1-second nod (scale: 0.85) (h) LL2-first nod (scale: 0.85)

Figure 56. SL and LL modules spatial profiles after subtraction of the background

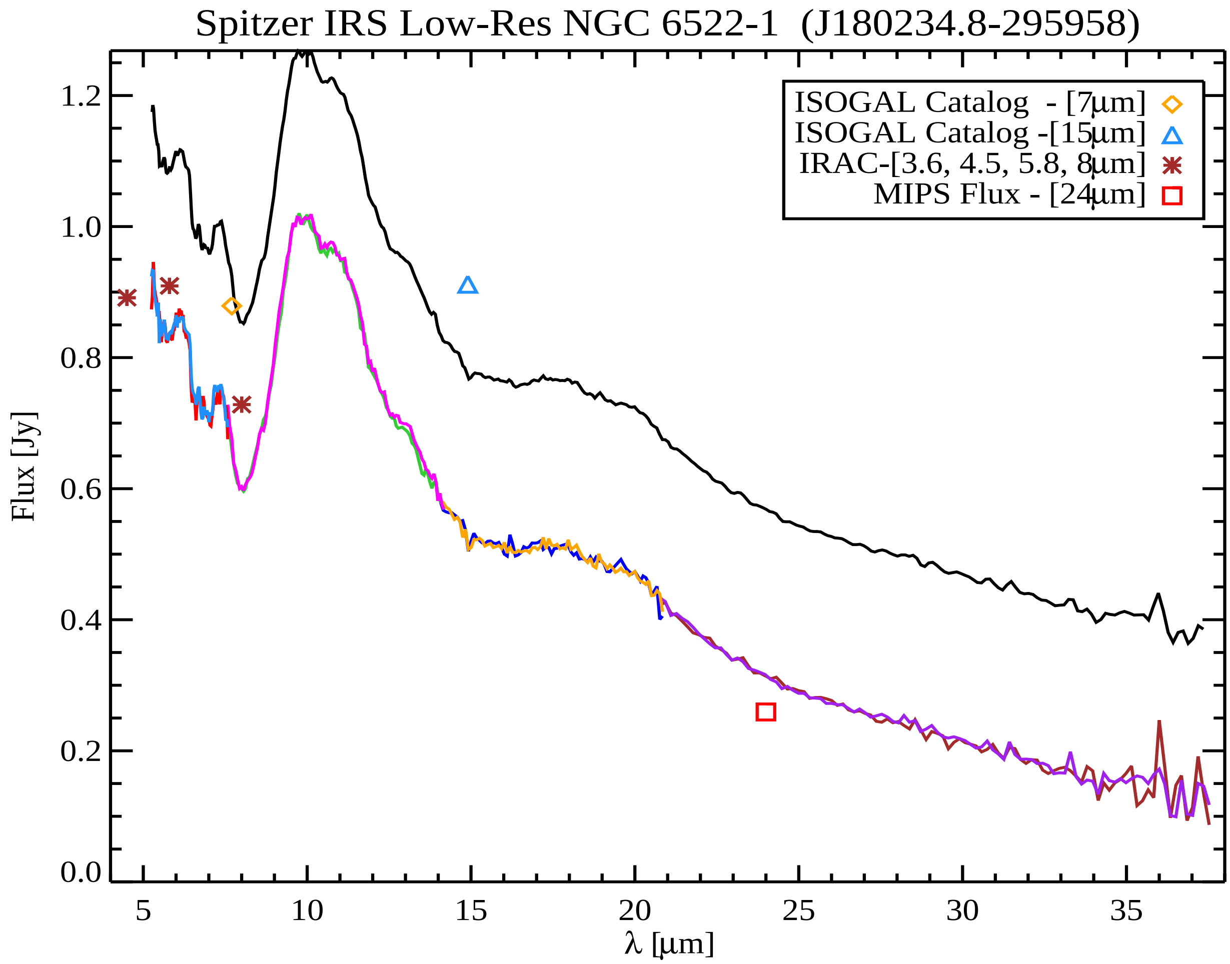

Figure 57. (NGC 6522-1) This is the final spectrum of NGC 6522-1. Figure 58 indicates the number of sources that have been extracted in each nod and module. After extraction the sharp and unrealistic residual features were masked (e.g. 19.5-μm). The background for this source is strong but it shows slightly less variation over the observed wavelength range, compared to other fields. This background was properly corrected through modeling. Finally, we scaled long low modules with respect to the short low modules using the following scale factors, in order to eliminate the mismatch between them and obtain the continuum shown here.

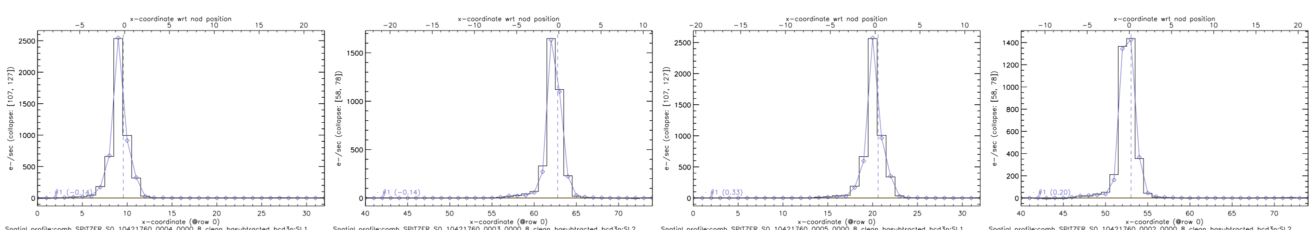

(a) SL1-first nod (scale: 1.0) (b) SL2-second nod (scale: 1.0) (c) SL1-second nod (scale: 1.0) (d) SL2-first nod (scale: 1.0)

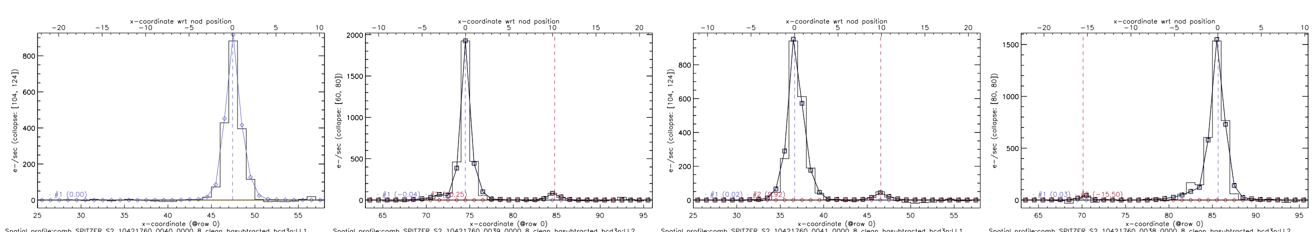

(e) LL1-first nod (scale: 0.90) (f) LL2-second nod (scale: 0.90) (g) LL1-second nod (scale: 0.90) (h) LL2-first nod (scale: 0.90)

Figure 58. SL and LL modules spatial profiles after subtraction of the background

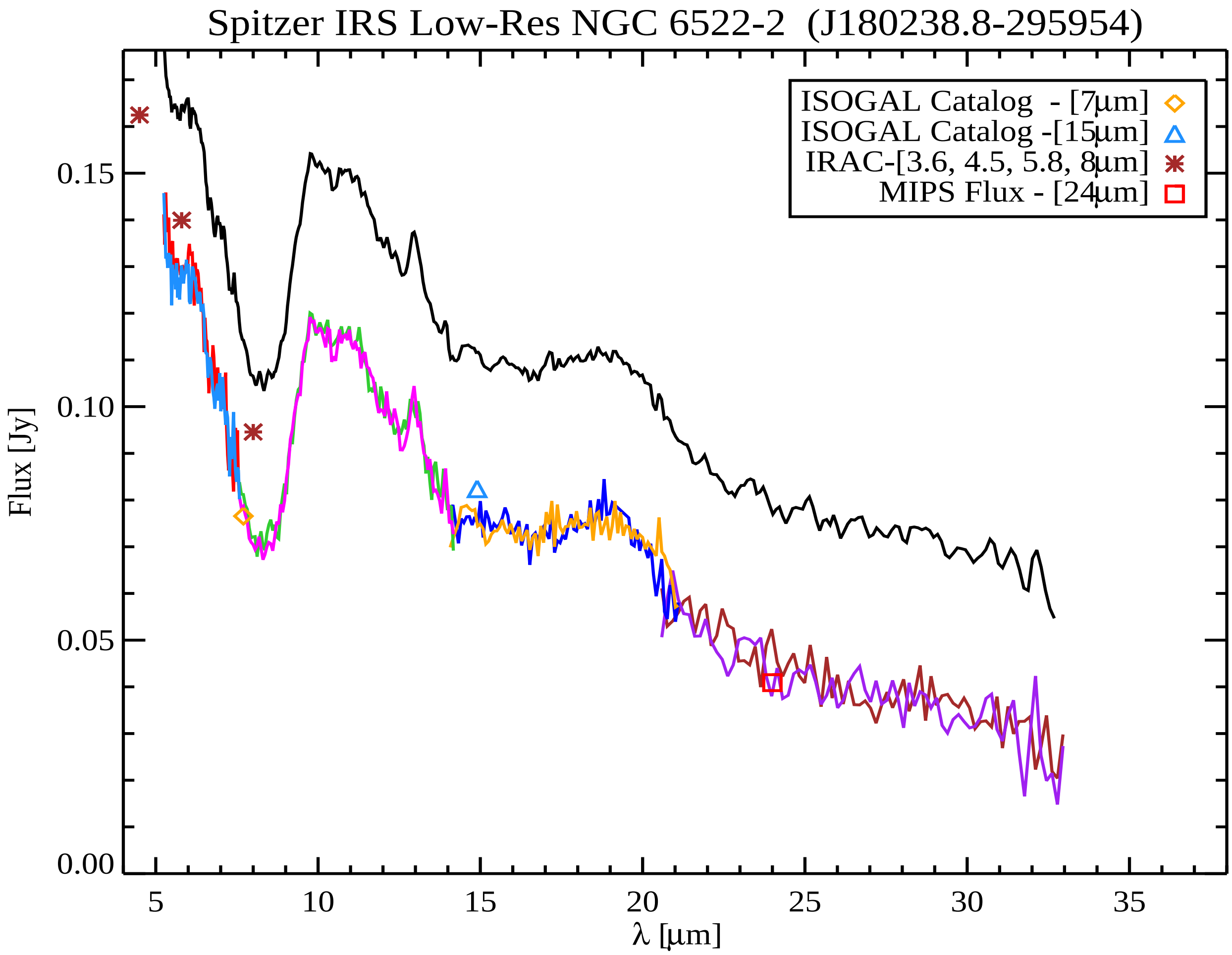

Figure 59. (NGC 6522-2) This is the final spectrum og NGC 6522-2. Figure 60 indicates the number of sources that have been extracted in each nod and module. There was a slight mismatch between the two nods of SL1 module which was removed by modifying the point spread function (central position and FWHM). After extraction the sharp and unrealistic residual features were masked (e.g. 19.5-μm). This source is located in the field covering NGC6522 and its background is similar to that of NGC 6522-1 therefore it was similarly corrected through modeling. Finally, we scaled long low modules with respect to the short low modules using the following scale factors, in order to eliminate the mismatch between them and obtain the continuum shown here.

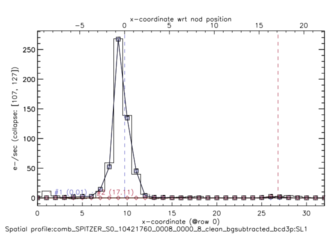
(a) SL1-first nod (scale: 1.0)

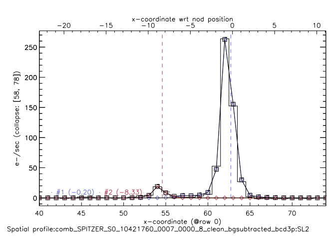
(b) SL2-second nod (scale: 1.0)

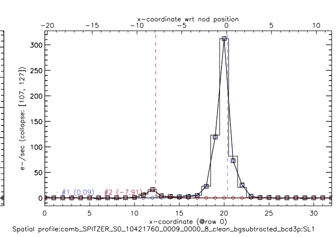
(c) SL1-second nod (scale: 1.0)

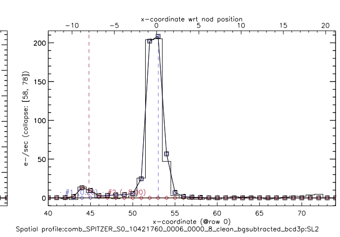
(d) SL2-first nod (scale: 1.0)

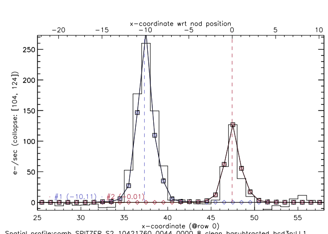
(e) LL1-first nod (scale: 0.90)

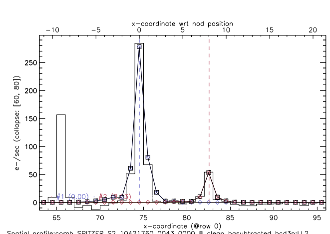
(f) LL2-second nod (scale: 0.85)

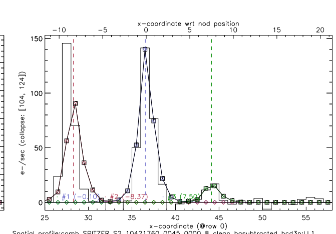
(g) LL1-second nod (scale: 0.90)

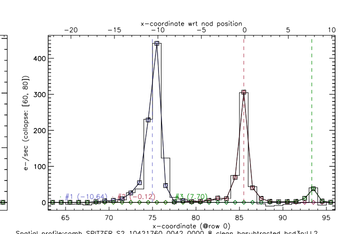
(h) LL2-first nod (scale: 0.85)

Figure 60. SL and LL modules spatial profiles after subtraction of the background

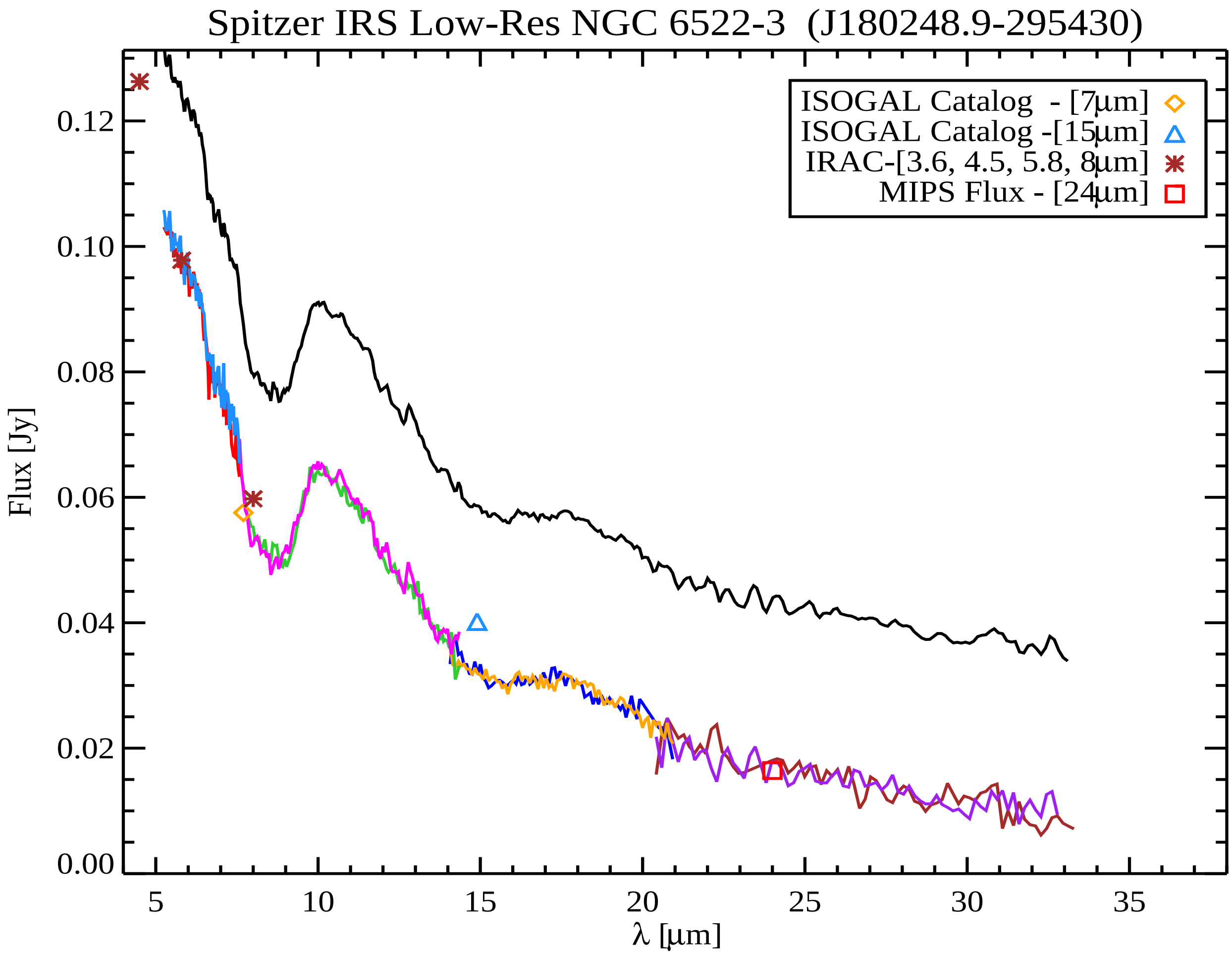

Figure 61. (NGC 6522-3) This is the final spectrum of NGC 6522-3. Figure 62 indicates the number of sources that have been extracted in each nod and module. After extraction the sharp and unrealistic residual features were masked (e.g. 20.5-μm). This source is located in the field covering NGC6522 and its background is similar to that of the rest of the field thus similarly it was corrected through modeling. Finally, we scaled long low modules with respect to the short low modules using the following scale factors, in order to eliminate the mismatch between them and obtain the continuum shown here.

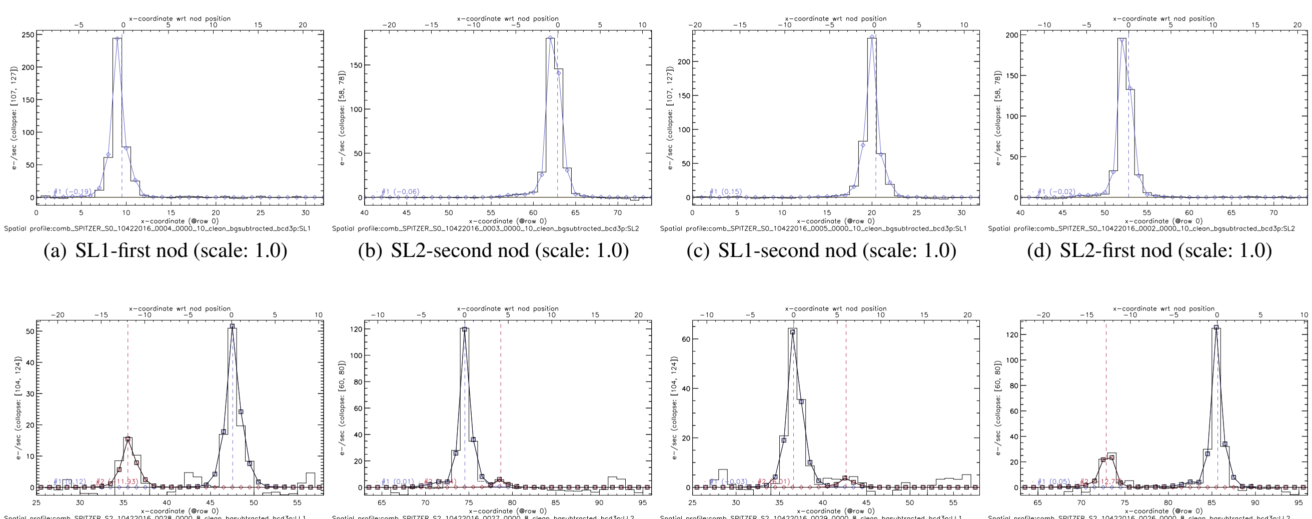

(a) SL1-first nod (scale: 1.0) (b) SL2-second nod (scale: 1.0) (c) SL1-second nod (scale: 1.0) (d) SL2-first nod (scale: 1.0)

(e) LL1-first nod (scale: 0.80) (f) LL2-second nod (scale: 0.80) (g) LL1-second nod (scale: 0.80) (h) LL2-first nod (scale: 0.80)

Figure 62. SL and LL modules spatial profiles after subtraction of the background

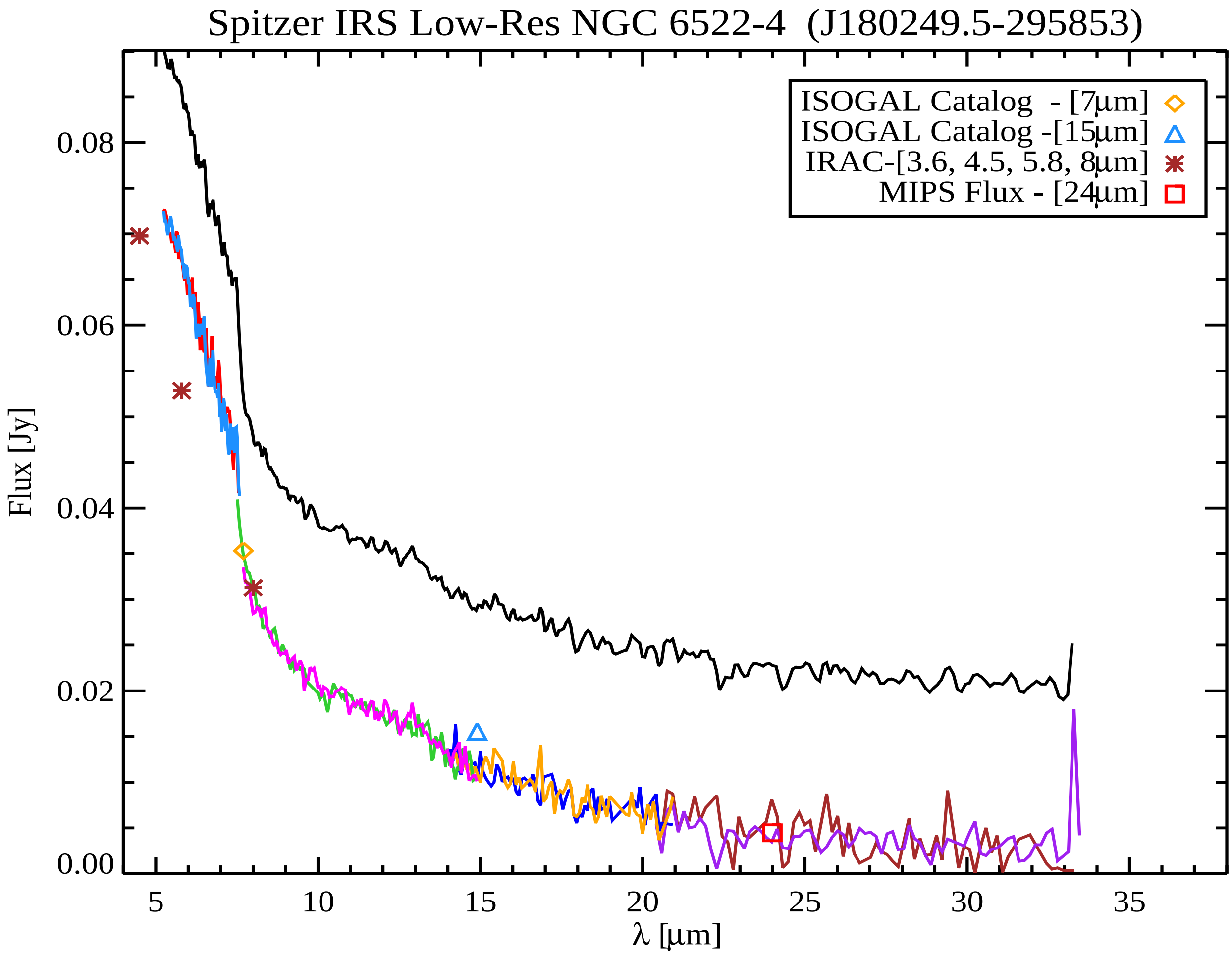

Figure 63. (NGC 6522-4) This is the final spectrum of NGC 6522-4. Figure 64 indicates the number of sources that have been extracted in each nod and module.There was a slight mismatch between the two nods of SL1 module which was removed by modifying the point spread function (central position and FWHM). After extraction, residual features were masked (e.g. 19.5-μm). This source is located in the field covering NGC6522 and its background is similar to that of the rest of the field thus similarly it was corrected through modeling. Finally, we scaled all modules with respect to the SL1 module using the following scale factors, in order to eliminate the mismatch between them and obtain the continuum shown here.

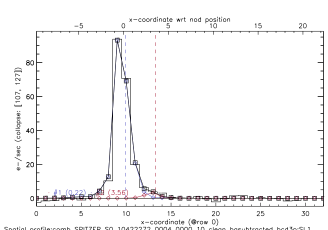
(a) SL1-first nod (scale: 1.0)

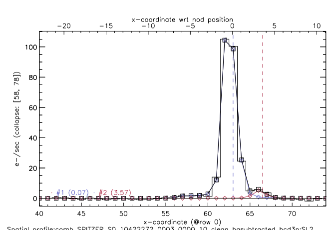
(b) SL2-second nod (scale: 1.1)

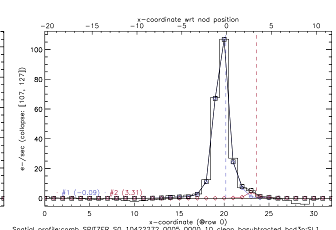
(c) SL1-second nod (scale: 1.0)

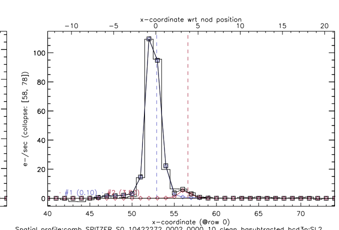
(d) SL2-first nod (scale: 1.1)

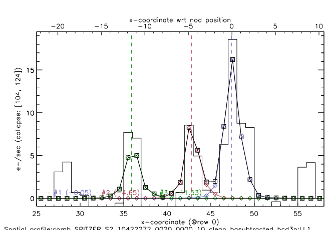
(e) LL1-first nod (scale: 0.60)

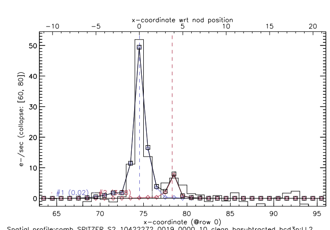
(f) LL2-second nod (scale: 0.70)

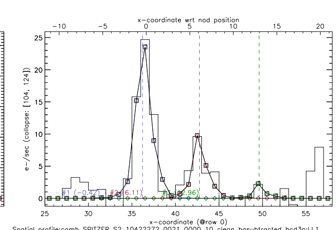
(g) LL1-second nod (scale: 0.60)

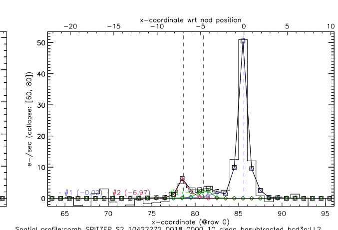
(h) LL2-first nod (scale: 0.70)

Figure 64. SL and LL modules spatial profiles after subtraction of the background

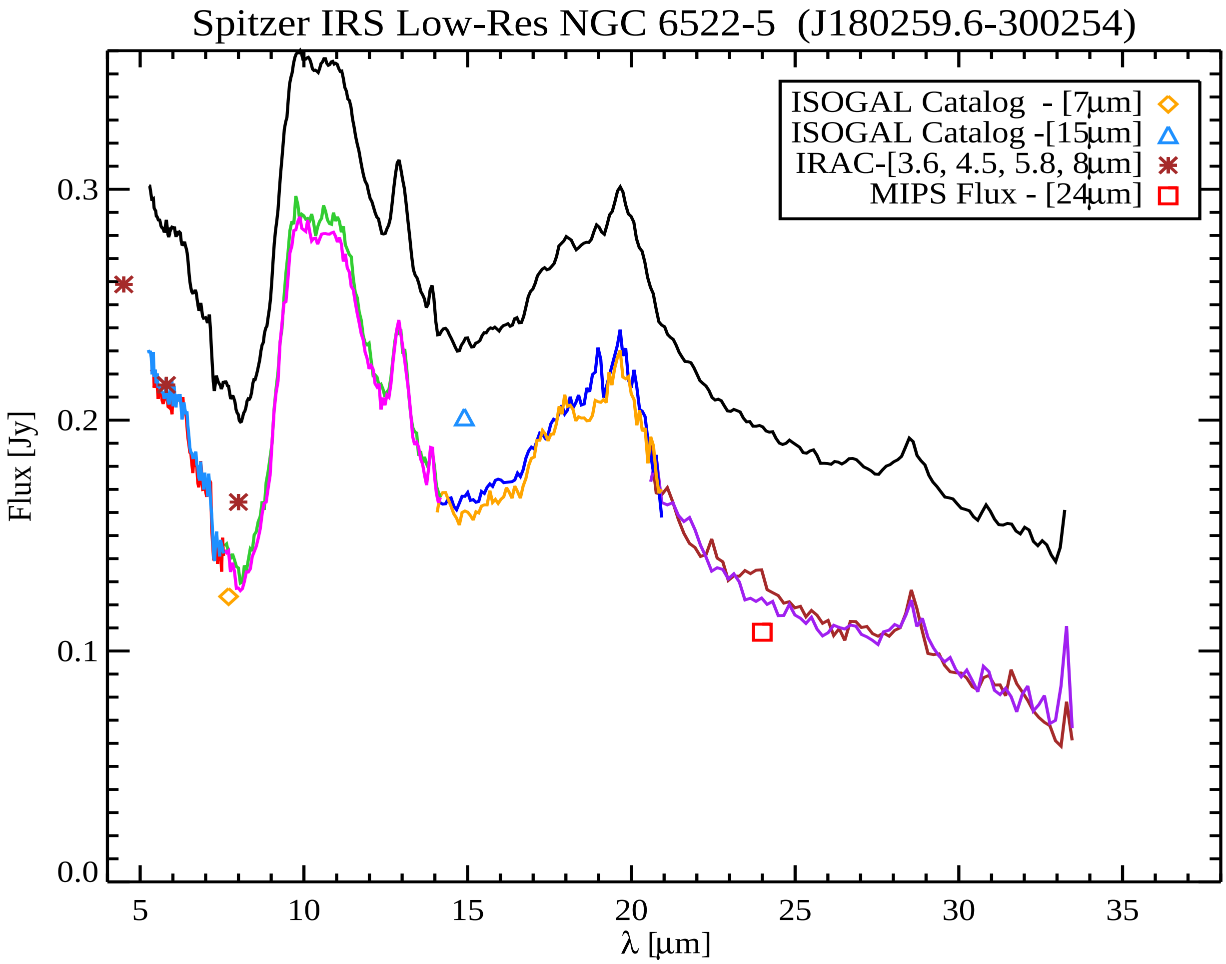

Figure 65. (NGC 6522-5) This is the final spectrum of NGC 6522-5. Figure 66 indicates the number of sources that have been extracted in each nod and module. After extraction the sharp and unrealistic residual features were masked (e.g. 19.5-μm). This source is located in the field covering NGC6522 and its background is similar to that of the rest of the field thus similarly it was corrected through modeling. Finally, we scaled long low modules with respect to the short low modules using the following scale factors, in order to eliminate the mismatch between them and obtain the continuum shown here.

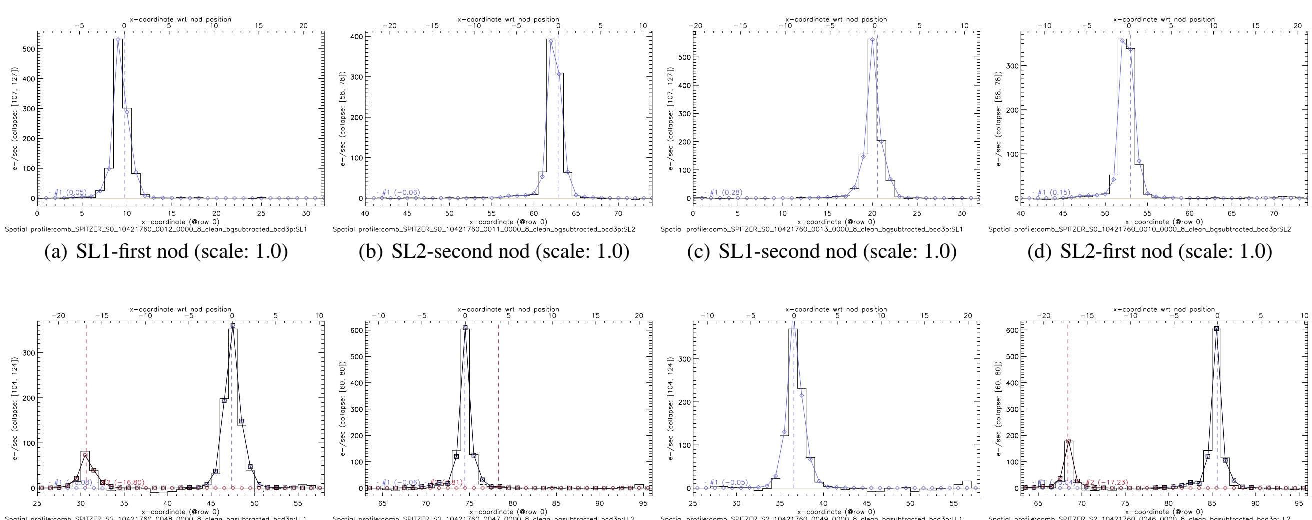

(a) SL1-first nod (scale: 1.0) (b) SL2-second nod (scale: 1.0) (c) SL1-second nod (scale: 1.0) (d) SL2-first nod (scale: 1.0)

(e) LL1-first nod (scale: 0.90) (f) LL2-second nod (scale: 0.90) (g) LL1-second nod (scale: 0.90) (h) LL2-first nod (scale: 0.90)

Figure 66. SL and LL modules spatial profiles after subtraction of the background

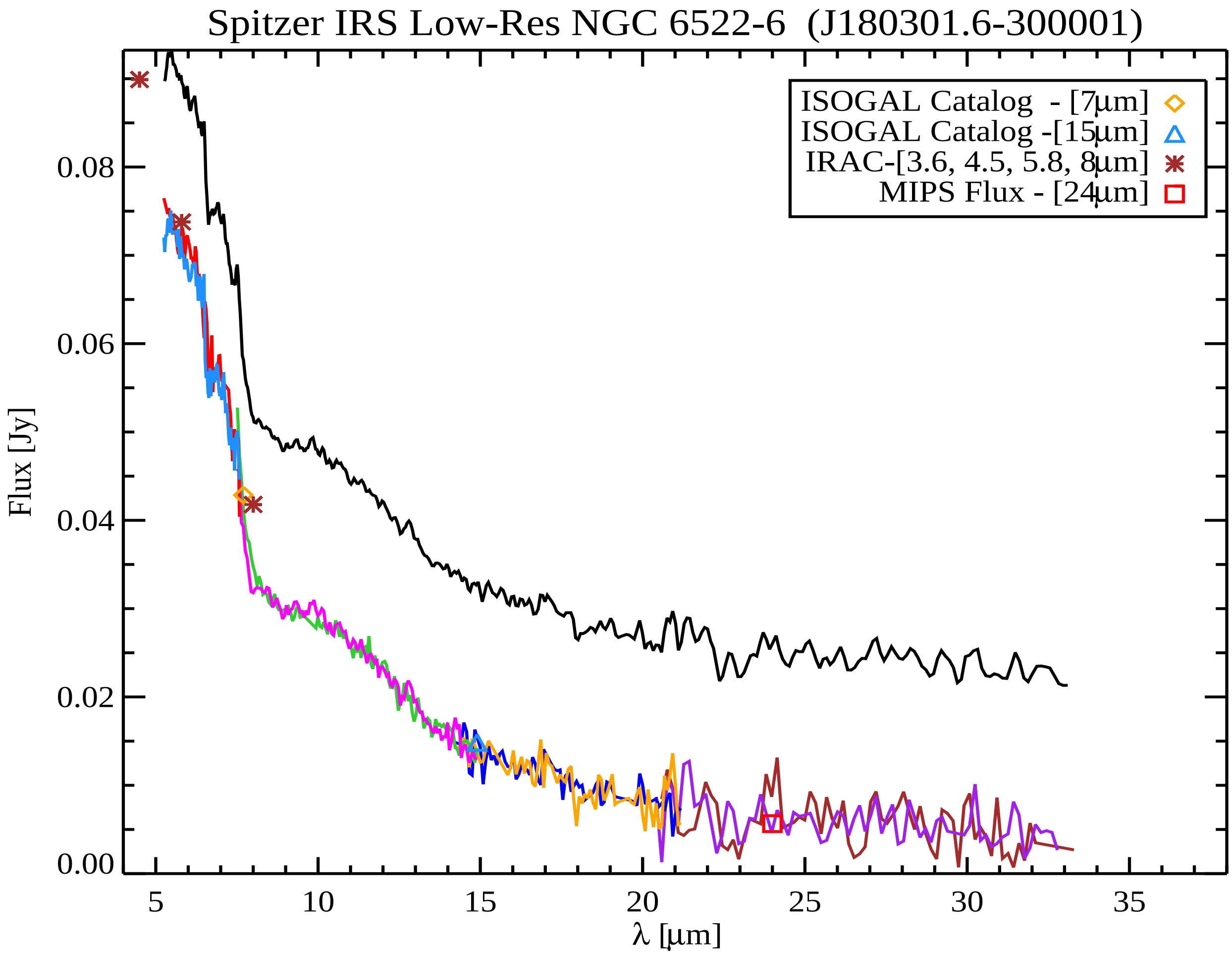

Figure 67. (NGC 6522-6) This is the final spectrum of NGC 6522-6. Figure 68 indicates the number of sources that have been extracted in each nod and module. After extraction, residual features were masked (e.g. 19.5-μm). This source is located in the field covering NGC6522 and its background is similar to that of the rest of the field thus similarly it was corrected through modeling. Finally, we scaled long low modules with respect to the short low modules using the following scale factors, in order to eliminate the mismatch between them and obtain the continuum shown here.

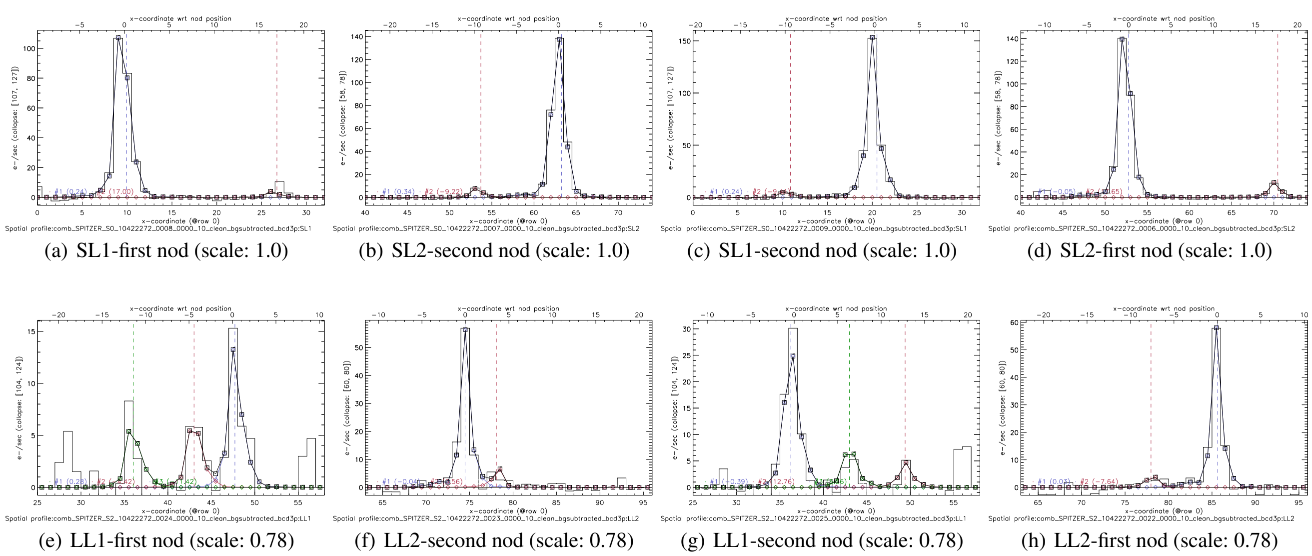

(a) SL1-first nod (scale: 1.0)
(b) SL2-second nod (scale: 1.0)
(c) SL1-second nod (scale: 1.0)
(d) SL2-first nod (scale: 1.0)
(e) LL1-first nod (scale: 0.78)
(f) LL2-second nod (scale: 0.78)
(g) LL1-second nod (scale: 0.78)
(h) LL2-first nod (scale: 0.78)

Figure 68. SL and LL modules spatial profiles after subtraction of the background

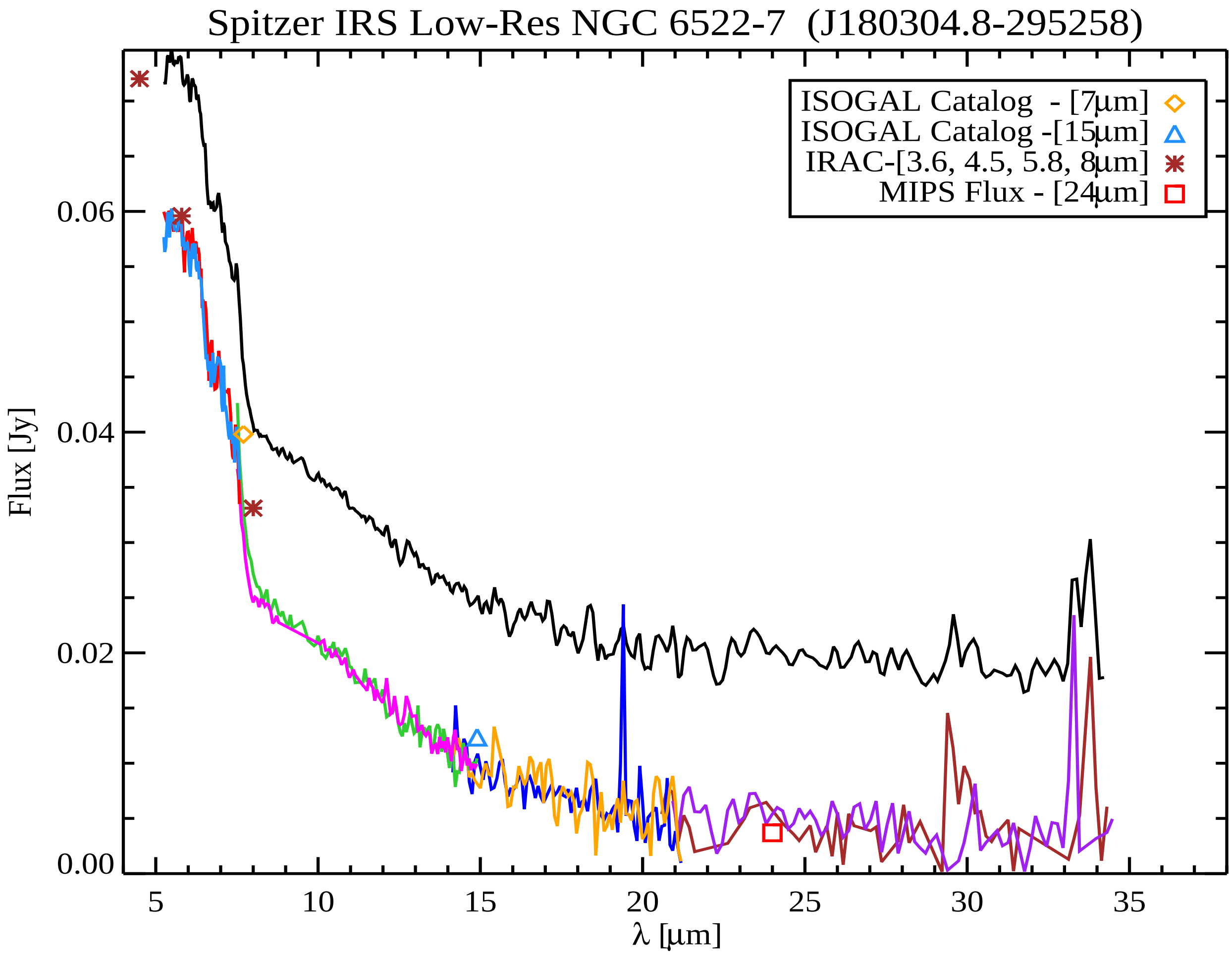

Figure 69. (NGC 6522-7) This is the final spectrum of NGC 6522-7. Figure 70 indicates the number of sources that have been extracted in each nod and module.There was a slight mismatch between the two nods of SL1 module which was removed by modifying the point spread function (central position and FWHM). After extraction, residual features were masked (e.g. 19.5-μm). This source is located in the field covering NGC6522 and its background is similar to that of the rest of the field thus similarly it was corrected through modeling. Finally, we scaled long low modules with respect to the short low modules using the following scale factors, in order to eliminate the mismatch between them and obtain the continuum shown here.

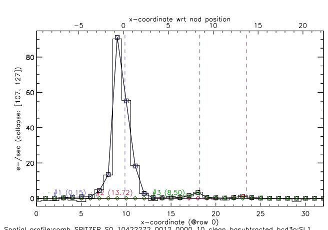
(a) SL1-first nod (scale: 1.0)

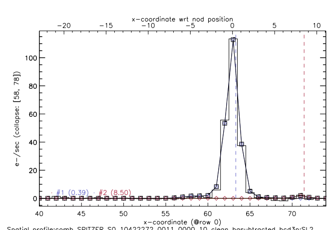
(b) SL2-second nod (scale: 1.0)

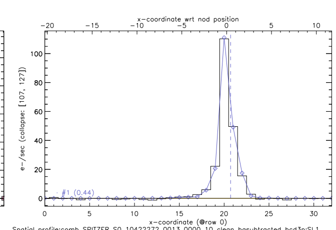
(c) SL1-second nod (scale: 1.0)

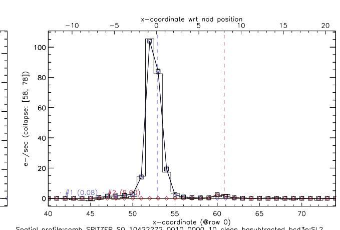
(d) SL2-first nod (scale: 1.0)

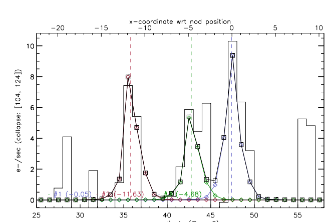
(e) LL1-first nod (scale: 0.85)

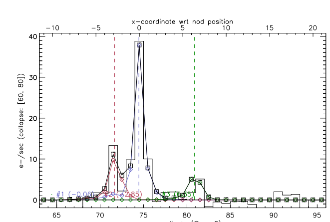
(f) LL2-second nod (scale: 0.80)

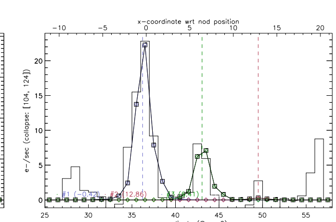
(g) LL1-second nod (scale: 0.85)

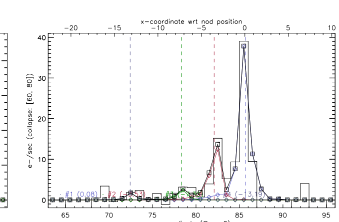
(h) LL2-first nod (scale: 0.80)

Figure 70. SL and LL modules spatial profiles after subtraction of the background

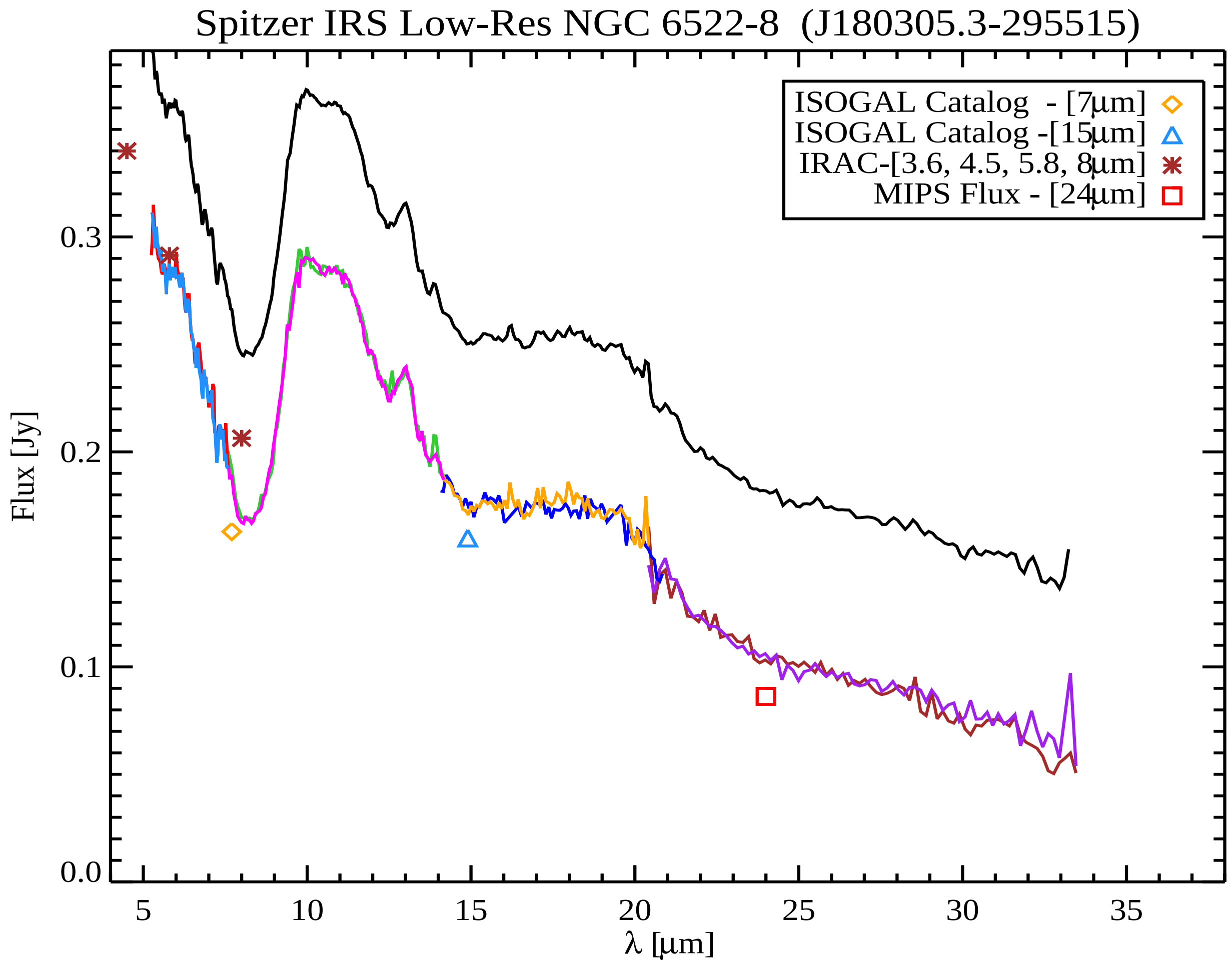

Figure 71. (NGC 6522-8) This is the final spectrum of NGC 6522-8. Figure 72 indicates the number of sources that have been extracted in each nod and module. There was a slight mismatch between the two nods of SL1 module which was removed by modifying the point spread function (central position and FWHM). After extraction the sharp and unrealistic residual features were masked (e.g. 19.5-μm). This source is located in the field covering NGC6522 and its background is similar to that of the rest of the field thus similarly it was corrected through modeling. Finally, we scaled long low modules with respect to the short low modules using the following scale factors, in order to eliminate the mismatch between them and obtain the continuum shown here.

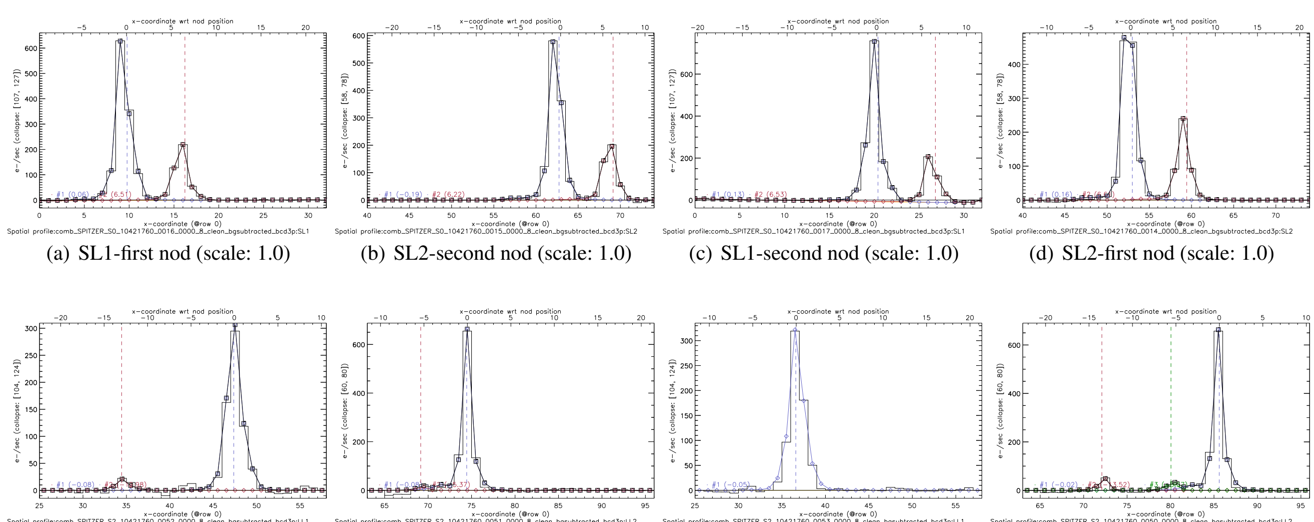

(a) SL1-first nod (scale: 1.0) (b) SL2-second nod (scale: 1.0) (c) SL1-second nod (scale: 1.0) (d) SL2-first nod (scale: 1.0)

(e) LL1-first nod (scale: 0.90) (f) LL2-second nod (scale: 0.90) (g) LL1-second nod (scale: 0.90) (h) LL2-first nod (scale: 0.90)

Figure 72. SL and LL modules spatial profiles after subtraction of the background

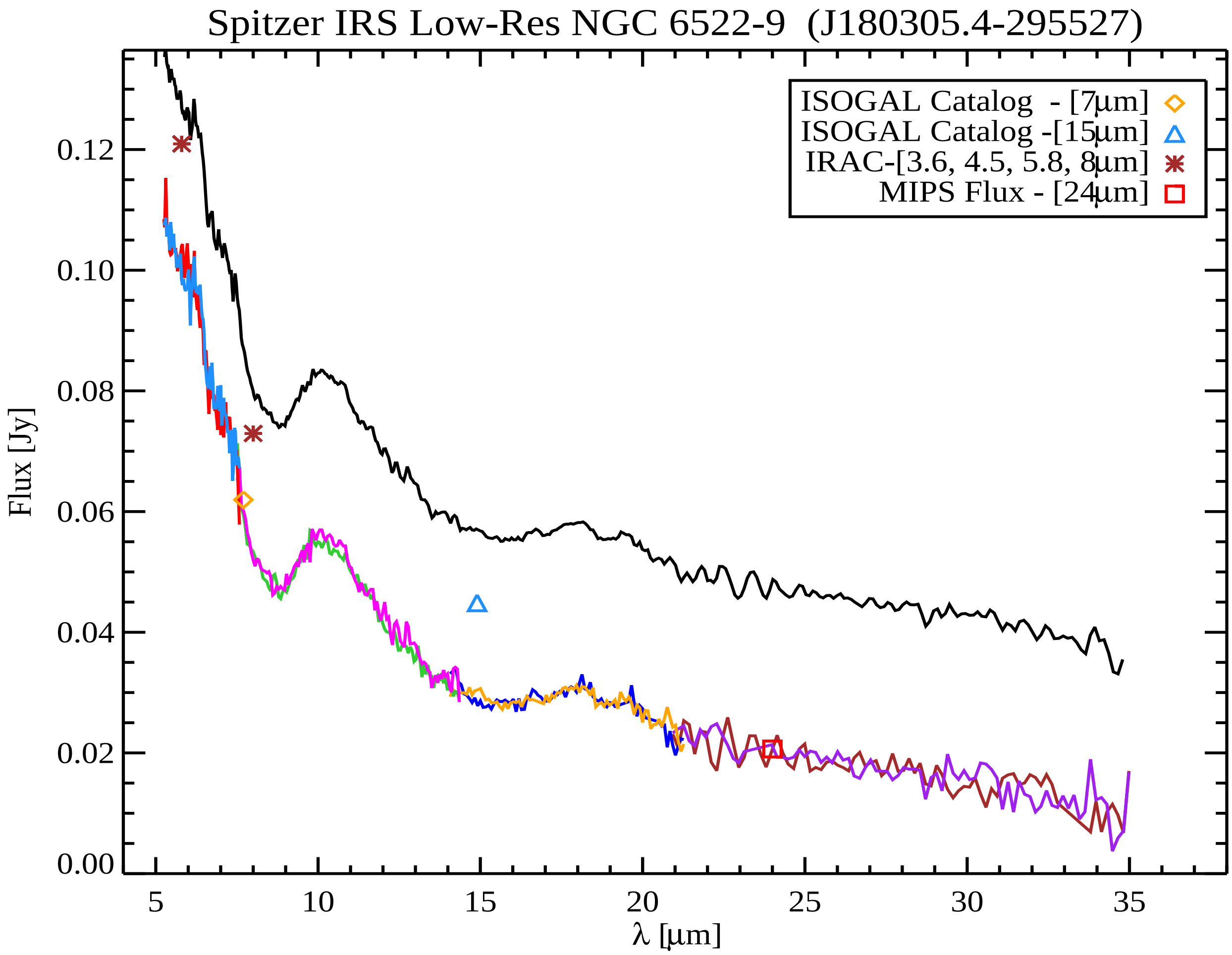

Figure 73. (NGC 6522-9) This is the final spectrum of NGC 6522-9. Figure 74 indicates the number of sources that have been extracted in each nod and module. After extraction the sharp and unrealistic residual features were masked (e.g. 19.5-μm). This source is located in the field covering NGC6522 and its background is similar to that of the rest of the field thus similarly it was corrected through modeling. Finally, we scaled long low modules with respect to the short low modules using the following scale factors, in order to eliminate the mismatch between them and obtain the continuum shown here.

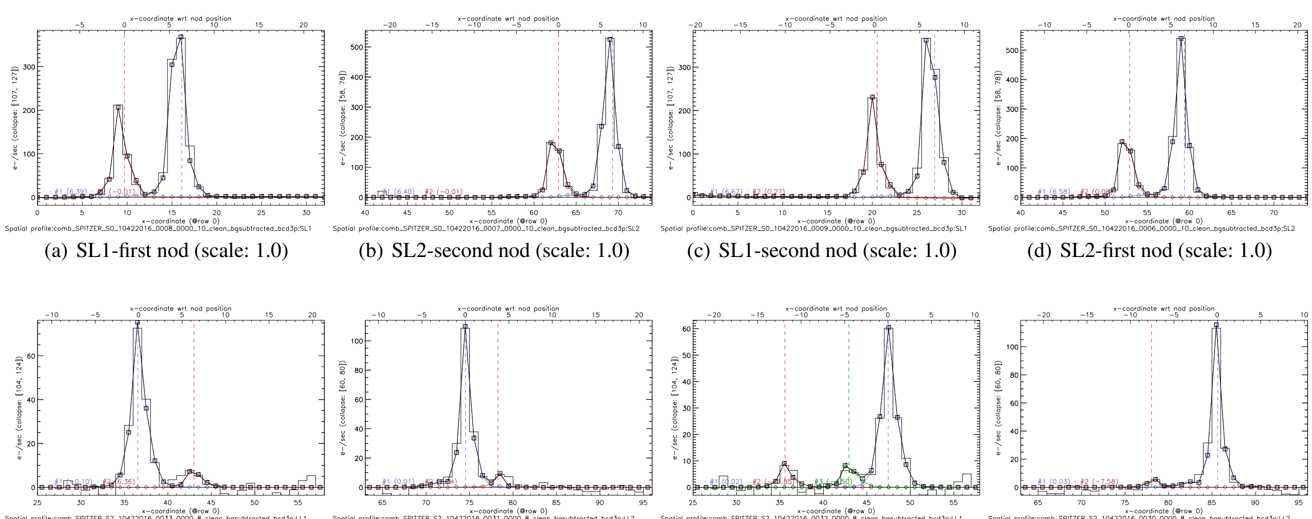

(a) SL1-first nod (scale: 1.0)
(b) SL2-second nod (scale: 1.0)
(c) SL1-second nod (scale: 1.0)
(d) SL2-first nod (scale: 1.0)
(e) LL1-first nod (scale: 0.75)
(f) LL2-second nod (scale: 0.80)
(g) LL1-second nod (scale: 0.75)
(h) LL2-first nod (scale: 0.80)

Figure 74. SL and LL modules spatial profiles after subtraction of the background

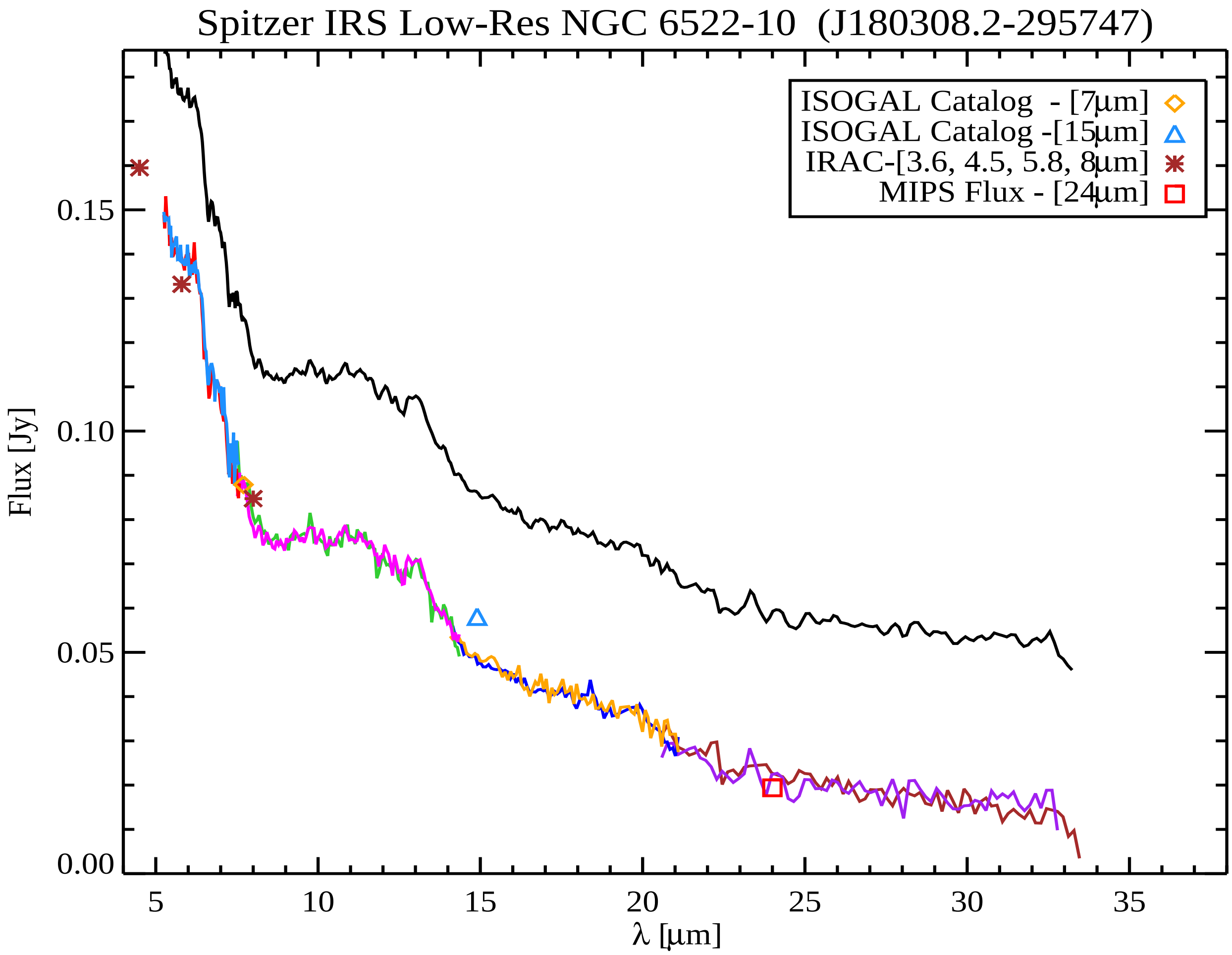

Figure 75. (NGC 6522-10) This is the final spectrum of NGC 6522-10.Figure 76 indicates the number of sources that have been extracted in each nod and module. After extraction the sharp and unrealistic residual features were masked (e.g. 19.5-μm). This source is located in the field covering NGC6522 and its background is similar to that of the rest of the field thus similarly it was corrected through modeling. Finally, we scaled long low modules with respect to the short low modules using the following scale factors, in order to eliminate the mismatch between them and obtain the continuum shown here.

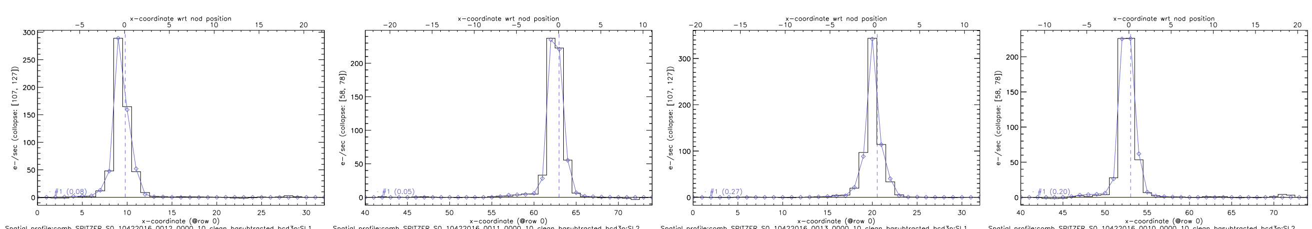

(a) SL1-first nod (scale: 1.0) (b) SL2-second nod (scale: 1.0) (c) SL1-second nod (scale: 1.0) (d) SL2-first nod (scale: 1.0)

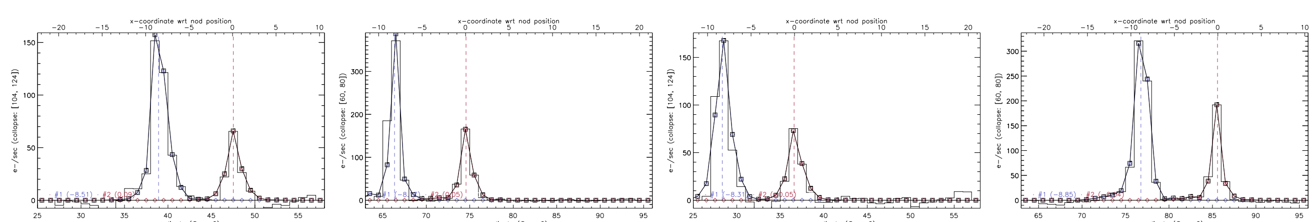

(e) LL1-first nod (scale: 0.85) (f) LL2-second nod (scale: 0.85) (g) LL1-second nod (scale: 0.85) (h) LL2-first nod (scale: 0.85)

Figure 76. SL and LL modules spatial profiles after subtraction of the background

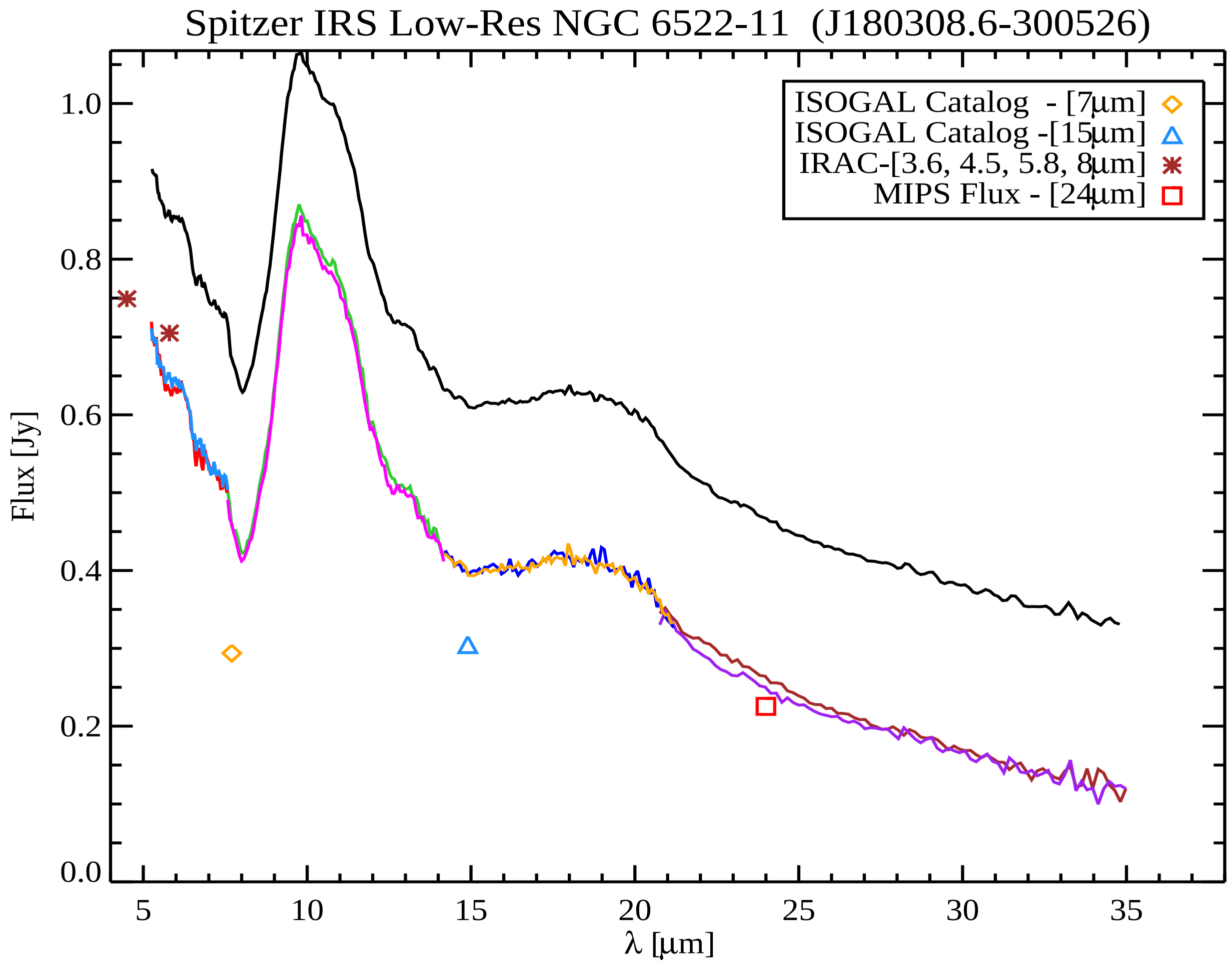

Figure 77. **(NGC 6522-11)** This is the final spectrum of NGC 6522-11. Figure 78 indicates the number of sources that have been extracted in each nod and module. There was a slight mismatch between the two nods of SL1 module which was removed by modifying the point spread function (central position and FWHM). After extraction the sharp and unrealistic residual features were masked (e.g. 19.5-μm). This source is located in the field covering NGC6522 and its background is similar to that of the rest of the field thus similarly it was corrected through modeling. Finally, we scaled long low modules with respect to the short low modules using the following scale factors, in order to eliminate the mismatch between them and obtain the continuum shown here.

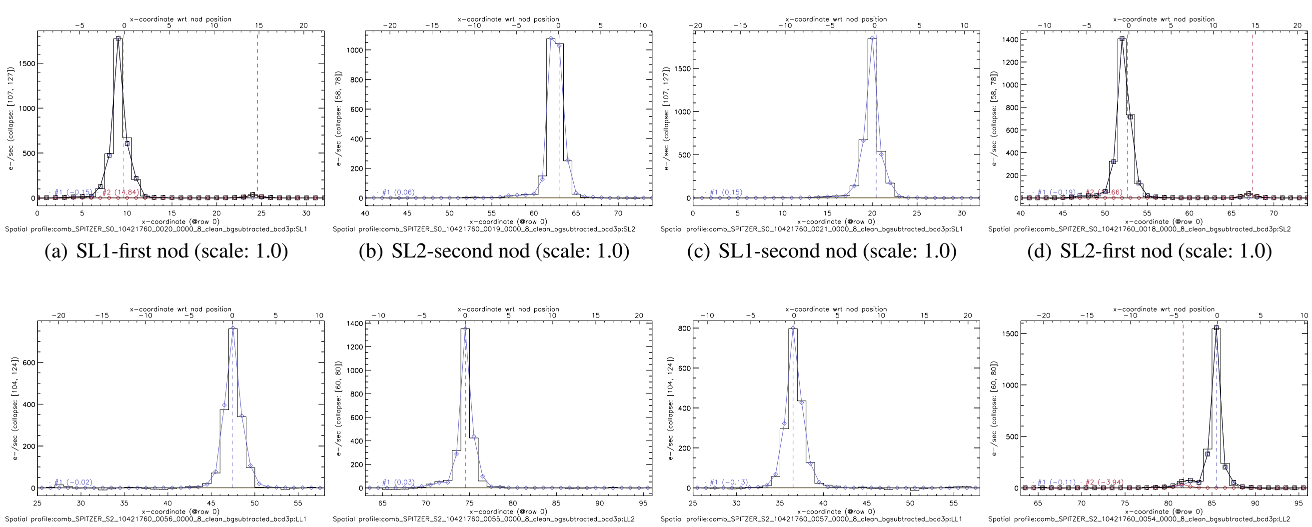

(a) SL1-first nod (scale: 1.0) (b) SL2-second nod (scale: 1.0) (c) SL1-second nod (scale: 1.0) (d) SL2-first nod (scale: 1.0)

(e) LL1-first nod (scale: 0.85) (f) LL2-second nod (scale: 0.90) (g) LL1-second nod (scale: 0.85) (h) LL2-first nod (scale: 0.90)

Figure 78. SL and LL modules spatial profiles after subtraction of the background

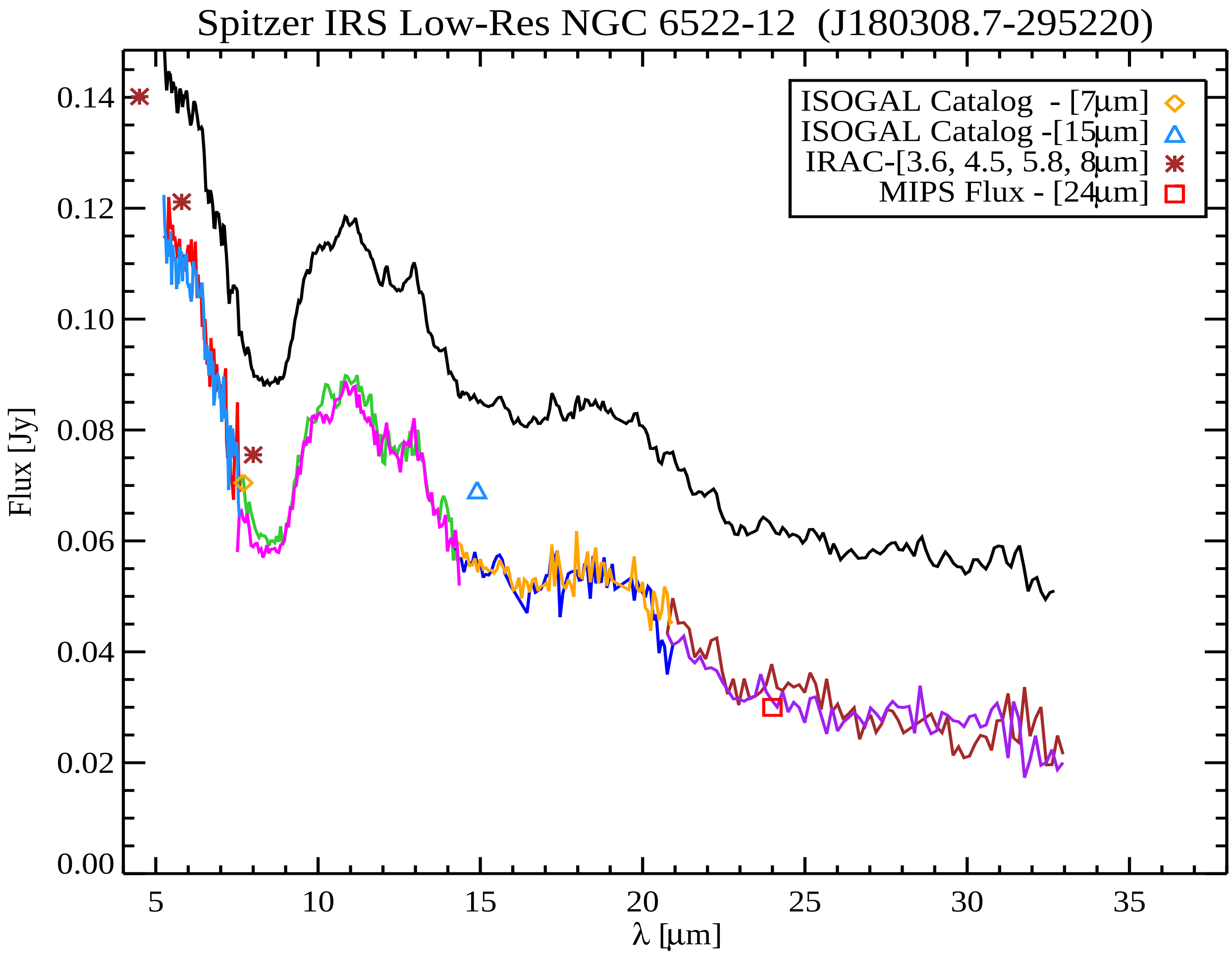

Figure 79. (NGC 6522-12) This is the final spectrum of NGC 6522-12. Figure 80 indicates the number of sources that have been extracted in each nod and module. There was a slight mismatch between the two nods of SL1 module which was removed by modifying the point spread function (central position and FWHM). After extraction the sharp and unrealistic residual features were masked (e.g. 19.5-μm). This source is located in the field covering NGC6522 and its background is similar to that of the rest of the field thus similarly it was corrected through modeling. Finally, we scaled long low modules with respect to the short low modules using the following scale factors, in order to eliminate the mismatch between them and obtain the continuum shown here.

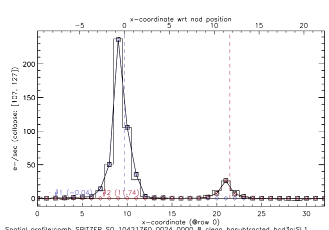

(a) SL1-first nod (scale: 1.0)

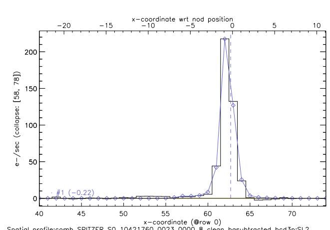

(b) SL2-second nod (scale: 1.0)

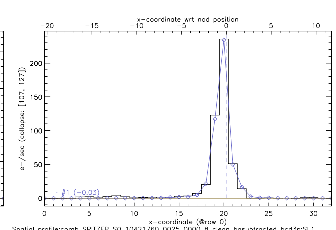

(c) SL1-second nod (scale: 1.0)

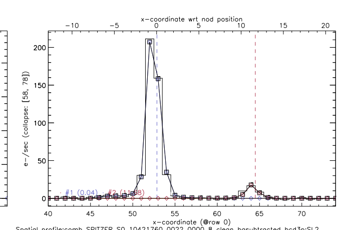

(d) SL2-first nod (scale: 1.0)

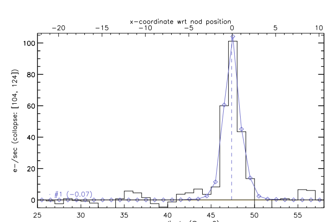

(e) LL1-first nod (scale: 0.78)

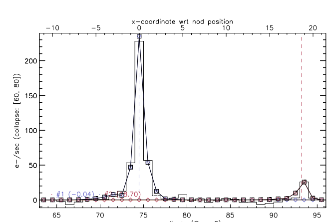

(f) LL2-second nod (scale: 0.78)

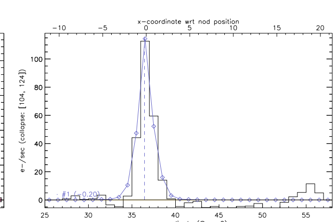

(g) LL1-second nod (scale: 0.78)

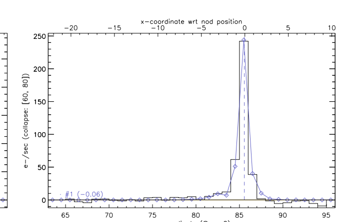

(h) LL2-first nod (scale: 0.78)

Figure 80. SL and LL modules spatial profiles after subtraction of the background

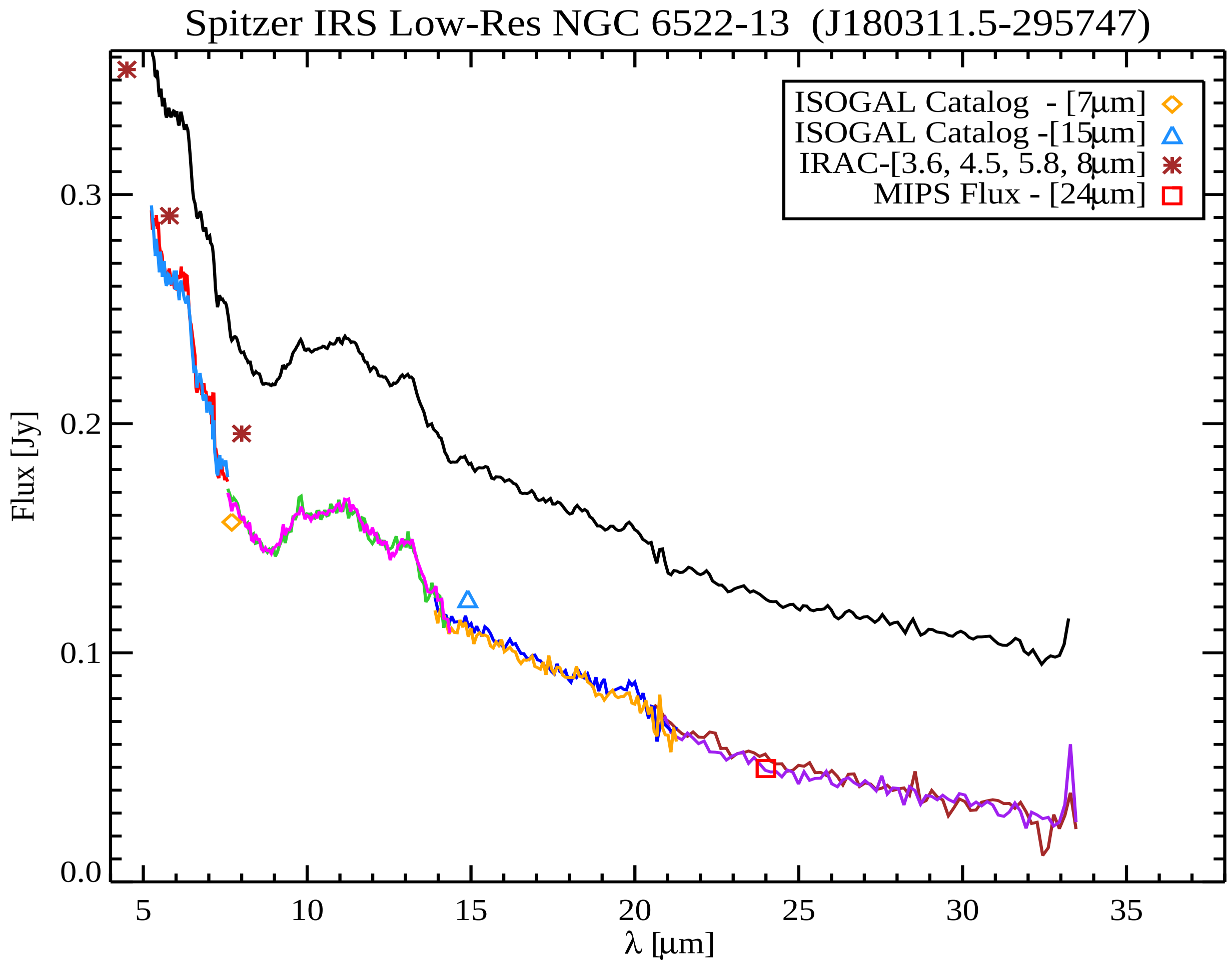

Figure 81. **(NGC 6522-13)** This is the final spectrum of NGC 6522-13. Figure 82 indicates the number of sources that have been extracted in each nod and module. After extraction the sharp and unrealistic residual features were masked (e.g. 19.5-μm). This source is located in the field covering NGC6522 and its background is similar to that of the rest of the field thus similarly it was corrected through modeling. Finally, we scaled long low modules with respect to the short low modules using the following scale factors, in order to eliminate the mismatch between them and obtain the continuum shown here.

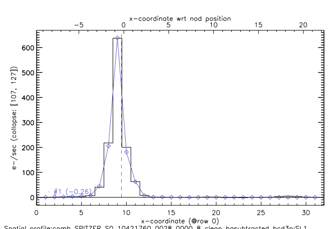
(a) SL1-first nod (scale: 1.0)

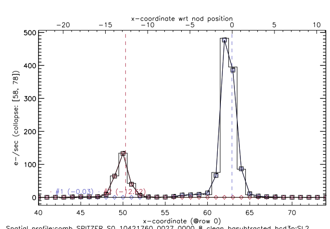
(b) SL2-second nod (scale: 1.0)

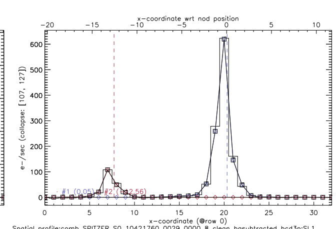
(c) SL1-second nod (scale: 1.0)

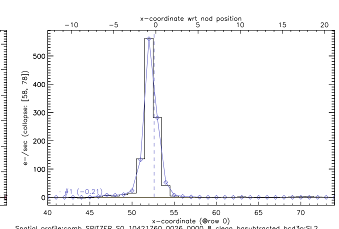
(d) SL2-first nod (scale: 1.0)

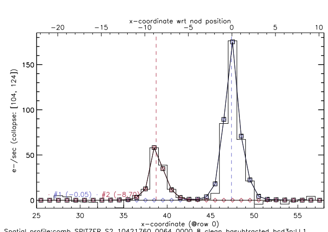
(e) LL1-first nod (scale: 0.80)

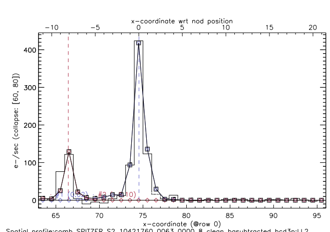
(f) LL2-second nod (scale: 0.80)

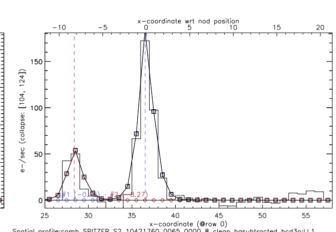
(g) LL1-second nod (scale: 0.80)

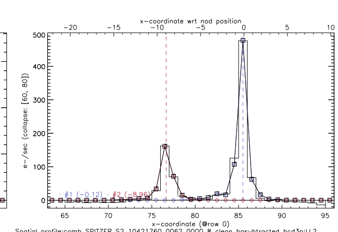
(h) LL2-first nod (scale: 0.80)

Figure 82. SL and LL modules spatial profiles after subtraction of the background

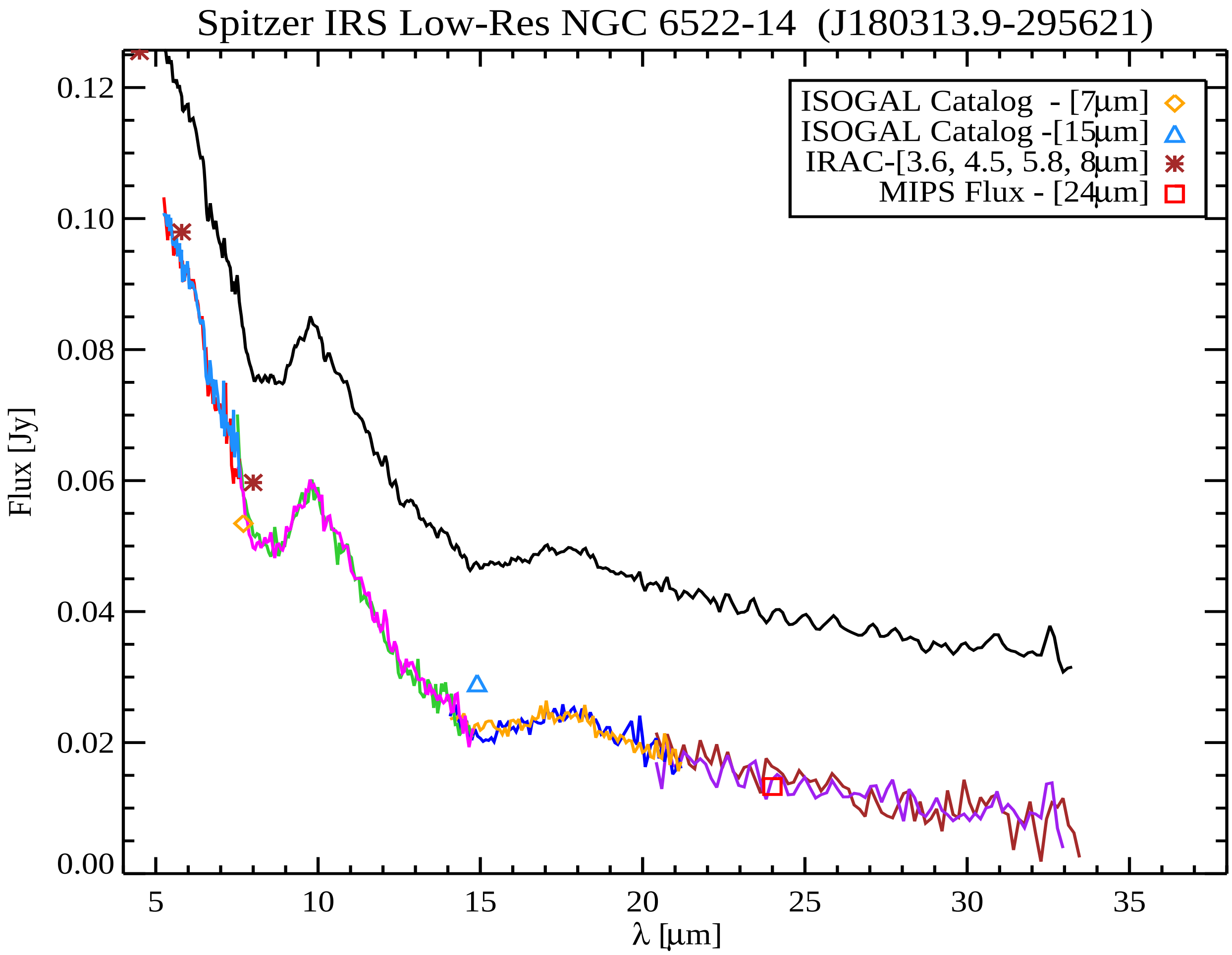

Figure 83. **(NGC 6522-14)** This is the final spectrum of NGC 6522-14. Figure 84 indicates the number of sources that have been extracted in each nod and module. After extraction the sharp and unrealistic residual features were masked (e.g. 19.5-μm). This source is located in the field covering NGC6522 and its background is similar to that of the rest of the field thus similarly it was corrected through modeling. Finally, we scaled long low modules with respect to the short low modules using the following scale factors, in order to eliminate the mismatch between them and obtain the continuum shown here.

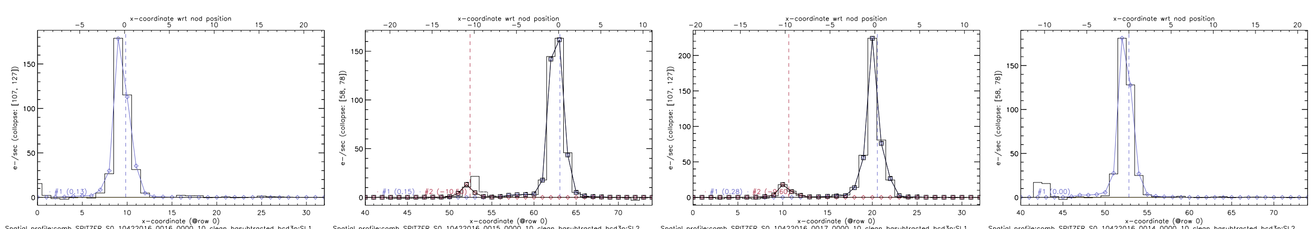

(a) SL1-first nod (scale: 1.0) (b) SL2-second nod (scale: 1.0) (c) SL1-second nod (scale: 1.0) (d) SL2-first nod (scale: 1.0)

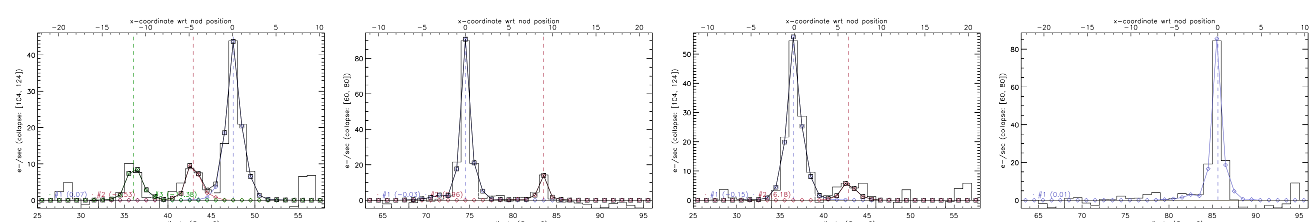

(e) LL1-first nod (scale: 0.80) (f) LL2-second nod (scale: 0.80) (g) LL1-second nod (scale: 0.80) (h) LL2-first nod (scale: 0.80)

Figure 84. SL and LL modules spatial profiles after subtraction of the background

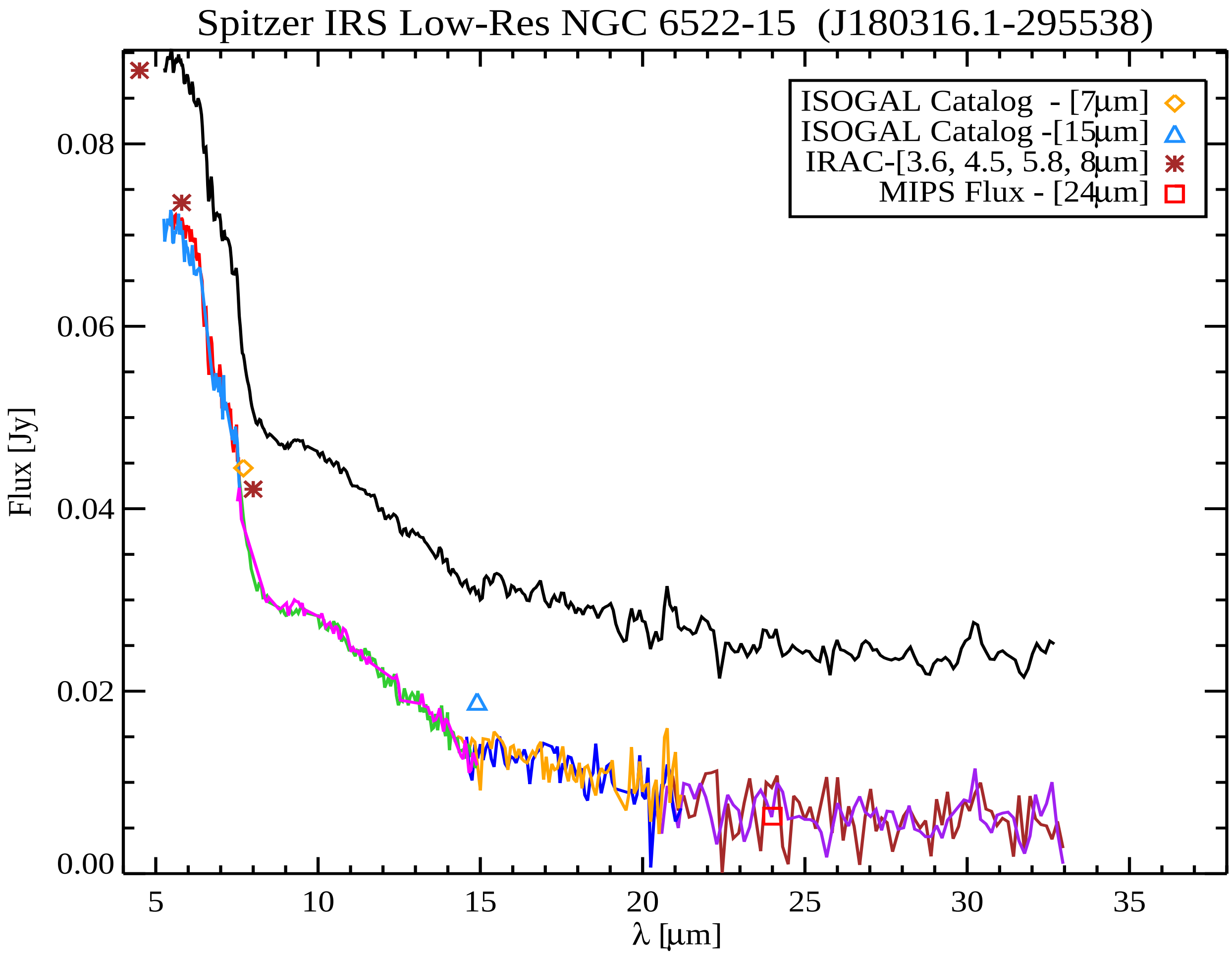

Figure 85. (NGC 6522-15) This is the final spectrum of NGC 6522-15. Figure 86 indicates the number of sources that have been extracted in each nod and module.There was a slight mismatch between the two nods of SL1 module which was removed by modifying the point spread function (central position and FWHM). After extraction, residual features were masked (e.g. 19.5-μm). This source is located in the field covering NGC6522 and its background is similar to that of the rest of the field thus similarly it was corrected through modeling. Finally, we scaled long low modules with respect to the short low modules using the following scale factors, in order to eliminate the mismatch between them and obtain the continuum shown here.

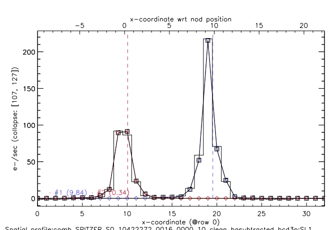
(a) SL1-first nod (scale: 1.0)

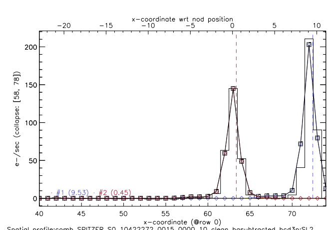
(b) SL2-second nod (scale: 1.0)

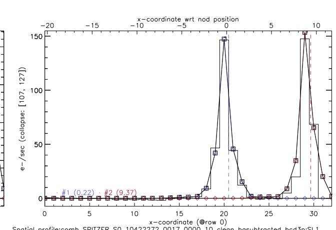
(c) SL1-second nod (scale: 1.0)

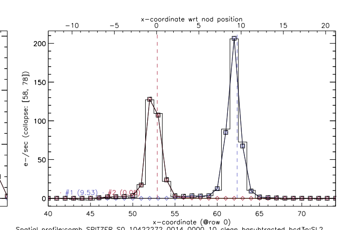
(d) SL2-first nod (scale: 1.0)

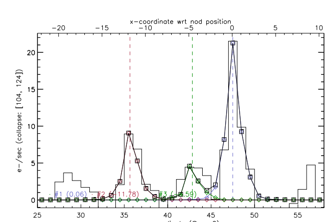
(e) LL1-first nod (scale: 0.75)

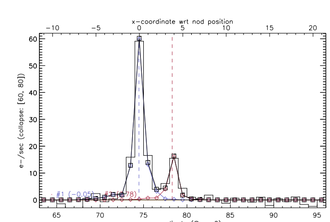
(f) LL2-second nod (scale: 0.75)

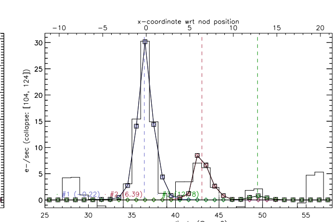
(g) LL1-second nod (scale: 0.75)

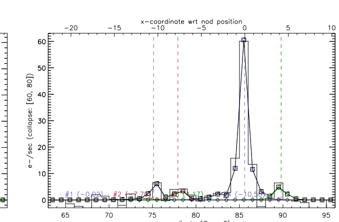
(h) LL2-first nod (scale: 0.75)

Figure 86. SL and LL modules spatial profiles after subtraction of the background

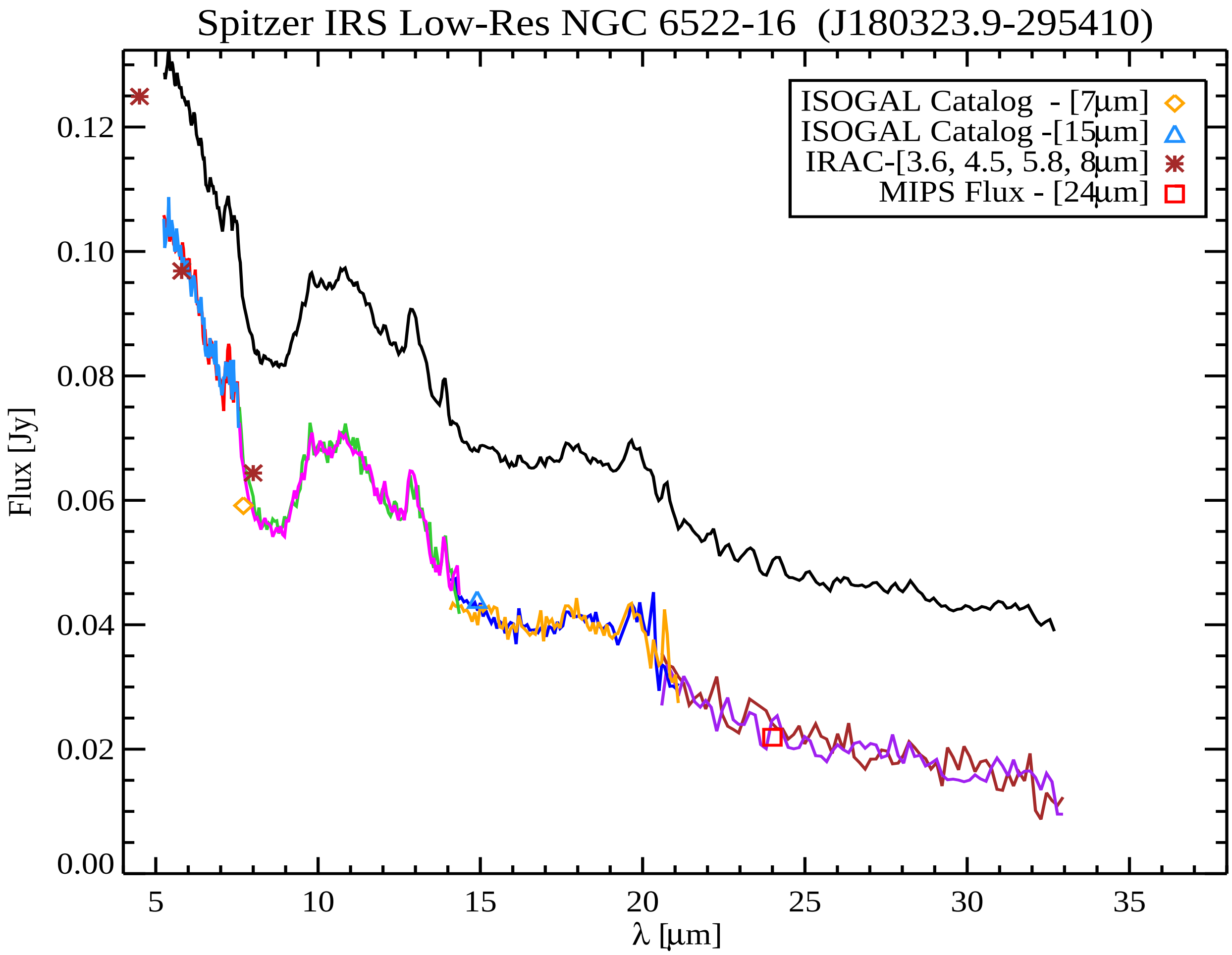

Figure 87. **(NGC 6522-16)** This is the final spectrum of NGC 6522-16. Figure 88 indicates the number of sources that have been extracted in each nod and module.There was a slight mismatch between the two nods of SL1 module which was removed by modifying the point spread function (central position and FWHM). After extraction the sharp and unrealistic residual features were masked (e.g. 19.5-μm). This source is located in the field covering NGC6522 and its background is similar to that of the rest of the field thus similarly it was corrected through modeling. Finally, we scaled long low modules with respect to the short low modules using the following scale factors, in order to eliminate the mismatch between them and obtain the continuum shown here.

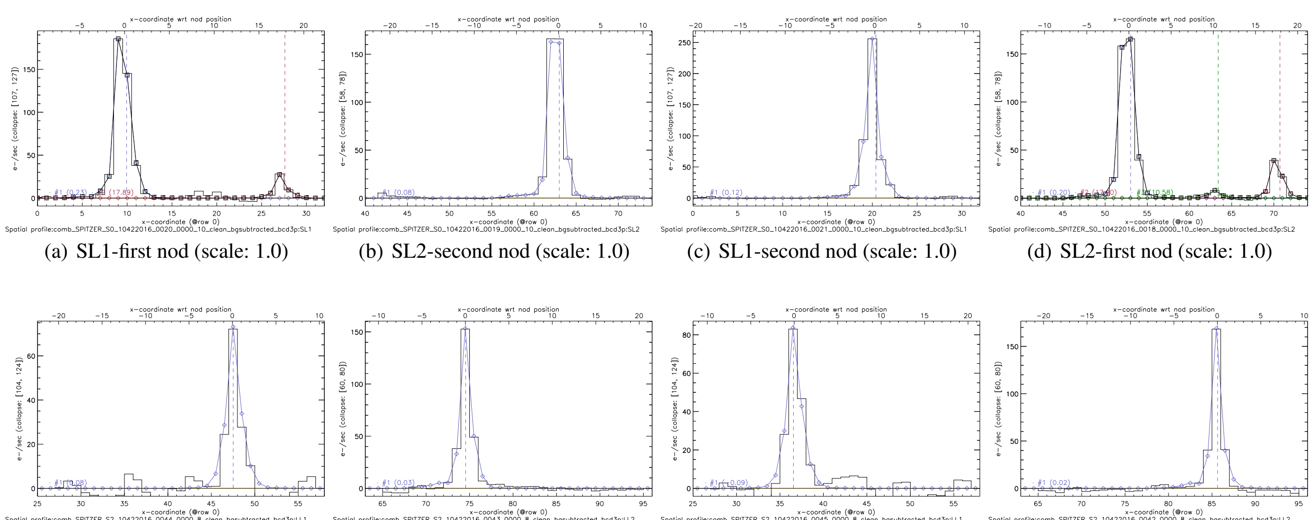

(a) SL1-first nod (scale: 1.0) (b) SL2-second nod (scale: 1.0) (c) SL1-second nod (scale: 1.0) (d) SL2-first nod (scale: 1.0)

(e) LL1-first nod (scale: 0.80) (f) LL2-second nod (scale: 0.80) (g) LL1-second nod (scale: 0.80) (h) LL2-first nod (scale: 0.80)

Figure 88. SL and LL modules spatial profiles after subtraction of the background

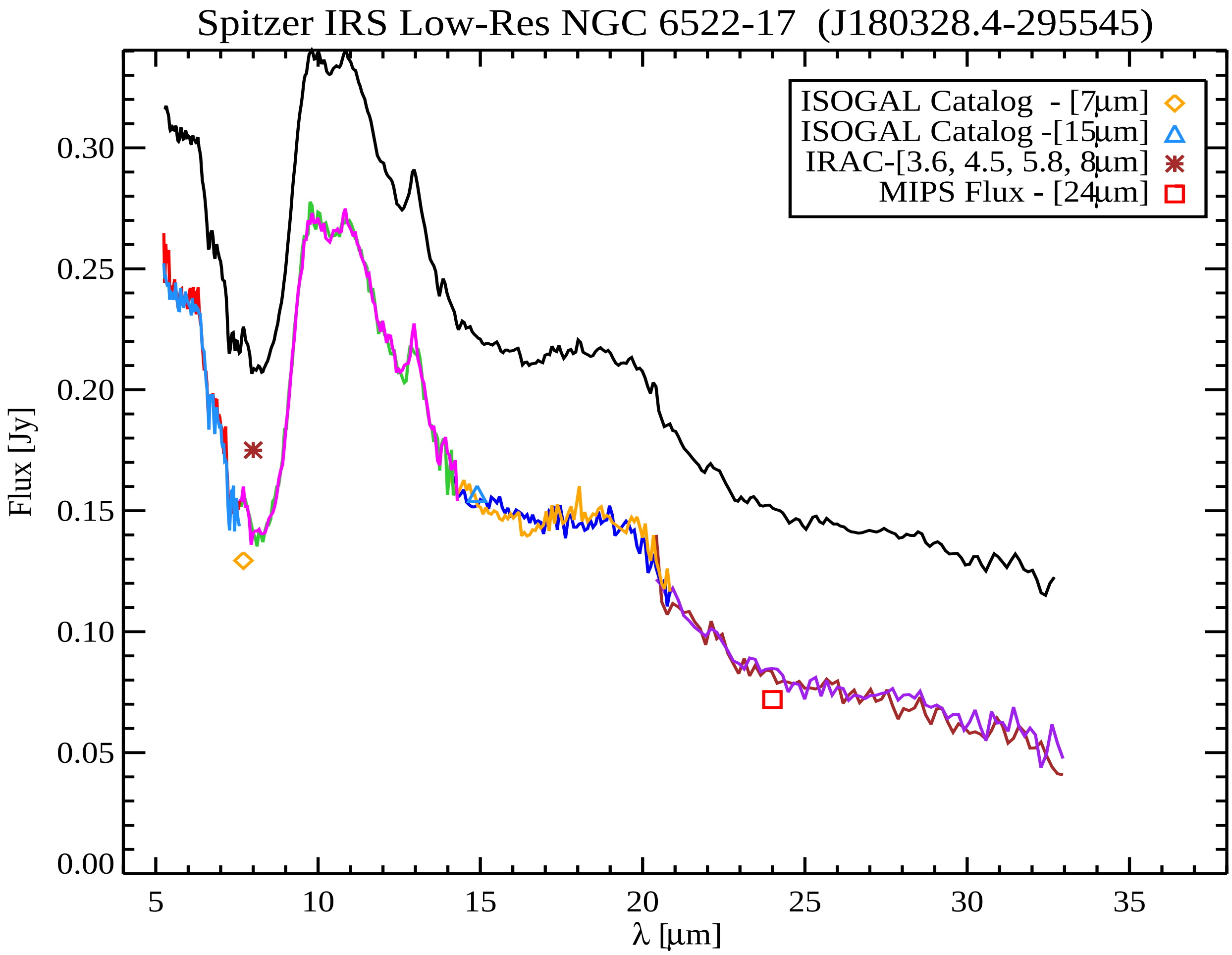

Figure 89. (NGC 6522-17) This is the final spectrum of NGC 6522-17. Figure 90 indicates the number of sources that have been extracted in each nod and module. After extraction the sharp and unrealistic residual features were masked (e.g. 19.5-μm). This source is located in the field covering NGC6522 and its background is similar to that of the rest of the field thus similarly it was corrected through modeling. Finally, we scaled long low modules with respect to the short low modules using the following scale factors, in order to eliminate the mismatch between them and obtain the continuum shown here.

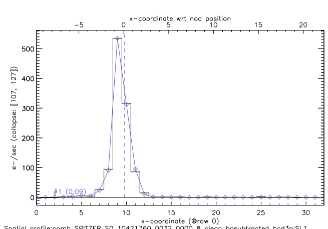
(a) SL1-first nod (scale: 1.0)

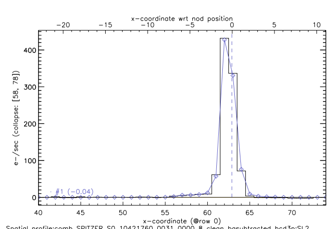
(b) SL2-second nod (scale: 1.0)

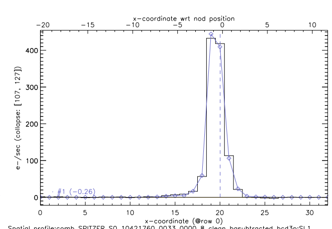
(c) SL1-second nod (scale: 1.0)

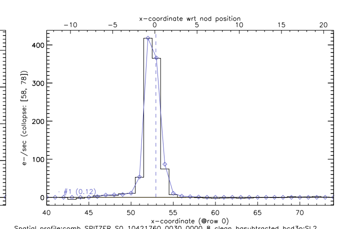
(d) SL2-first nod (scale: 1.0)

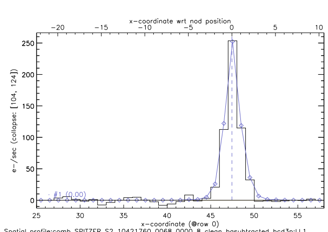
(e) LL1-first nod (scale: 0.85)

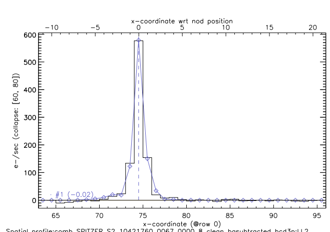
(f) LL2-second nod (scale: 0.85)

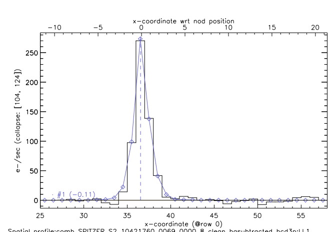
(g) LL1-second nod (scale: 0.85)

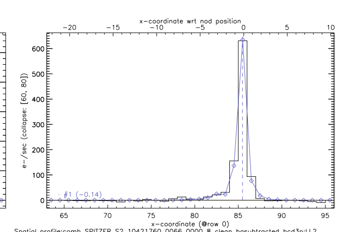
(h) LL2-first nod (scale: 0.85)

Figure 90. SL and LL modules spatial profiles after subtraction of the background

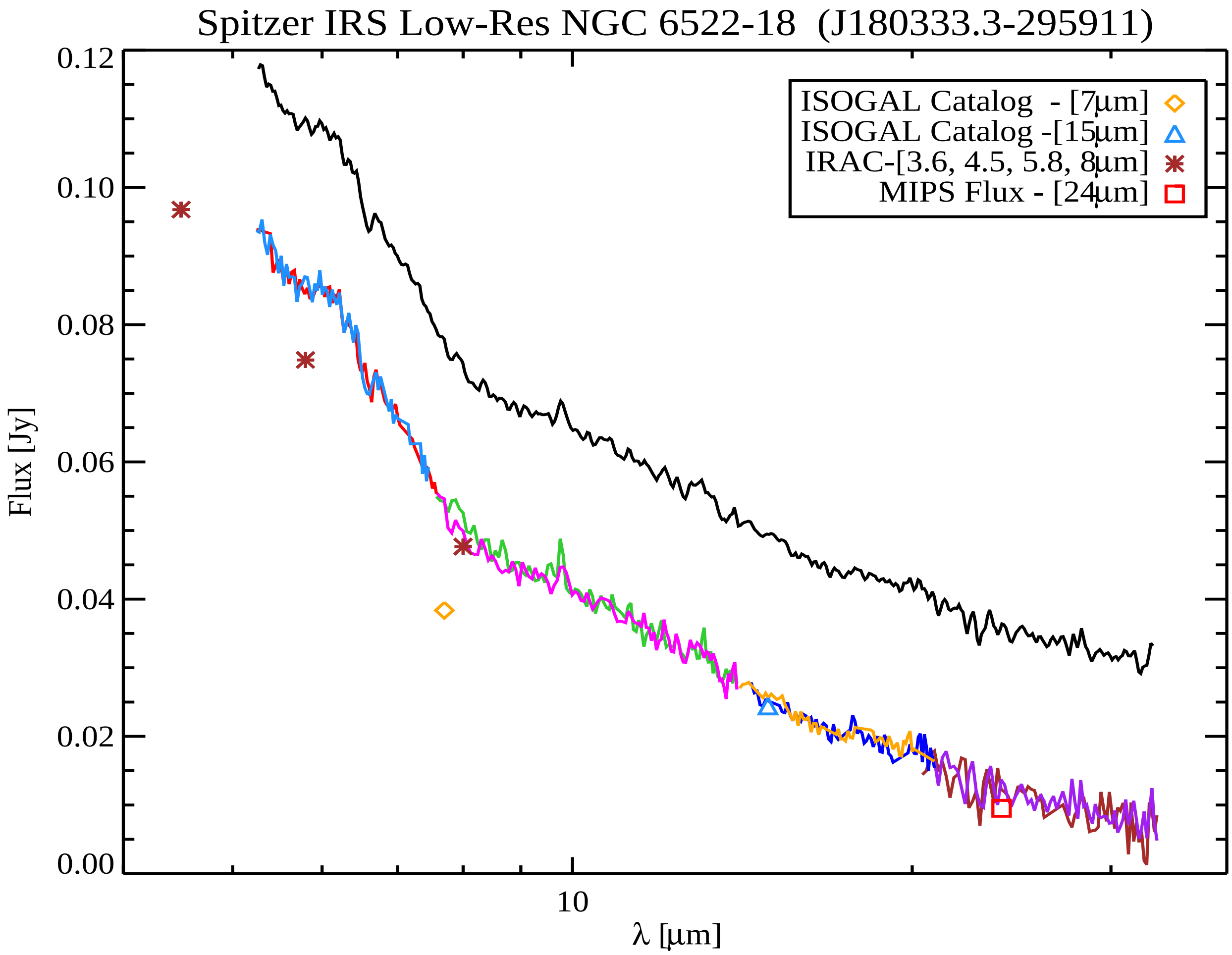

Figure 91. **(NGC 6522-18)** This is the final spectrum of NGC 6522-18. Figure 92 indicates the number of sources that have been extracted in each nod and module. After extraction, residual features were masked (e.g. 19.5-μm). This source is located in the field covering NGC6522 and its background is similar to that of the rest of the field thus similarly it was corrected through modeling. Finally, we scaled long low modules with respect to the short low modules using the following scale factors, in order to eliminate the mismatch between them and obtain the continuum shown here.

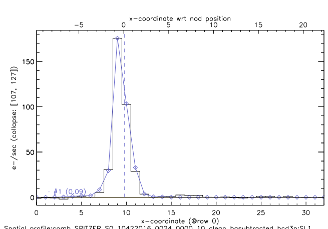

(a) SL1-first nod (scale: 1.0)

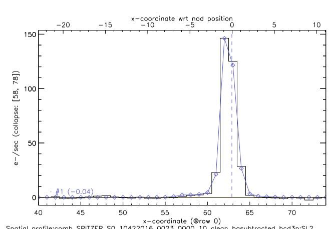

(b) SL2-second nod (scale: 1.0)

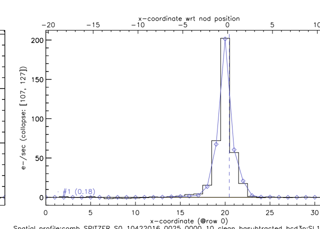

(c) SL1-second nod (scale: 1.0)

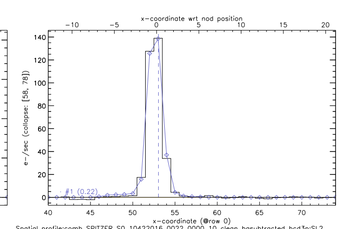

(d) SL2-first nod (scale: 1.0)

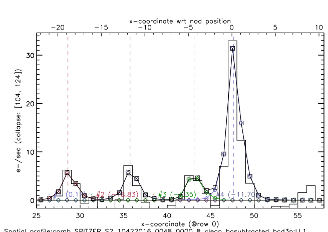

(e) LL1-first nod (scale: 0.85)

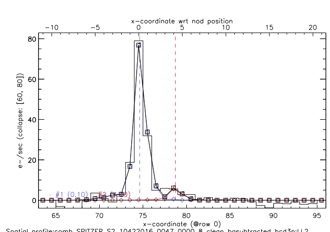

(f) LL2-second nod (scale: 0.85)

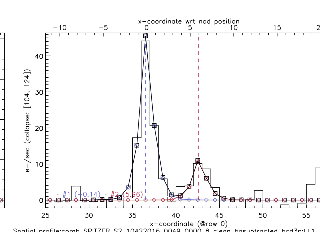

(g) LL1-second nod (scale: 0.85)

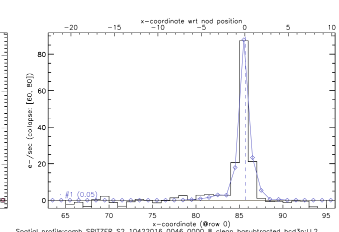

(h) LL2-first nod (scale: 0.85)

Figure 92. SL and LL modules spatial profiles after subtraction of the background

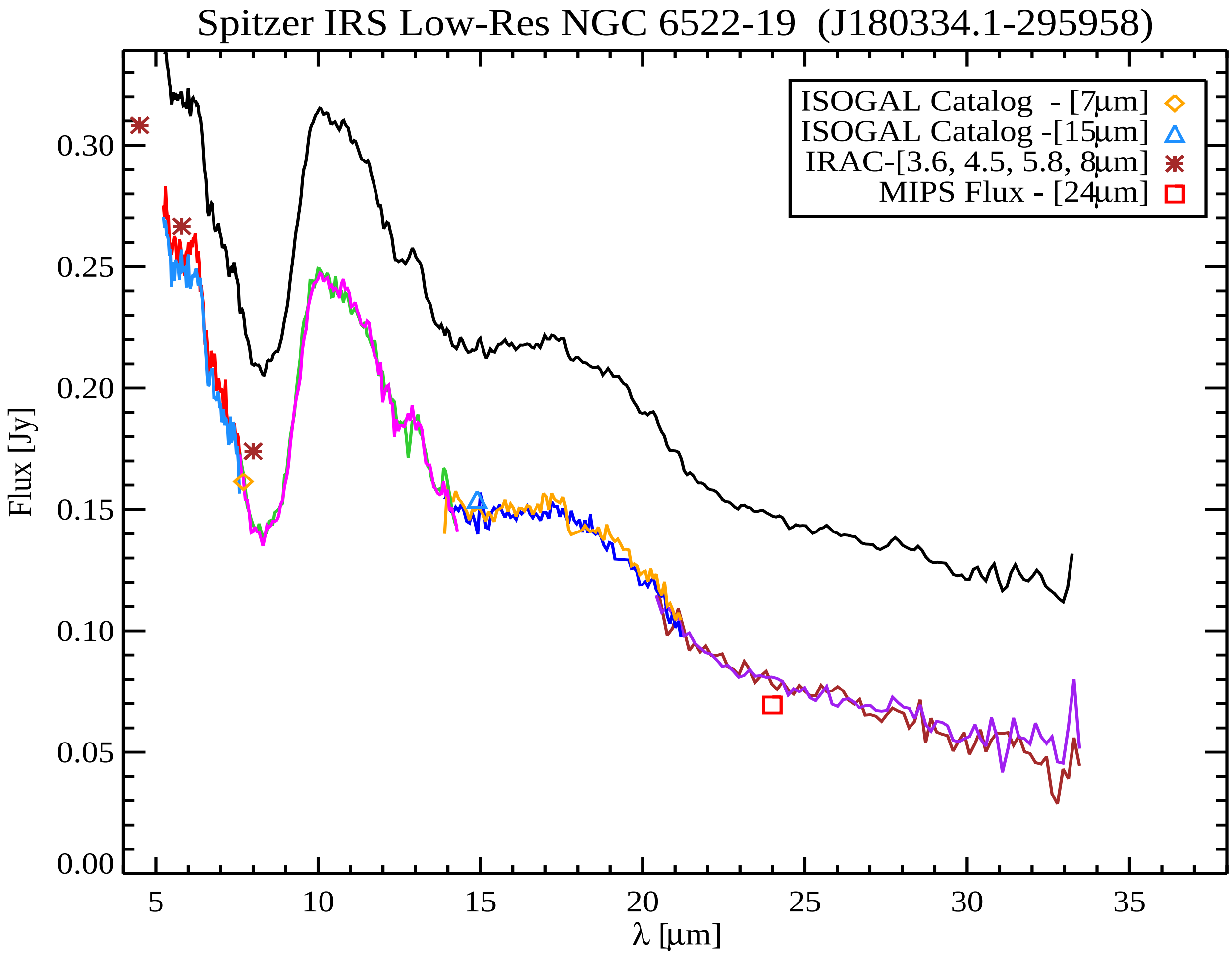

Figure 93. (NGC 6522-19) This is the final spectrum of NGC 6522-19. Figure 94 indicates the number of sources that have been extracted in each nod and module. After extraction the sharp and unrealistic residual features were masked (e.g. 19.5-μm). This source is located in the field covering NGC6522 and its background is similar to that of the rest of the field thus similarly it was corrected through modeling. Finally, we scaled long low modules with respect to the short low modules using the following scale factors, in order to eliminate the mismatch between them and obtain the continuum shown here.

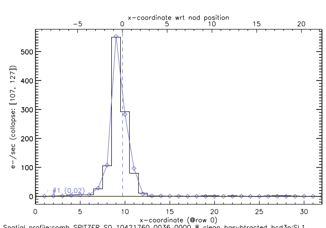
(a) SL1-first nod (scale: 1.0)

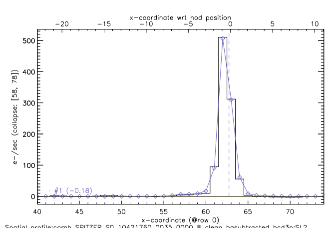
(b) SL2-second nod (scale: 1.0)

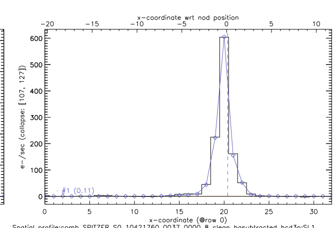
(c) SL1-second nod (scale: 1.0)

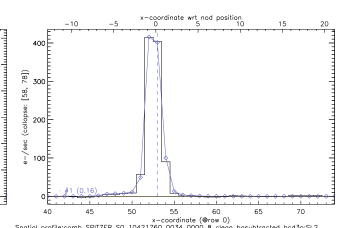
(d) SL2-first nod (scale: 1.0)

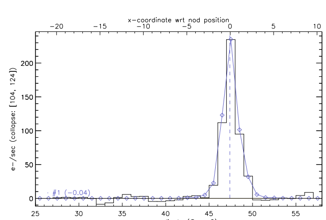
(e) LL1-first nod (scale: 0.85)

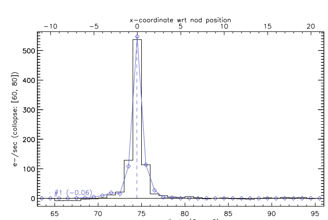
(f) LL2-second nod (scale: 0.90)

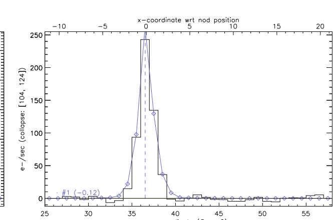
(g) LL1-second nod (scale: 0.85)

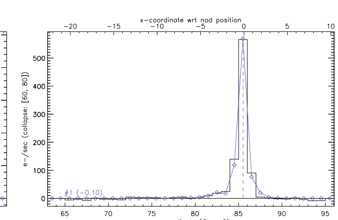
(h) LL2-first nod (scale: 0.90)

Figure 94. SL and LL modules spatial profiles after subtraction of the background

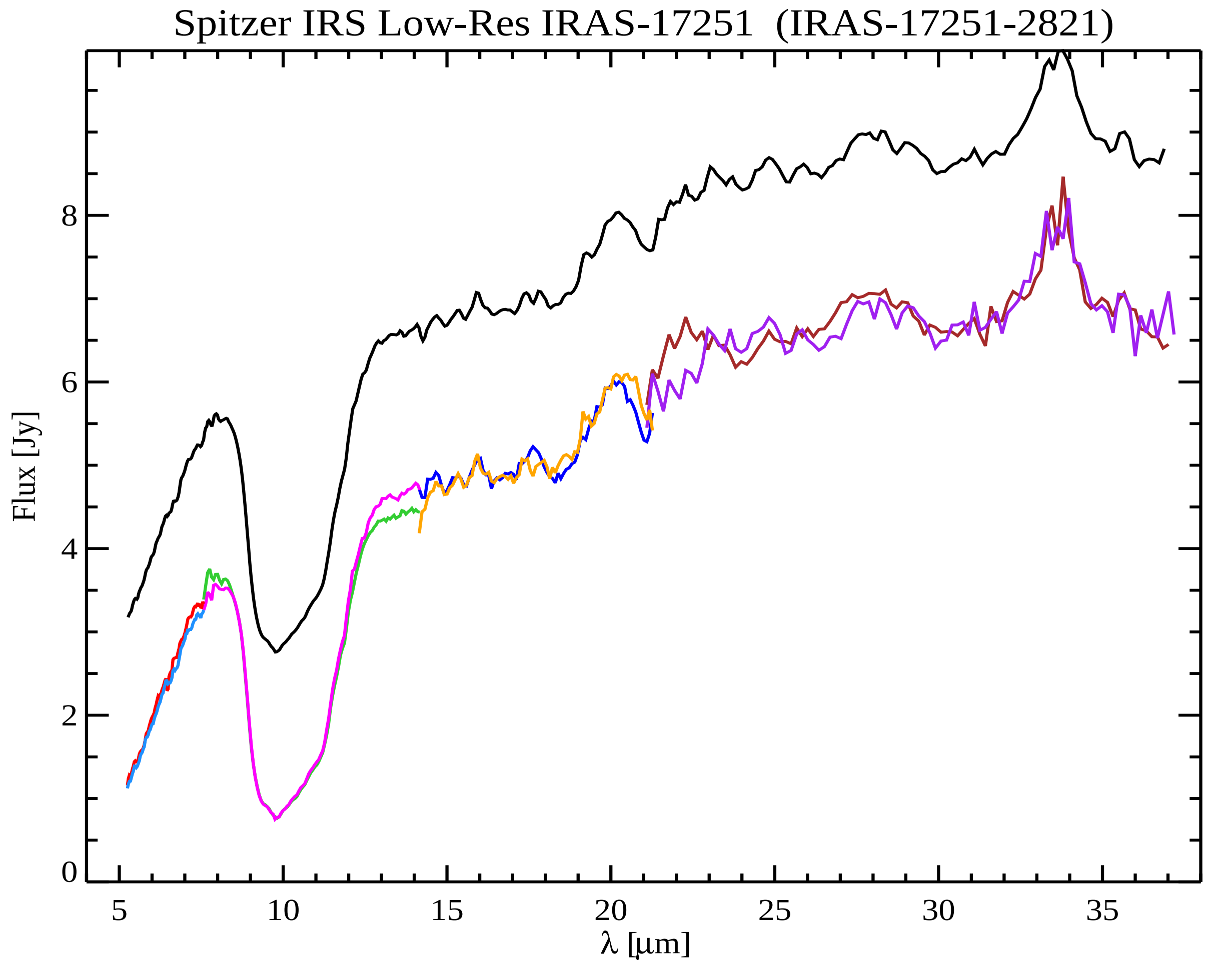

Figure 95. (IRAS-17251-2821) This is the final spectrum of IRAS-17251-2821. Figure 96 indicates the number of sources that have been extracted in each nod and module. After extraction, residual features were masked (e.g. 16.5-μm). This background was corrected through modeling. Finally, we scaled all modules with respect to the SL1 modules using the following scale factors, in order to eliminate the mismatch between them and obtain the continuum shown here.

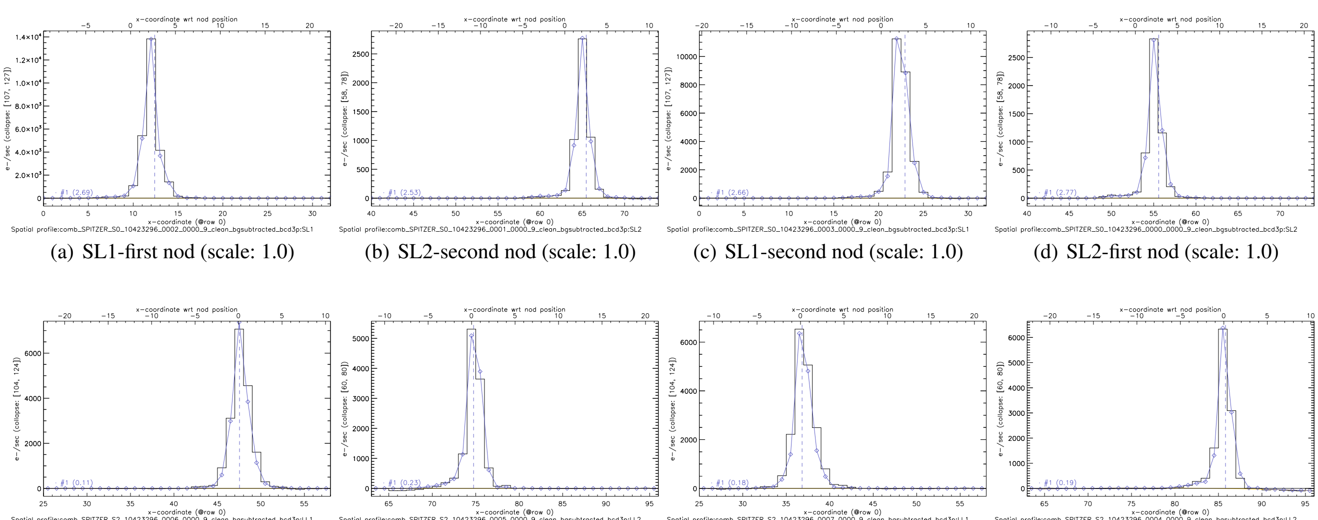

(a) SL1-first nod (scale: 1.0) (b) SL2-second nod (scale: 1.0) (c) SL1-second nod (scale: 1.0) (d) SL2-first nod (scale: 1.0)

(e) LL1-first nod (scale: 2.0) (f) LL2-second nod (scale: 2.0) (g) LL1-second nod (scale: 2.0) (h) LL2-first nod (scale: 2.0)

Figure 96. SL and LL modules spatial profiles after subtraction of the background

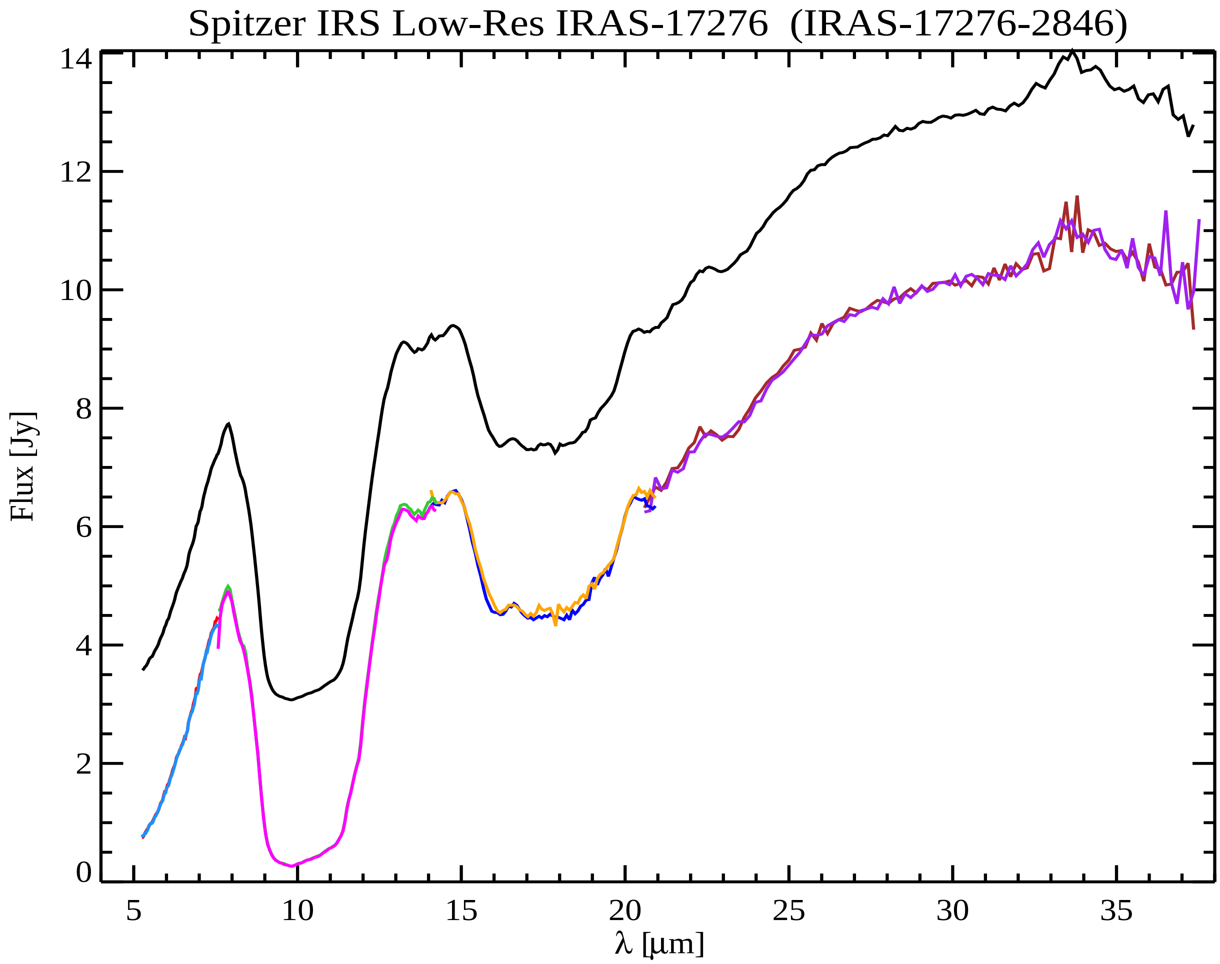

Figure 97. (IRAS-17276-2846) This is the final spectrum of IRAS-17276-2846. Figure 98 indicates the number of sources that have been extracted in each nod and module. After extraction, residual features were masked (e.g. 16.5-μm). The background was corrected through **modeling except that, in the long low modules,** there were residuals left from the background. We removed those residuals by further **subtracting a constant offset (zeroth order polynomial)**. This particular case results in no mismatch between the modules therefore the continuum shown here is obtained without any further scaling.

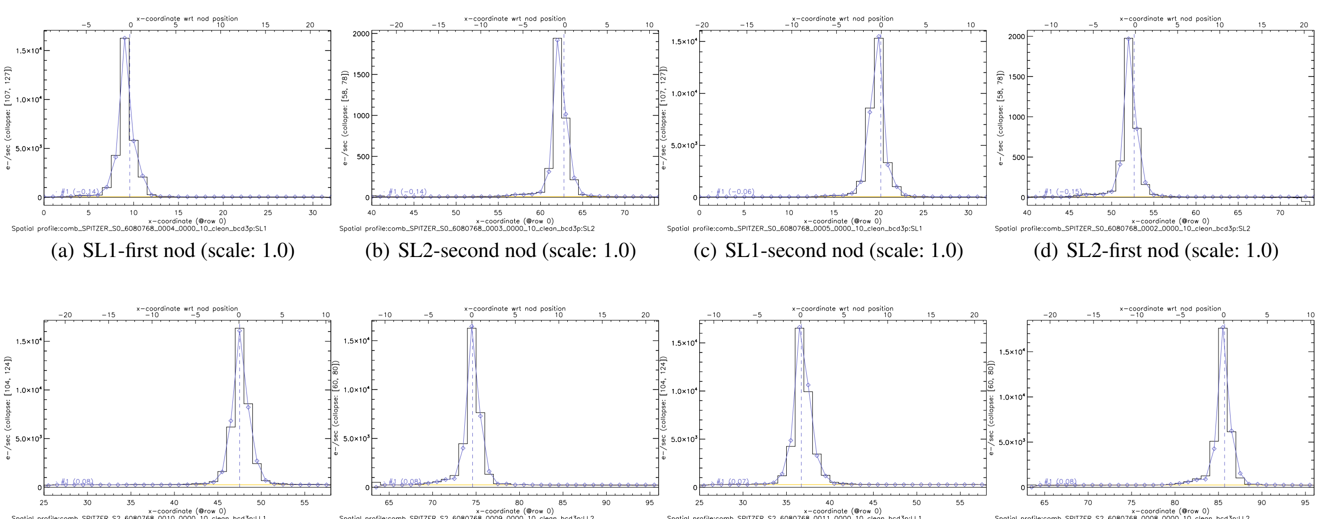

(a) SL1-first nod (scale: 1.0) (b) SL2-second nod (scale: 1.0) (c) SL1-second nod (scale: 1.0) (d) SL2-first nod (scale: 1.0)

(e) LL1-first nod (scale: 1.0) (f) LL2-second nod (scale: 1.0) (g) LL1-second nod (scale: 1.0) (h) LL2-first nod (scale: 1.0)

Figure 98. SL and LL modules spatial profiles after subtraction of the background

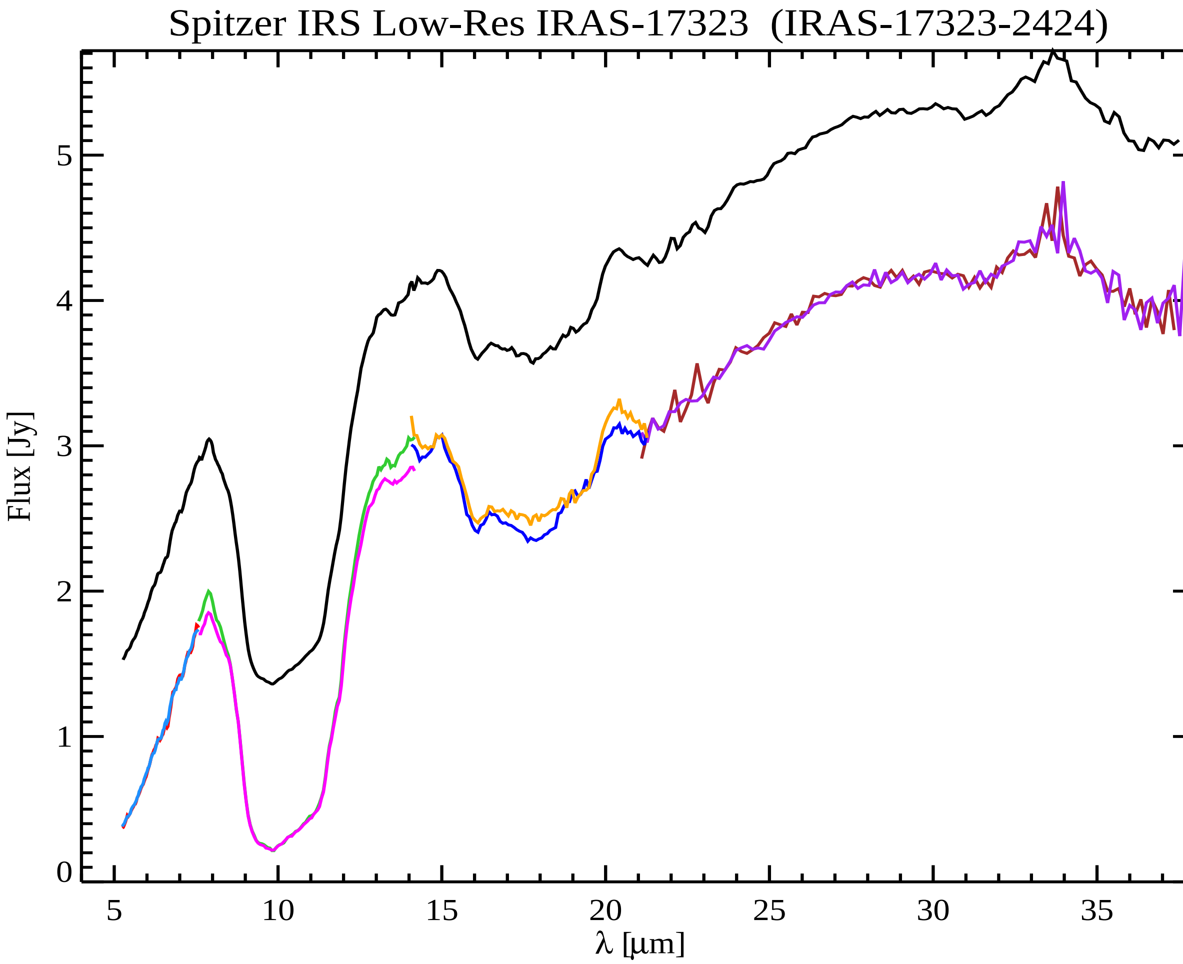

Figure 99. (IRAS-17323-2424) This is the final spectrum of IRAS-17323-2424. Figure 100 indicates the number of sources that have been extracted in each nod and module. After extraction, no significant residual was left to mask. The background was corrected through modeling. Finally, we scaled long low modules with respect to the short low modules using the following scale factors, in order to eliminate the mismatch between them and obtain the continuum shown here.

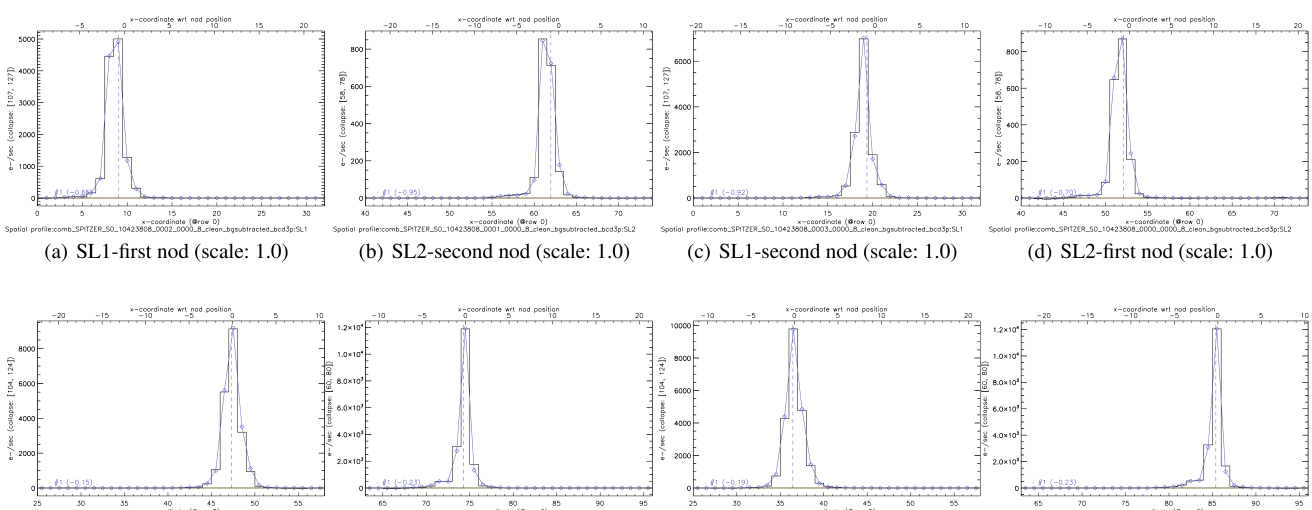

(a) SL1-first nod (scale: 1.0) (b) SL2-second nod (scale: 1.0) (c) SL1-second nod (scale: 1.0) (d) SL2-first nod (scale: 1.0)

(e) LL1-first nod (scale: 0.80) (f) LL2-second nod (scale: 0.85) (g) LL1-second nod (scale: 0.80) (h) LL2-first nod (scale: 0.85)

Figure 100. SL and LL modules spatial profiles after subtraction of the background

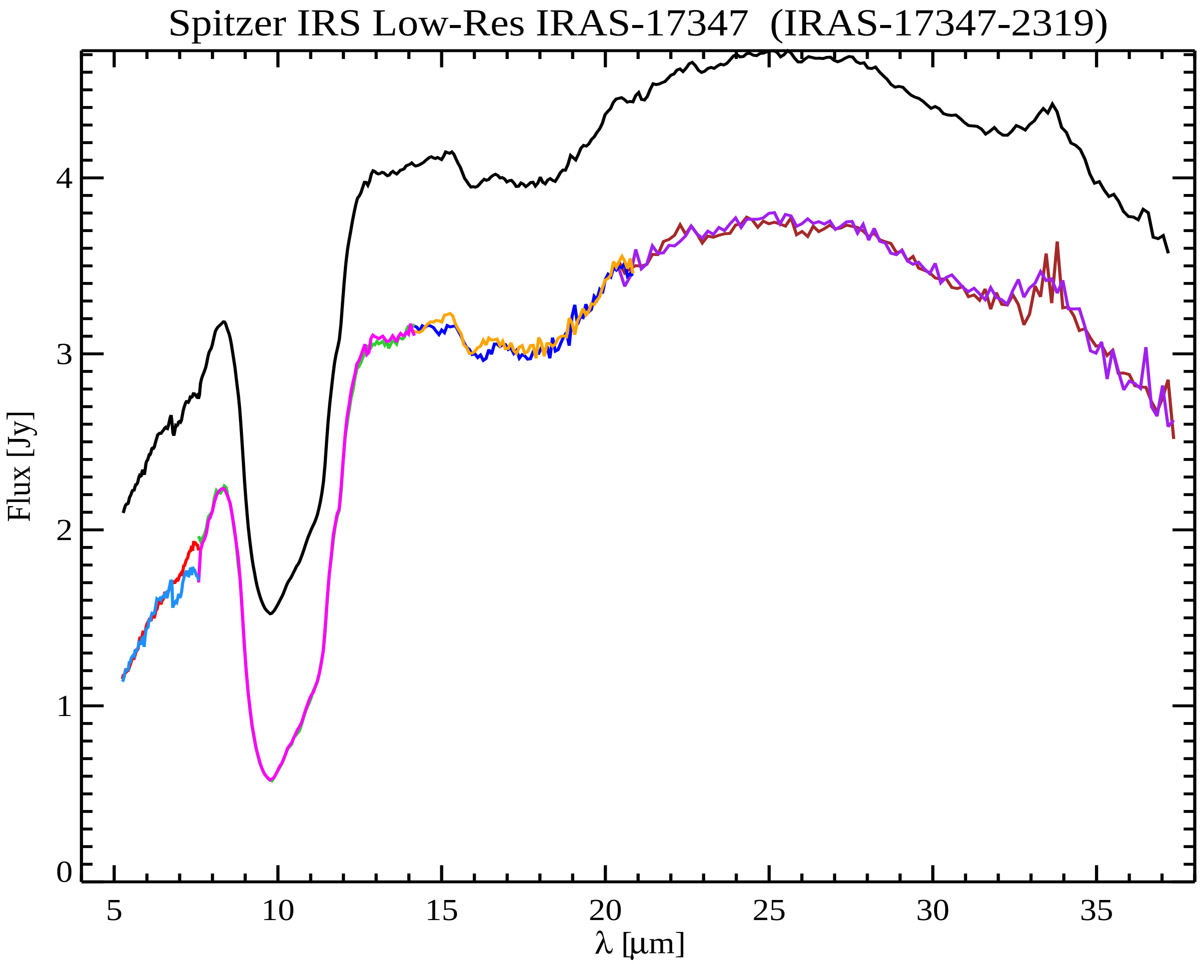

Figure 101. (IRAS-17347-2319) This is the final spectrum of IRAS-17347-2319. Figure 102 indicates the number of sources that have been extracted in each nod and module. After extraction, no significant residual was left to mask. The background was corrected through modeling **except that, after modeling, there was** still residuals left from the background. Therefore we have corrected the residuals with **further subtracting a constant offset (polynomial order zero)**. Finally, we scaled long low modules with respect to the short low modules using the following scale factors, in order to eliminate the mismatch between them and obtain the continuum shown here.

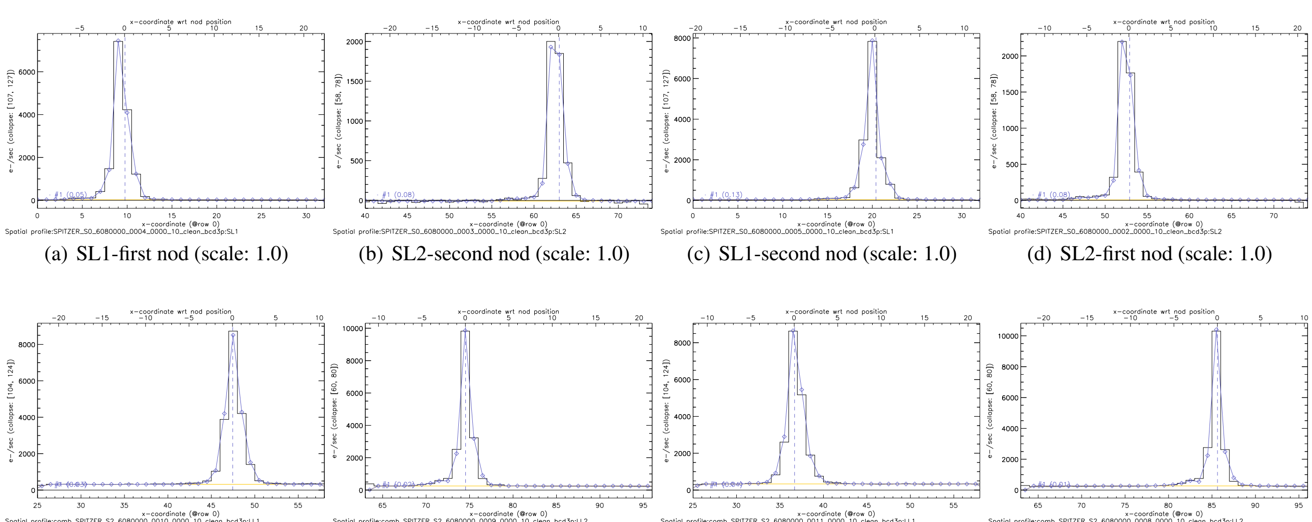

(a) SL1-first nod (scale: 1.0) (b) SL2-second nod (scale: 1.0) (c) SL1-second nod (scale: 1.0) (d) SL2-first nod (scale: 1.0)

(e) LL1-first nod (scale: 0.97) (f) LL2-second nod (scale: 0.97) (g) LL1-second nod (scale: 0.97) (h) LL2-first nod (scale: 0.97)

Figure 102. SL and LL modules spatial profiles after subtraction of the background

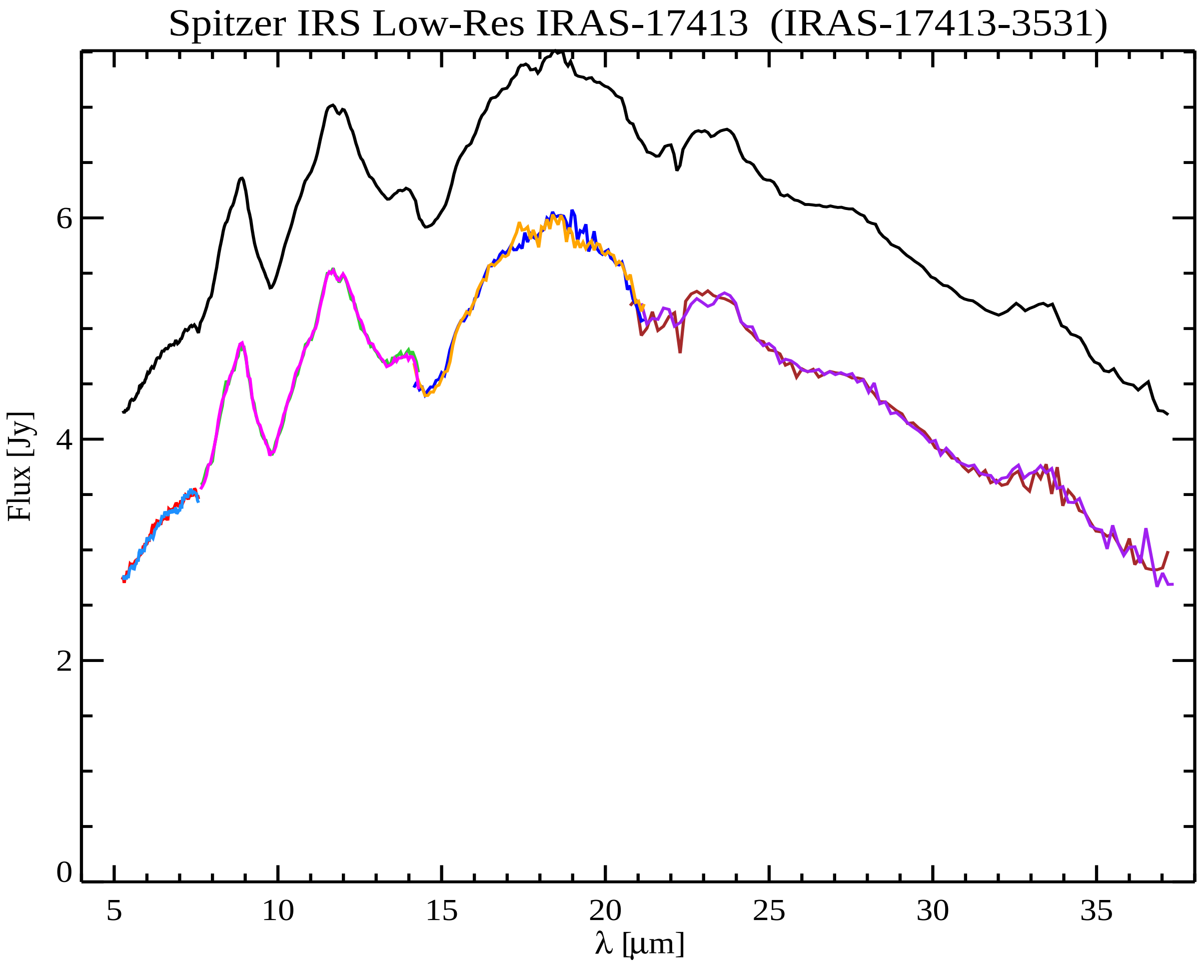

Figure 103. (IRAS-17413-3531) This is the final spectrum of IRAS-17413-3531. Figure 104 indicates the number of sources that have been extracted in each nod and module. After extraction, no significant residual was left to mask. The background was corrected through modeling **except that, in the long low modules,** there were residuals left from the background. We removed those residuals by further **subtracting a constant offset (polynomial order zero)**. Finally, we scaled all modules with respect to the SL1 modules using the following scale factors, in order to eliminate the mismatch between them and obtain the continuum shown here.

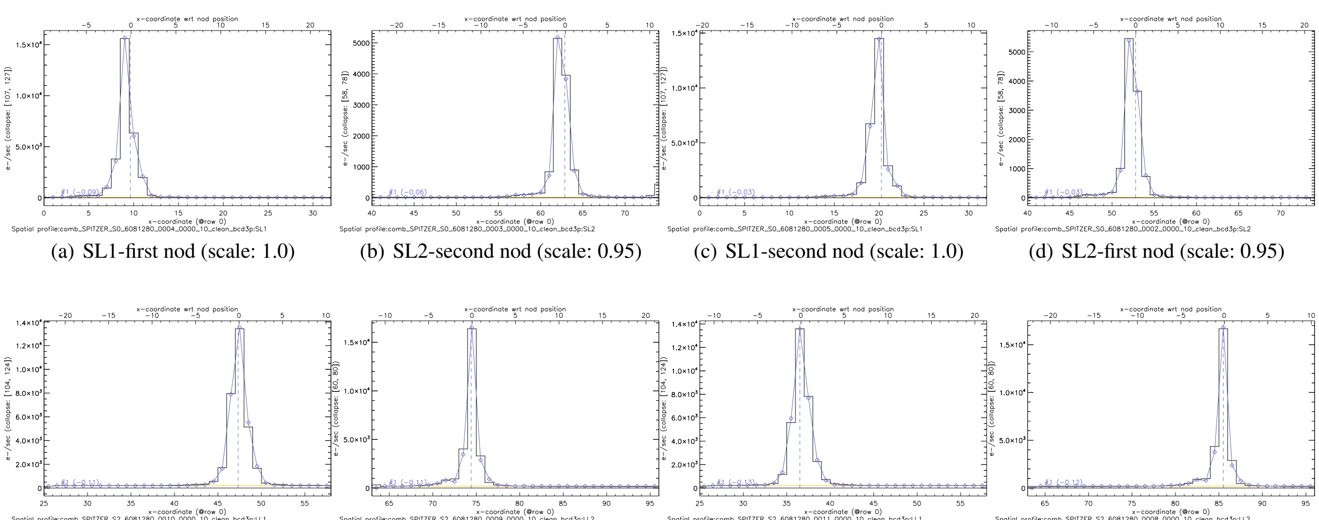

(a) SL1-first nod (scale: 1.0) (b) SL2-second nod (scale: 0.95) (c) SL1-second nod (scale: 1.0) (d) SL2-first nod (scale: 0.95)

(e) LL1-first nod (scale: 0.85) (f) LL2-second nod (scale: 0.90) (g) LL1-second nod (scale: 0.85) (h) LL2-first nod (scale: 0.90)

Figure 104. SL and LL modules spatial profiles after subtraction of the background

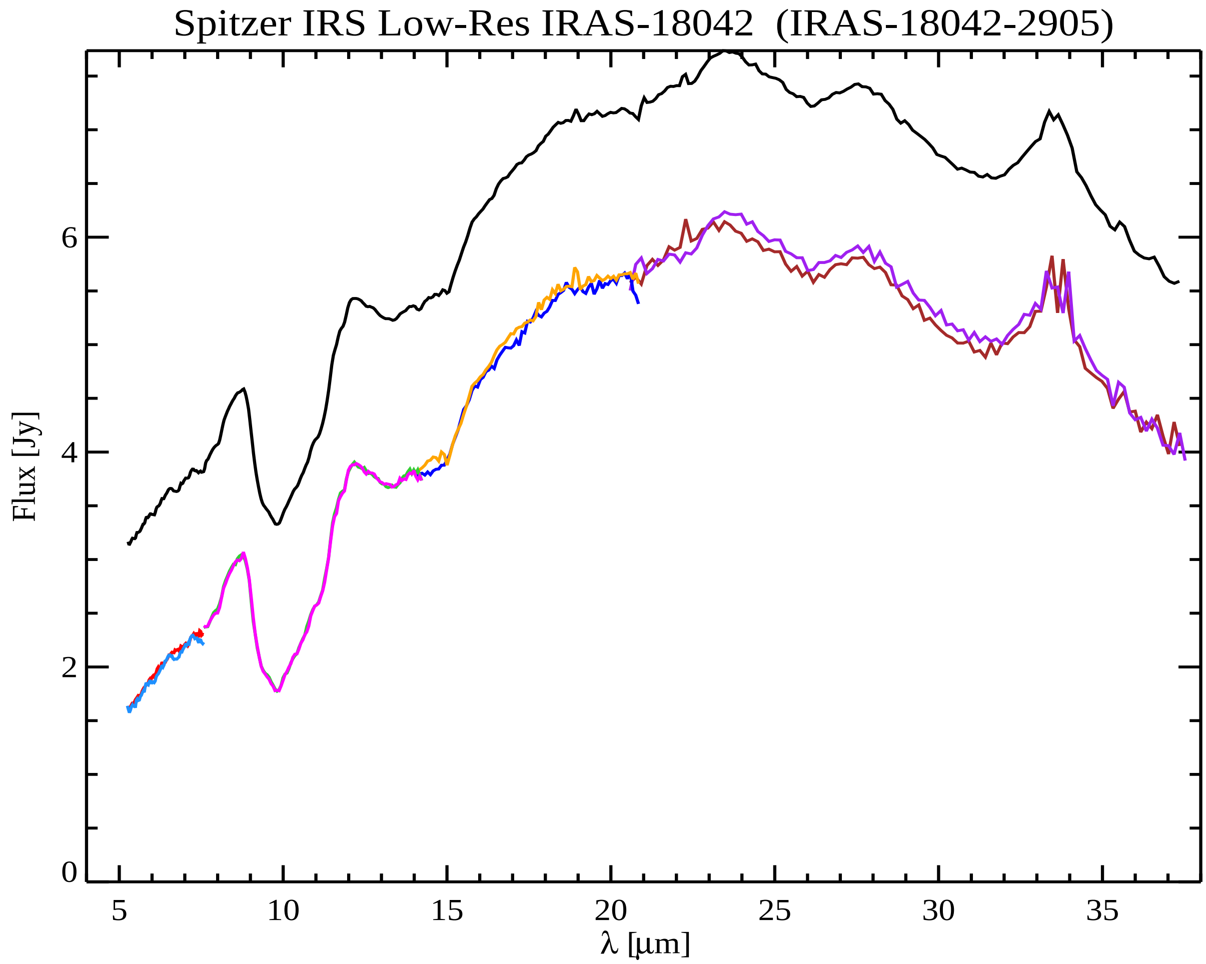

Figure 105. (IRAS-18042-2905) This is the final spectrum of IRAS-18042-2905. Figure 106 indicates the number of sources that have been extracted in each nod and module. After extraction, no significant residual was left to mask. The background was corrected through modeling. Finally, we scaled all modules with respect to the SL1 modules using the following scale factors, in order to eliminate the mismatch between them and obtain the continuum shown here.

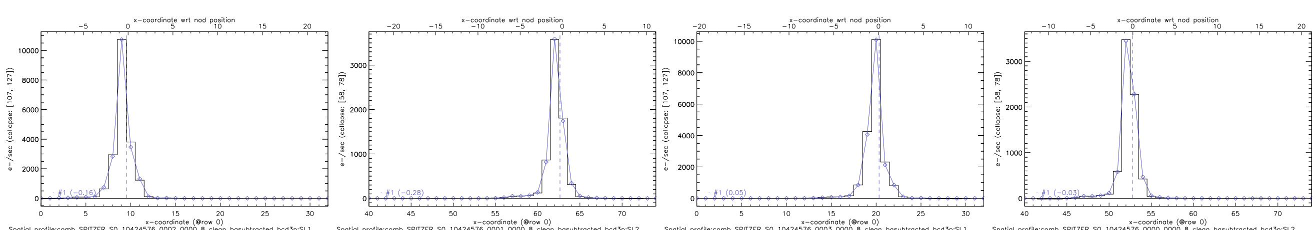

(a) SL1-first nod (scale: 1.0) (b) SL2-second nod (scale: 0.95) (c) SL1-second nod (scale: 1.0) (d) SL2-first nod (scale: 0.95)

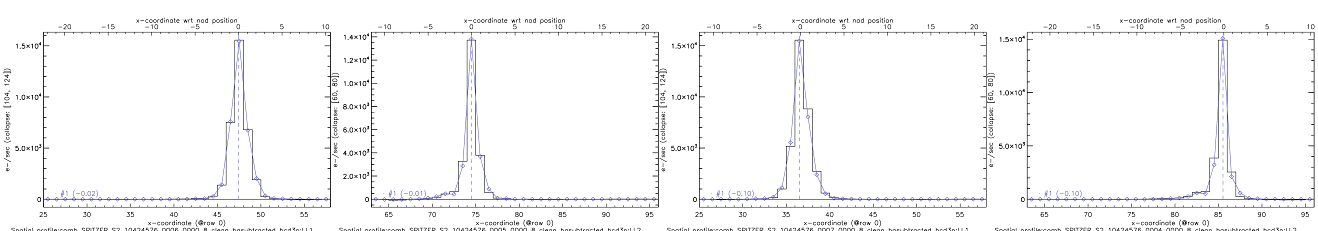

(e) LL1-first nod (scale: 0.90) (f) LL2-second nod (scale: 0.90) (g) LL1-second nod (scale: 0.90) (h) LL2-first nod (scale: 0.90)

Figure 106. SL and LL modules spatial profiles after subtraction of the background